DOCTORAL DISSERTATION

Control of Various Physical Properties
Using Structural Changes of
Redox Active Aromatic Amines

（芳香族アミンの酸化還元に基づく構造変化を利用した

多彩な物性制御に関する研究）

Wataru Nojo

Graduate School of Chemical
Sciences and Engineering
Hokkaido University

2020

Contents

Chapter 1

General Introduction

1-1. Organic redox systems in modern society 1

1-2. History of organic redox systems 2

1-3. The importance of partial charge-transfer state 3

1-4. Mixed-valence (MV) compound 4

1-5. A dream of molecular electronics 5

1-6. Molecular design 6

1-7. Content of this thesis 7

References 8

Chapter 2

Selective Creation of Mixed-Valence Oligomers based on π-Expanded Aromatic Diamines

2-1. Mixed-valence of pure organic molecules 10

2-2. Benzindolocarbazole (BIC) 13

2-3. Molecular design for MV-oligomers 17

2-4. Preparation of BIC dimers with an alkylene chain (n = 3, 4, 5) 19

2-5. UV-Vis and fluorescence spectra of **2a**, **2b**, **2c** 21

2-6. Cyclic and difference pulse voltammograms of **2a**, **2b**, **2c** 22

2-7. Spectroelectrograms of **2a**, **2b**, **2c** 25

2-8. Preparation of BIC dimers with a xylylene spacer (*o*-, *m*-, *p*-) 27

2-9. Cyclic and differential pulse voltammograms of **2d**, **2e**, **2f** 29

2-10. Spectroelectrograms of **2d'** and **2e'** 31

2-11. Preparation of BIC dimers with another aromatic spacer 33

2-12. Cyclic and differential pulse voltammograms of **2g**, **2h**, **2i** 34

2-13. Consideration on the distance between the connecting sites 35

2-14. Pimer formation of *m*-xylylene-bridged BIC 36

2-15. Determination of the spacer structure for oligomers 38

2-16. Preparation of BIC oligomers (**2** ~ **8**) 40

2-17. Electrochemical properties of BIC oligomers 44

2-18. Spectroscopic analyses of BIC oligomers 47
2-19. X-ray crystallography of dication diradical of tetramer **4** 50
2-20. Even–odd dependency of half-filled MV states 52
2-21. Conclusion for the linear BIC oligomers 53
2-22. The dendrimeric BIC with multiple *m*-xylylene structure 54
2-23. CV and DPV measurements of BIC triad and tetrad 55
Experimental 58
References 92

Chapter 3
Development of aromatic amine with molecular film forming ability applicable to molecular diode/junction
3-1. Conventional diodes and molecular diodes
3-2. A history of molecular diodes
3-3. Molecular diodes for next generation
3-4. New design of molecular diode in this study
3-5. Preparation of novel molecular diode
3-6. Electrochemical properties of the molecular diode
3-7. UV-Vis-NIR spectra of the molecular diode
3-8. Molecular junction: principal, progress, and problem
3-9. Molecular junction with conductivity ON/OFF switching
3-10. Electrically-switchable molecular junction
3-11. Challenges of Electrically-switchable molecular junction
3-12. Dynamic redox (*dyrex*) system
3-13. Preliminary examination of previously synthesized molecule
3-14. Considerations for accelerating the reaction rate
3-15. Molecular design for superior molecular junction
3-16. Preparation of new BDAE compounds undergoing rapid response
3-17. Electrochemical properties of newly prepared BDEA compounds
Experimental
References

Acknowledgements

Chapter 1

General Introduction

1-1. Organic redox systems in modern society

Recently, much attention has been focused on organic π-electron systems in the field of organic materials chemistry since those compounds are the promising candidates for developing organic electroluminescence (EL) materials,[1-5] organic field effect transistors (OFET),[6-10] and organic solar cells (OSC).[11-15] The HOMO and LUMO energy levels of those compounds are the determinant factors of the devices derived there from, and thus examination of their redox properties gives indispensable information for developing the future materials.

1-2. History of organic redox systems

Besides the importance in related to the organic materials chemistry, the studies on organic redox systems have been long conducted with producing a plethora of knowledge on organic conductors/superconductors or electrochromic materials. Tetrathiafulvalene (TTF) is one of the most important redox molecules,[16] which was first synthesized in 1965 as the mixture of dimethyl and diphenyl derivatives.[17] The good electron-donating ability is partly on account of aromatization from dithiolylidene to dithiolium moiety upon oxidation process. On the other hand, tetracyanoquinodimeth-ane (TCNQ) is also representative electronic acceptor molecule, which was synthesized in DuPont in mid-1960s.[18] Like TTF, aromatization plays an important role in the reversible two-step one-electron reduction at lower potentials. The redox systems that acquires aromaticity by being oxidized/reduced such as TTF/TCNQ are called Weitz/Wurster-type redox system, respectively (Scheme 1).[19]

Scheme 1 | Redox process and electronic structure of TTF and TCNQ.

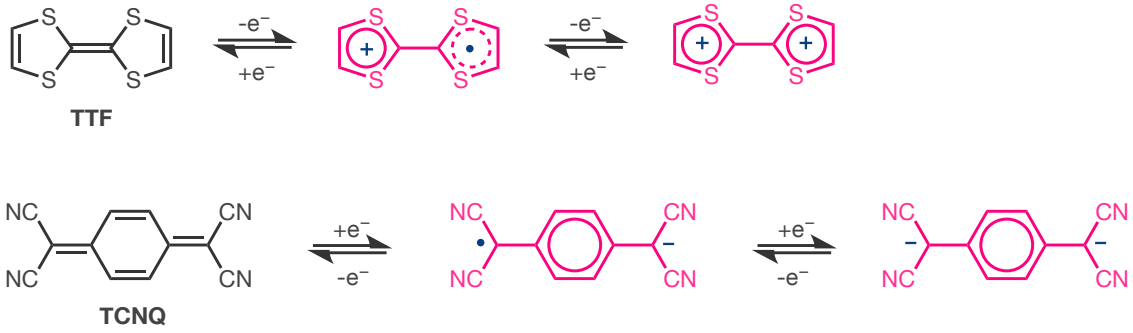

1-3. The importance of partial charge-transfer-state

The charge-transfer (CT) complex of TTF and TCNQ[20-22] shows high electronic conductivity about 100 S cm^{-1} at room temperature. Also, the conductivity rises promptly with decreasing temperature and then, decreased rapidly at 54 K. The high conductivity and temperature-dependency of the complex is shown that there are free electrons as seen in metallic solids, therefore the TTF-TCNQ complex is called molecular metal. The characteristics of crystal structure of the TTF-TCNQ complex is that each of TTF, and TCNQ unit stacked in one-dimension (segregated stacking structure) and the distances between each unit are all same (Figure 2). In addition to the feature of crystal structure, it is also important that the degree of charge transfer (σ) is 0.59. The state where the value of charge transfer is $0 < \sigma < 1$ is called "partial charge-transfer state". In this state, the total energy is not changed when carrier exchange occur between neutral and radical ion molecules, so that carrier can freely move through the crystals.

Figure 2 | Schematic diagram of the crystal structure of TTF-TCNQ charge transfer complex.

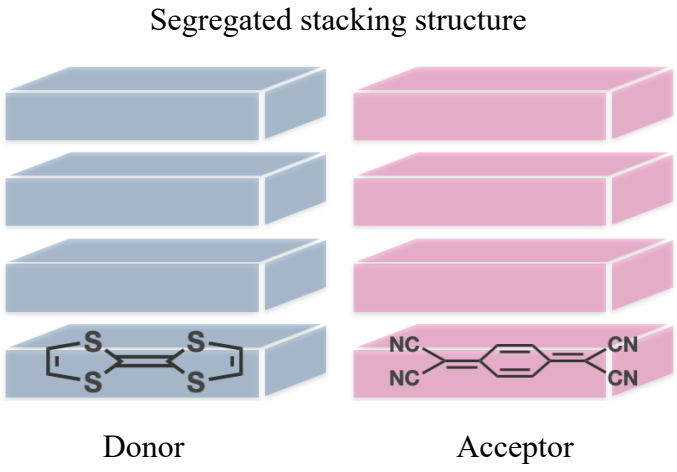

1-4. Mixed-valence (MV) compound

As mentioned in the previous section, creating partial charge-transfer state is important for exploring the electronic functions of organic molecules, and it is the mixed-valence (MV) state that can form this state within the molecule.[23] Mixed-valence states have unique magnetic or opto-electronic behaviors, due to the fact that they exhibit facile electron-transfer and/or charge-delocalization.[24, 25] Dinuclear metal complexes are representative materials that adopt MV states, which have two chemically equivalent sites with different redox states. In coordination polymers with multiple redox sites, even long-range interaction could be observed.[26]

In contrast to the plethora of metal-based MV materials, less is known about pure organic MV molecules, partly due to the poor stability of its radical ionic states. However, fine-tuning of the MV state could be realized by the proper design of redox-active organic chromophores.

Figure 3 | MV states of **a)** Creutz-Taube ion,[23] and **b)** metal-organic complex oligomer.[26]

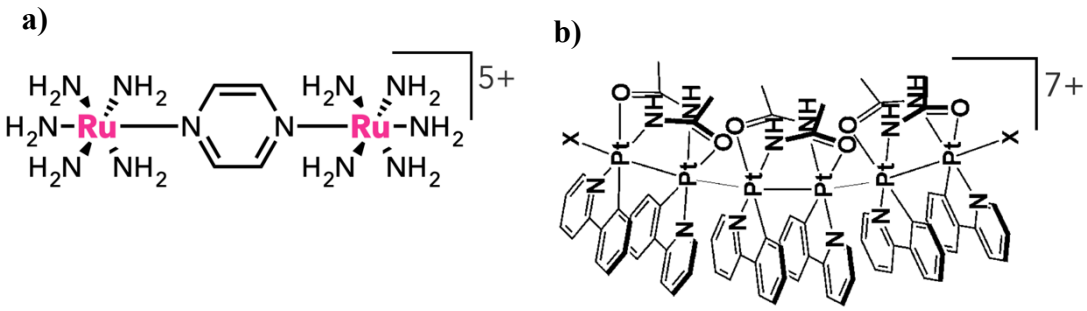

1-5. A dream of molecular electronics

The idea of molecular electronics stems from the theoretical proposal of molecular diode by Aviram and Ratner in 1974.[27] They considered the rectification effects of electrons flowing between electrodes by calculating the molecular orbital of a D-σ-A linked molecule in which TTF and TCNQ are linked by non-conjugating spacer (Figure 4). Although research has been conducted by various researchers by using a single molecule element or a molecular film system with a small number of molecules since this paper published,[28] the development of effective molecular diode has not been realized for 40 years. It is like a so-called "dream" in this research area.

Figure 4 | a) Molecular structure of Aviram and Ratner's molecular diode, and b) current (I)-voltage (V) properties of a theoretical molecular diode.

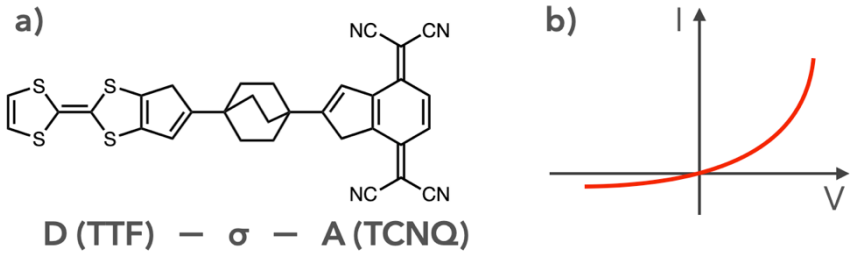

1-6. Molecular design for the PhD study

Based on the above-mentioned background, this PhD thesis has conducted research aiming at the further development of the field of molecular electronics. The author set two point as guidelines for molecular design: they are “using aromatic amines” and “controlling physical properties by structural changes”.

Aniline, which is the simplest structure among aromatic amine compounds, first appeared in 1826 as the very first man-made redox molecule.[29] Also, one-electron oxidized product of *N,N,N′,N′*-tetramethyl-*p*-phenylenediamine (TMPD) has been known as a stable chemical species called Wurster’s Blue radical cation for more than 140 years (Figure 5b).[30] This compound has a dimethylamino group containing a sp^3 nitrogen atom that acts as an electron-donating substituent to stabilize its charge state. As described above, aromatic amine compounds are of great significance historically, but it seems that there are fewer studies on the development of their usefulness compared to TTF and TCNQ.

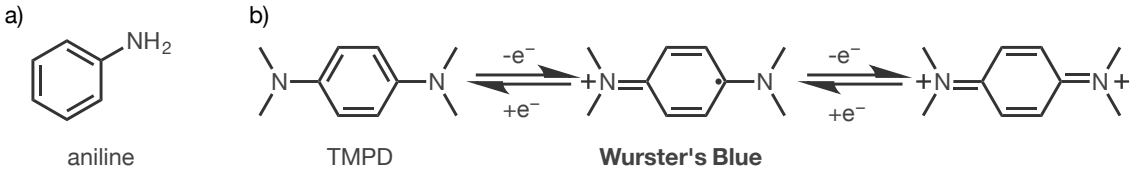

Figure 5 | Molecular structure of **a)** aniline, and **b)** TMPD and its cation radical (Wurster’s Blue).

It can be finally brought out the characteristics of the charged state by stabilizing its cation/anion state. There are several methods for stabilization, and the author focused on the delocalization of charge or unpaired electron by using redox-induced structural changes.

1-7. Content of this thesis

The author has been conducting a series of studies toward development of molecular electronics based on the aromatic amines that can undergo drastic structural change upon electron-transfer to stabilize the charged state.

Beside this introduction (Chapter 1), there are two chapters as follows.

Chapter 2: Selective Creation of Mixed-Valence Oligomers based on π-Expanded Aromatic Diamines

Chapter 3: Development of aromatic amine with molecular film forming ability applicable to molecular diode/junction

Reference

[1] C. W. Tang, S. A. VanSlyke, *Appl. Phys. Lett.* **1987**, *51*, 913–915.

[2] J. R. Sheats, H. Antoniadis, M. Hueschen, W. Leonard, J. Miller, R. Moon, D. Roitman, A. Stocking, *Science* **1996**, *273*, 884–888.

[3] G. M. Farinola, R. Ragni, *Chem. Soc. Rev.* **2011**, *40*, 3467–3482.

[4] R. Ieuji, K. Goushi, C. Adachi, *Nat. Commun.* **2019**, *10*, 5283.

[5] J. U. Kim, I. S. Park, C.-Y. Chan, M. Tanaka, Y. Tsuchiya, H. Nakanotani, C. Adachi, *Nat. Commun.* **2020**, *11*, 1765.

[6] G. Horowitz, *Adv. Mater.* **1998**, *10*, 365–377.

[7] J. Zaumseil, H. Sirringhaus, *Chem. Rev.* **2007**, *107*, 1296–1323.

[8] H. Sirringhaus, *Adv. Mater.* **2014**, *26*, 1319–1335.

[9] J. T. E. Quinn, J. Zhu, X. Li, J. Wang, Y. Li, *J. Mater. Chem.* **2017**, *5*, 8654–8681.

[10] H. Chen, W. Zhang, M. Li, G. He, X. Guo, *Chem. Rev.* **2020**, *120*, 2879–2949.

[11] H. Hoppe, N. S. Sariciftci, *J. Mater. Res.* **2004**, *19*, 1924–1945.

[12] S. Günes, H. Neugebauer, N. S. Sariciftci, *Chem. Rev.* **2007**, *107*, 1324–1338.

[13] J.-L. Brédas, J. E. Norton, J. Cornil, V. Coropceanu, *Acc. Chem. Res.* **2009**, *42*, 1691–1699.

[14] P. Cheng, X. Zhan, *Chem. Soc. Rev.* **2016**, *45*, 2544–2582.

[15] S. Liu, J. Yuan, W. Deng, M. Luo, Y. Xie, Q. Liang, Y. Zou, Z. He, H. Wu, Y. Cao, *Nat. Photonics* **2020**, *14*, 300–305.

[16] J. L. Segura, N. Martín, *Angew. Chem. Int. Ed Engl.* **2001**, *40*, 1372–1409.

[17] H. Prinzbach, H. Berger, A. Lüttringhaus, *Angew. Chem. Int. Ed Engl.* **1965**, *4*, 435–435.

[18] D. S. Acker, W. R. Hertler, *J. Am. Chem. Soc.* **1962**, *84*, 3370–3374.

[19] K. Nakasuji, M. Nakatsuka, I. Murata, *J. Synth. Org. Chem Jpn.* **1983**, *41*, 204–220.

[20] J. Ferraris, D. O. Cowan, V. Walatka, J. H. Perlstein, *J. Am. Chem. Soc.* **1973**, *95*, 948–949.

[21] M. J. Cohen, L. B. Coleman, A. F. Garito, A. J. Heeger, *Physical Review B* **1974**, *10*, 1298–1307.

[22] B. Y. T. J. Kistenmacher, T. E. Phillips, D. O. Cowan, *Acta Cryst.* **1974**, *B30*, 763–768.

[23] D. E. Richardson, H. Taube, *Coord. Chem. Rev.* **1984**, *60*, 107–129.

[24] A. Heckmann, C. Lambert, *Angew. Chem. Int. Ed Engl.* **2012**, *51*, 326–392.

[25] T. Matsumoto, G. N. Newton, T. Shiga, S. Hayami, Y. Matsui, H. Okamoto, R. Kumai, Y. Murakami, H. Oshio, *Nat. Commun.* **2014**, *5*, 3865.

[26] M. Yoshida, N. Yashiro, H. Shitama, A. Kobayashi, M. Kato, *Chem. Eur. J.* **2016**, *22*, 491–495.

[27] A. Aviram, M. A. Ratner, *Chem. Phys. Lett.* **1974**, *29*, 277–283.

[28] M. Iwane, S. Fujii, M. Kiguchi, *Sensors* **2017**, *17*, 956–971.

[29] O. Unverdorben, *Ann. Phys.* **1826**, *84*, 397–410.

[30] C. Wurster, E. Schobig, *Chem. Ber.* **1879**, *12*, 1807–1813.

Chapter 2

Selective creation of mixed-valence oligomers based on π-expanded aromatic diamines

2-1. Mixed-valence of pure organic molecules

As shown in Chapter 1, the mixed-valence states in pure organic compounds are few compared to those in metal-based MV.[1] However, fine-tuning of the MV state could be realized by the proper design of redox-active organic chromophores.[2,3] There are two major methods for developing mixed-valence states in pure organic compounds.

The first one is to use a π-conjugating spacer. The electronic interactions between two redox sites can be modulated by connecting them with a series of π-conjugating spacers, as recently reported for stable carbene-based cation radicals (**I**) (figure 1).[4] Due to the rigid structure of the spacer, MV characteristics can be discussed in detail in terms of dichromophoric cyclophanes[5,6] with a well-defined framework.

On the other hand, there is another type of organic MV state, which is attained through a drastic structural change upon electronic transfer[7] [e.q., bis(dimethoxybenzene) derivative (**II**)[8] with an *o*-xylylene-α,α'-diyl (*o*-xylylene)-type spacer] (Figure 1). Due to the non-conjugating and flexible nature of *o*-xylylene, the neutral state of **II** adopts an extended *anti*-conformation whereas one-electron oxidation causes a geometrical change into a folded *syn*-conformation to maximize the charge-transfer (CT) interaction between the two chromophores with different redox states (0 and +1). Thus, $\mathbf{II}^{+\bullet}$ is an intramolecular pimer with MV characteristics (Scheme 1). The *o*-xylylene spacer also enables the bis(phenothiazine) donor to achieve the MV state upon one-electron oxidation.[9]

Although there have been only a few reported examples of pure organic compounds in this category, their MV states accompanied by a redox-induced geometrical change would enable modification of the MV character by external signals,[10,11] as in the case of stimulus-responsive foldamers[12-15] or calixarenes.[16,17]

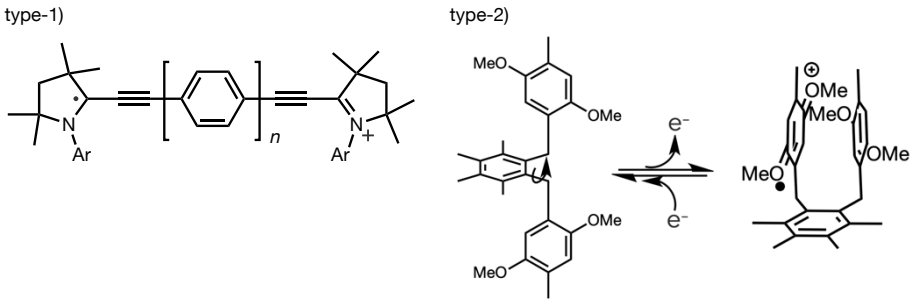

Figure 1 | Molecular structure of type-1) stable carbene-based cation radicals (**I**), and type-2) bis(dimethoxybenzene) derivative (**II**).

In pursing the MV state accompanied by a change in geometry, one of the difficulties is selection of the proper spacer unit, as shown by the fact that *o*-xylynene is not always suitable for pimer formation in dichromophoric systems.[18] For example, π-dimer, not pimer, formation is facilitated by the *o*-xylylene spacer in a bis(paraquat)-type molecule.[19] The resulting π-dimer does not exhibit the MV state. Since both of the redox sites are in a cation-radical state and exhibit radical-pair interaction[20,21] to stabilize the folded geometry.

Thus, its electronic structure is far different from that of the pimer, whose folded geometry is favored by CT interaction and/or by electron exchange. Accordingly, to obtain the MV state selectively for a certain dichromophoric system, it is most important to use the perfect spacer, which facilitates formation of the pimer (0 and +1), but not that of the corresponding π-dimer (+1 and +1).

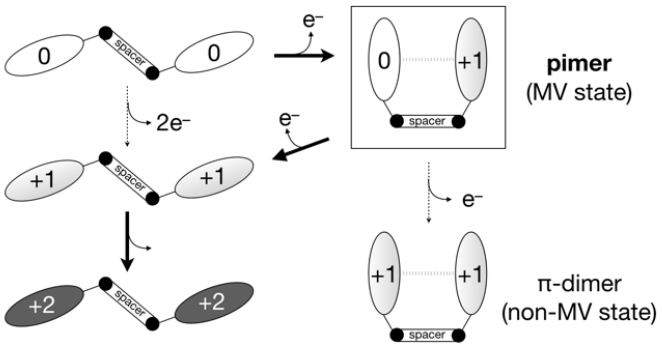

Scheme 1 | Formation of MV state (pimer) through redox-induced geometrical change of dichromophoric systems.

Once the best-matched spacer for a certain dichromophoric systems is determined, the pure organic and long-range MV state would become accessible for the first time in the non-crystalline state by redox reaction of linearly bridged oligomers with multiple organic redox sites connected by the best spacer (Scheme 2a). Through repeated interactions between the neighboring chromophores over the whole oligomeric units, the resulting MV species would adopt a one-dimensional (1D) columnar stack structure, where the spins and charges are delocalized over all of the repeating units. Such species are quite unique in the sense that they can mimic the electronic structure of the crystalline MV state of organic conductors [e.g., TTF-TCNQ or $(TMTSF)_2^{+\bullet}ClO_4^-$].[22, 23]

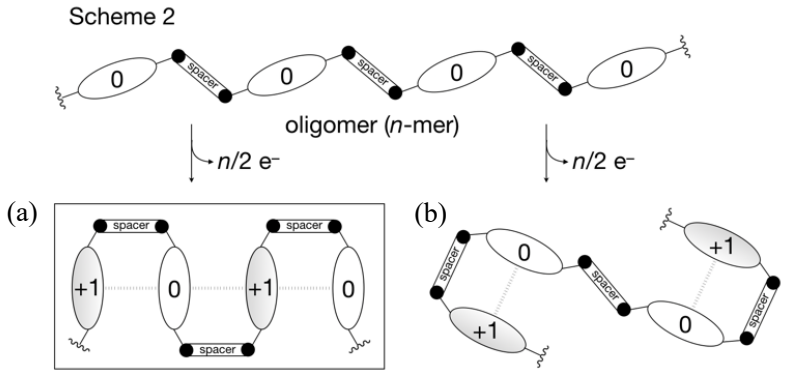

Scheme 2 | (a) Formation of long-range MV state in the half-filled polycations of oligomers through redox-induced geometrical change into a 1D columnar stack. (b) Formation of cluster of pimers in the half-filled polycations of oligomers which cannot form a 1D columnar stack.

2-2. Benzindolocarbazole (BIC)

There are a lot of nitrogen-containing heterocycles and aromatic diamines having redox properties which are responsible for reversible electron transfer. Methyl viologen (MV), which is widely used as a pesticide acting on electron transfer systems, is an electrochromic molecule exhibiting reversible color changes by electrochemical redox. In addition, the cation radical of *N,N,N′,N′*-tetramethyl-*p*-phenylenediamine (TMPD) is a very stable compound, which has been known as "Wruster's Blue cation radical" for over 100 years.

In the research group to which the author belongs, some members have got interested in the multi-output response system with additional function to the common electrochromic response systems. Electrochromic systems are widely used as display and light control material. If the electrochromic molecules are endowed with fluorescence properties in either the neutral or oxidized states, it is possible to impart to the molecule not only color change but also ON/OFF switching property of fluorescence, by using the electrochemical oxidation as an external stimulus.

Phenylenedimamines, which are representative electrochromic molecules as described above, do not emit fluorescence, whereas carbazole derivatives are, in general, known as the molecules with luminescence properties. In this way, the hybrid compound based on phenylenediamine having carbazole skeletons would be promising candidates to exhibit electrochromism with fluorescence switching. In this way, 5,10-dihydrobenzo[*a*]indolo[2,3-*c*]carbazole (**BIC**)[24-28] had been designed, in which three benzene nuclei are attached to 1,4-phenylenediamine moiety (Figure 2).

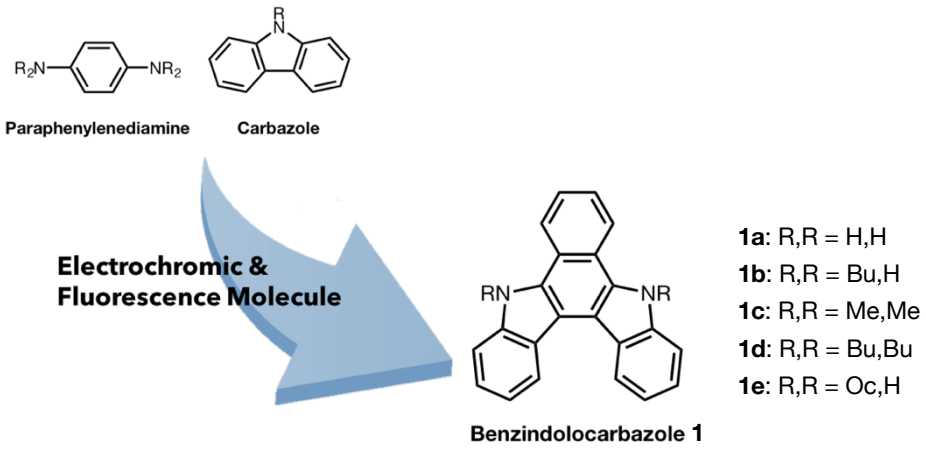

Figure 2 | Molecular design for benziondolocarbazole (BIC).

N,N'-dimethyl derivative of BIC **1c** shows strong absorption bands only in the UV region and shows very high fluorescence quantum yield (Φ_F: 0.71) (Figure 3).

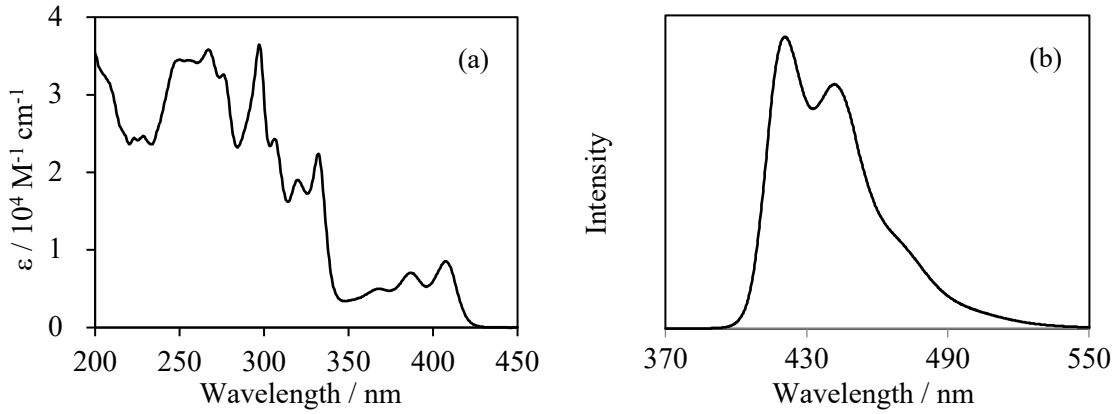

Figure 3 | (a) UV/Vis and (b) fluorescence spectra of 1c measured in MeCN at 298 K.

Upon treatment of **1c** with one equivalent of $(4\text{-}BrC_6H_4)_3N^{+\bullet}X^-$ (X = BF_4 or $SbCl_6$), cation radical salts $\mathbf{1c}^{+\bullet}X^-$ were isolated as stable blue-green solids. By the X-ray crystallography, $\mathbf{1c}^{+\bullet}BF_4^-$ forms a one-dimensional columnar stacked structure. It exhibits a broad absorption band in the NIR region with an absorption tail that extends to λ = 1000 nm, which is assignable to the HOMO–SOMO transition (Figures 4-6).

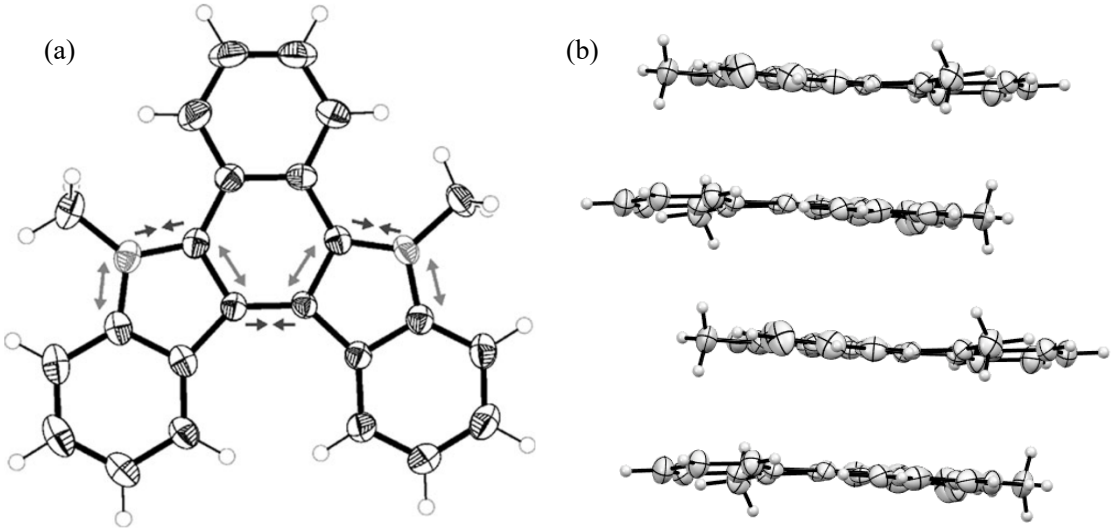

Figure 4 | (a) ORTEP drawing of $\mathbf{1c}^{+\bullet}$ in $\mathbf{1c}^{+\bullet}BF_4^-$ salt as determined from X-ray structural analysis at 123 K. (b) Packing structure of $\mathbf{1c}^{+\bullet}BF_4^-$.

The electrochromic behavior of **1c** was demonstrated by the UV/Vis/NIR spectral changes upon oxidation. At the same time a continuous decrease in emission intensity was observed, which demonstrated dual electrochromic behavior.

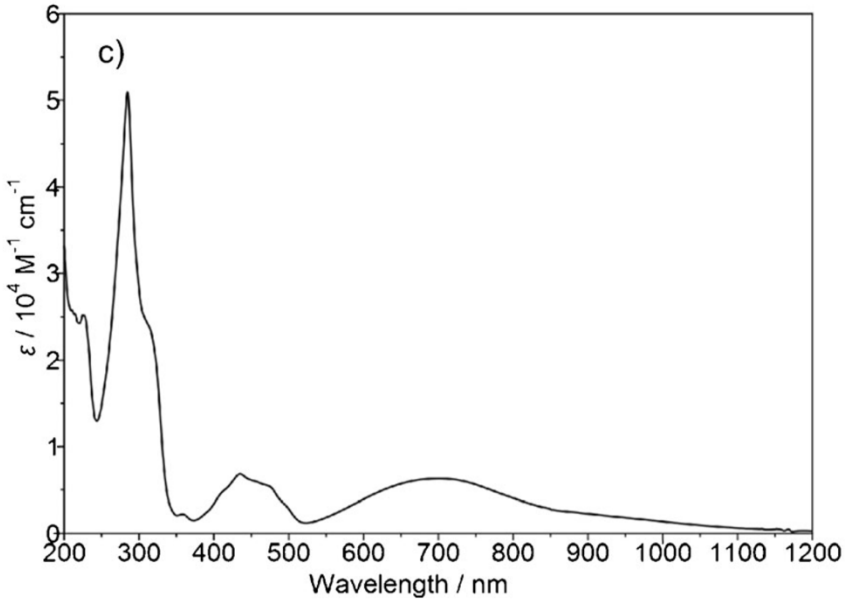

Figure 5 | UV/Vis/NIR spectrum of $\mathbf{1c}^{+\bullet}BF_4^-$ measured in MeCN.

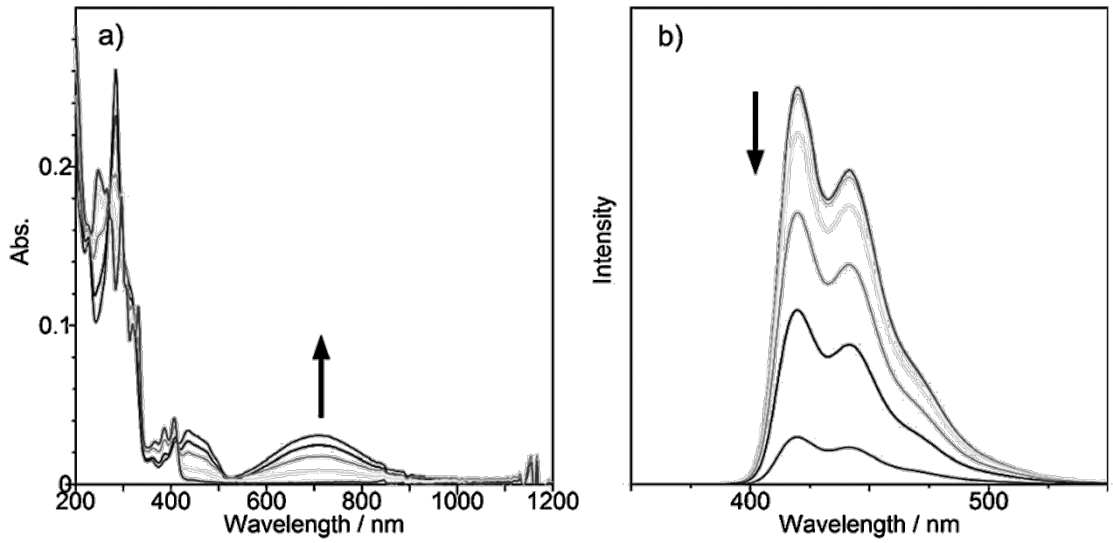

Figure 6 | Continuous changes in (a) UV/Vis/NIR and (b) fluorescence spectra upon constant current electrochemical oxidation of **1c** (20 μA, every 2 min) in MeCN that contained 0.05 M Et_4NClO_4 as the electrolyte.

2-3. Molecular design for MV-oligomers

To stabilize the polycationic state of the oligomers,[29-34] BIC is selected as a monomer unit in this study, which is a 1,4-phenylenediamine analogue that undergoes two-stage one-electron oxidation. As shown in the previous section, similar to other condensed π-systems,[35-39] the large disk-shaped skeleton of BIC would be suitable for the formation of π-stacked structures, which was actually observed in its cation radical salt. The spacer should be connected at the N atoms of BIC, so that it can induce close contact between the atoms with large orbital coefficients in the HOMO.[25]

It should be noted that, the BIC dimers and oligomers also have an advantage in achievement of the structural change with the formation of a folded structure in the oxidized state, which could be isolated stable entities. In the dimers, a neutral unfolded structure changes into a folded structure upon partial oxidation and the further changes back into an unfolded structure upon further oxidation as shown in scheme 3.

Scheme 3 | Redox scheme for dimeric BIC.

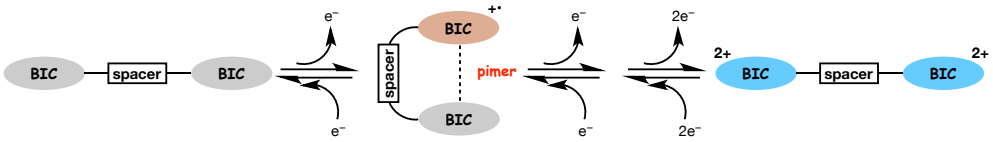

Based on the above consideration, the author decided to start the research by determining the best spacer that favors the formation of oligomers pimer by screening spacer structures. After that, the author prepared a series of BIC up to hexamer using the selected spacer to propose the novel method for creating +*n*/2 valence state, which is a mixed -valence state, selectively.

First of all, the author started the studies on the dimers consisting of two units of BIC and designed a series of molecules with some non-conjugating spacer. Their redox behavior is altered depending on the spacer or the number of units, as investigated by voltammetric analyses, the spectrum changes upon constant current oxidation, and X-

ray crystallography. Upon oxidation of BIC unit, not only NIR-region absorption but also strong fluorescent would be changed, which makes it possible to investigate the conformational change in oxidized state by the modified change in fluorescence emission as well as the NIR absorption.

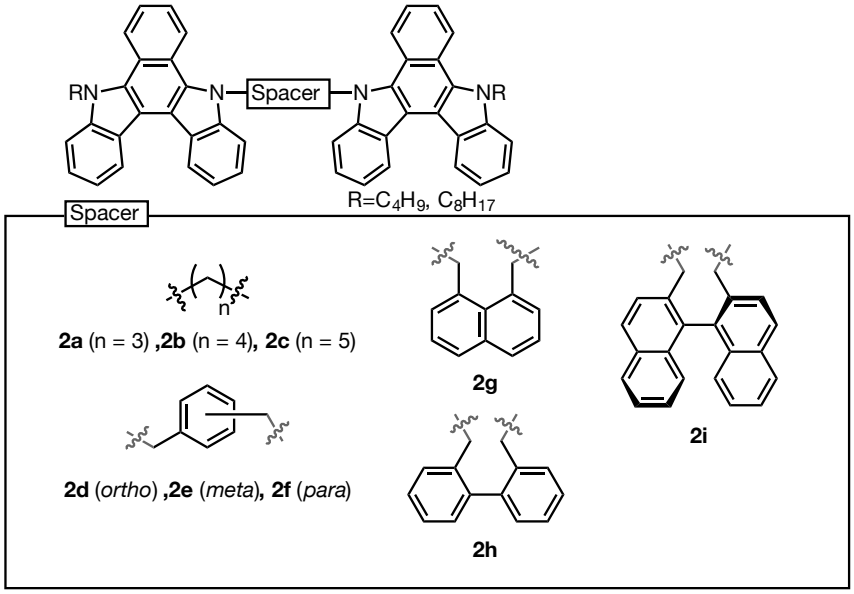

Figure 7 | Twin-BIC donors **2a**-**2i** with an alkylene, a xylylene or an arylenedimethylene spacer designed in this work.

Additionally, the choice of spacer plays a very important role for the structural switching from the unfolded to the folded form. It was shown, by the study on the dimer consisting of methyl viologen or dimethoxybenzene as chromophores, that a trimethylene (n = 3) chain or an *o*-xylylene spacer is suitable for the geometrical switching between the unfolded and folded forms, and these spacer have been widely used for the molecular design of other systems. However, the author have a unique hypothesis, that is “the effective spacer should be changed depending on the kind of redox chromophores”, so in chapter 2, the author began his study with preparation of a series of dimers with nine kinds of different spacer, whose redox properties are investigated in detail.

2-4. Preparation of BIC dimers with an alkylene chain (n = 3, 4, 5)

The twin-BIC donors with an alkylene chain (n = 3, 4, 5) would be obtained by the reaction of mono-alkylated-BIC with α,ω-dibromoalkane. The preliminary study showed that the dimers of mono-methylated-BIC are less soluble in common organic solvents, and the introduction of a longer chain on nitrogen atom is favored. So, the author firstly prepared the monobutylated-BIC according to the previously reported synthesis method on mono-methylated-BIC (**1f**).[25]

Thus, using 2-bromoacetophenone and phenylhydrazine as starting materials, 2-(2'-bromophenyl) indole **9** was obtained by Fischer indole synthesis. 2-(2'-Ethynylphenyl) indole **11** was prepared by a Sonogashira cross-coupling of **9** and ethynyltrimethylsilane, followed by desilylation. The second Sonogashira coupling of **11** with 2-iodophenyl-azide gave **12**. Hydroarylation of **12** proceeded smoothly upon treatment with JohnPhos-AuNTf$_2$ in dichloromethane to give **13**.

Scheme 4 | Preparation of benzocarbazole **13**, which is a common intermediate for BIC units.

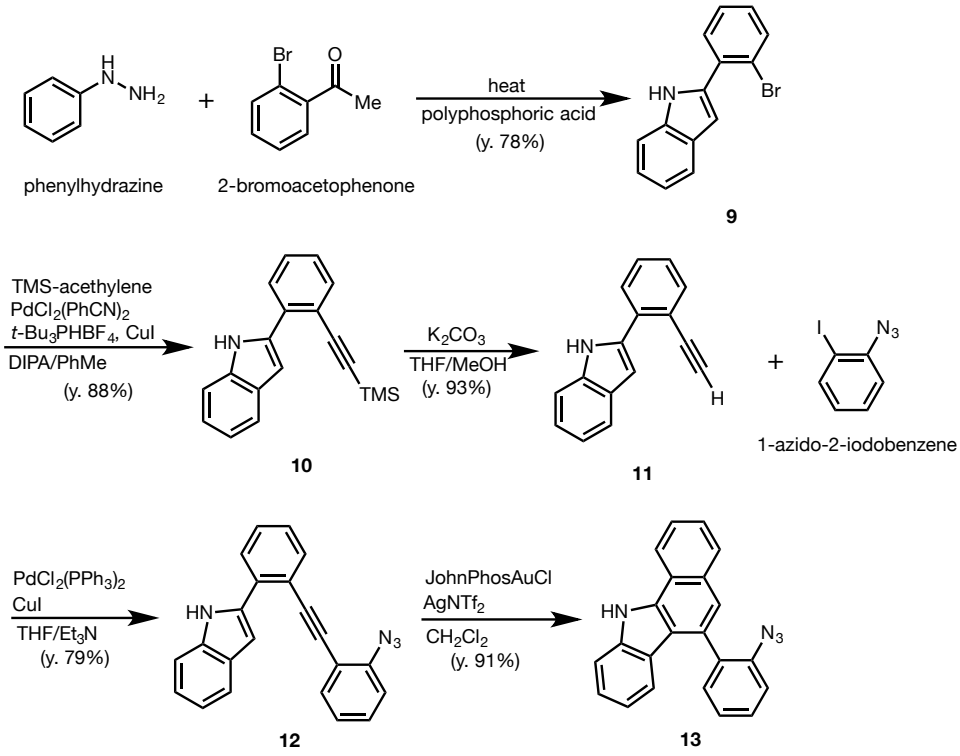

N-butyl derivative **14b** was obtained upon treatment of **13** with NaH and 1-bromobutane in DMF. Exposure of **14b** to the nitrene insertion conditions at 160 °C in 1,2-dichlorobenzene provided monobutylated-BIC **1b**.

Scheme 5 | Preparation of mono-butylated-BIC **1b**.

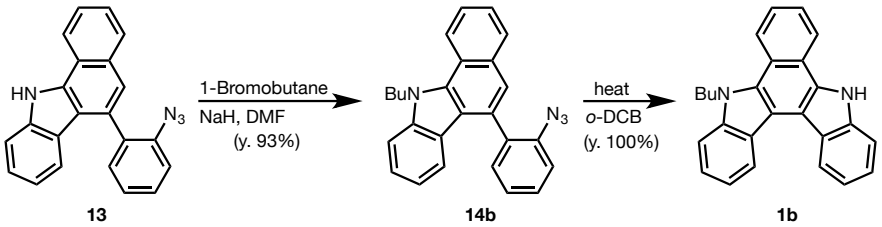

By the reaction with NaH followed by 1,3-dibromopropane, 1,4-dibromobutane or 1,5-dibromo pentane in DMF, the desired twin-BIC donors **2a** (*n* = 3, y. 17%), **2b** (*n* = 4, y. 72%), and **2c** (*n* = 5, y. 84%) were prepared as pale yellow crystals. The low yield of **2a** is due to the by-production of *N*-allylated compound by competing of E2 reaction with S_N2 reaction.

Scheme 6 | Preparation of twin-BIC donors **2a**-**2c** with a trimethylene (n = 3), tetramethylene (n = 4), or pentamethylene (n = 5) chain.

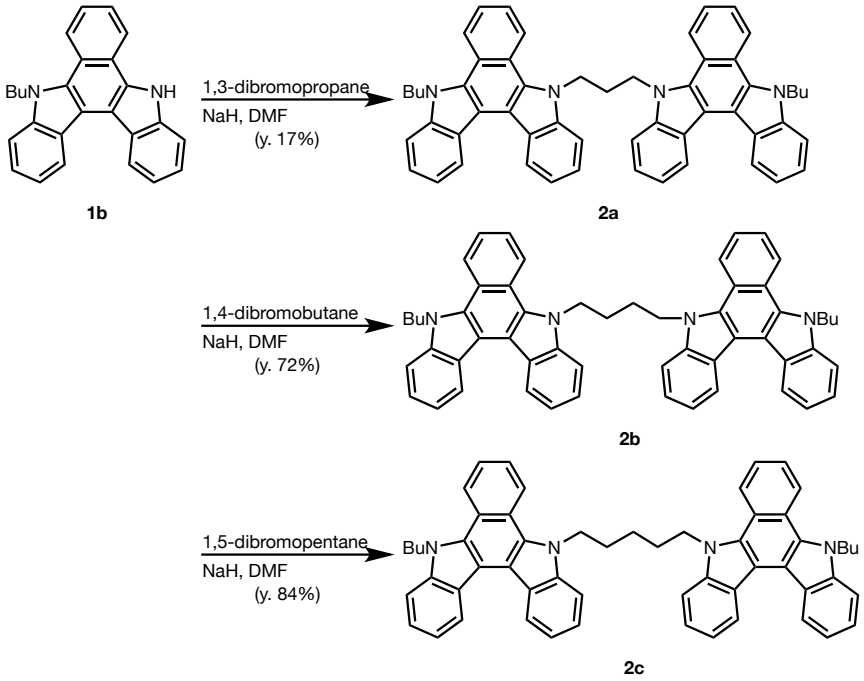

2-5. UV-Vis and fluorescence spectra of 2a, 2b, 2c

The UV-Vis absorption spectra of the dimers with a trimethylene (**2a**, n = 3), tetramethylene (**2b**, n = 4), and pentamethylene (**2c**, n = 5) measured in 1,1,2-trichloroethane show strong absorption bands which are very close to that of monomeric BIC (**1f**) measured under the similar conditions (Figure 8). Also, their fluorescence spectra resemble to the monomeric BIC, and excimer emission in the long wavelength region is not observed. Therefore, the twin-BIC donors with an alkylene chain have the similar electronic structure with the monomeric di-alkylated-BIC (**1c**), and it is assumed that each of these dimers mainly adopts the unfolded form at the neutral state.

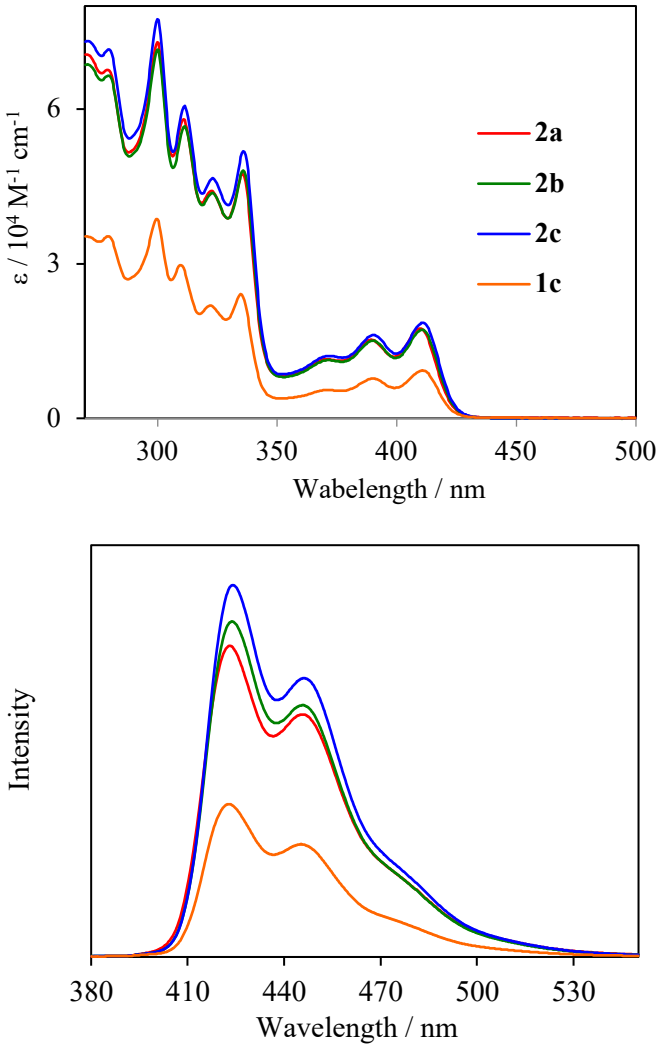

Figure 8 | (a) UV/Vis and (b) fluorescence spectra of **2a**-**2c** and **1c** measured in 1,1,2-trichloroethane.

2-6. Cyclic and differential pulse voltammograms of 2a, 2b, 2c

In the voltammogram of dimethylated-BIC (**1c**) measured in dichloromethane, there are two major peaks. The first wave corresponds to the process, in which BIC is oxidized to the cation radical. The second wave corresponds to the oxidation process to give the closed shell dication. Figure 9 shows the voltammograms of the twin-BIC donors **2a**, **2b**, **2c** measured in 1,1,2,2-tetrachloroethane. In this measurement, characteristic properties depending on the length of the alkylene chain were found.

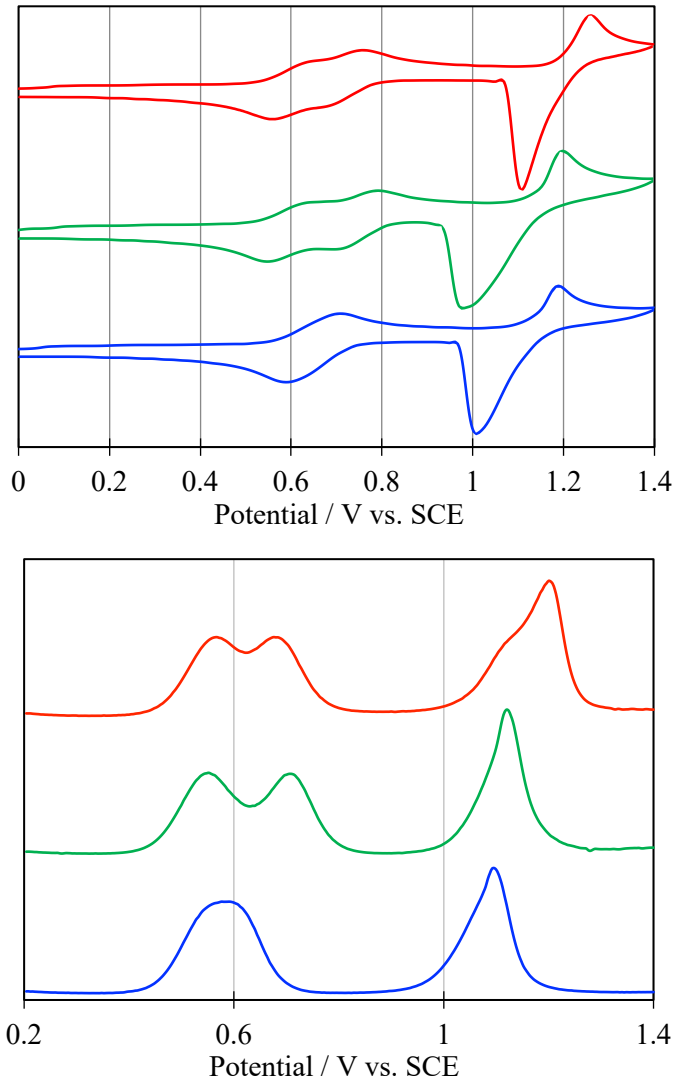

Figure 9 | **(a)** Cyclic and **(b)** differential pulse voltammograms of **2a**-**2c** measured in 1,1,2,2-tetrachloroethane (0.1 M Bu_4NPF_6, *E*/V vs. SCE, Pt electrode, 100 mVs^{-1}).

Table 1 | Oxidation potentials of **2a**-**2c**.

sample	E1	E2	E3 = E4
2a	+ 0.62	+ 0.76	+ 1.26 (2e)
2b	+ 0.61	+ 0.79	+ 1.20 (2e)
2c	+ 0.71 (2e)		+ 1.19 (2e)

Twin donors **2c** with the pentamethylene chain (n = 5) undergoes two-stage two-electron oxidation. The oxidation potentials are very close to those of monomeric BIC measured under the similar conditions. Thus, the two electrophores in **2c** are oxidized independently, showing that its dication diradical and tetracationic species adopt the extended form. In contrast, stepwise one-electron oxidation into the corresponding cation radical and dication diradical was observed for the twin donor **2a** with the trimethylene chain (n = 3), showing that the cation radical of **2a** is the pimer with the stacked geometry where the two electrophores are interacting through the π-π overlap. The next oxidation peak of **2a** is shifted to the anode compared to the corresponding peak in **2c** and **1c**, showing that dication diradical of **2a** also adopts the stacked form (π-dimer) to encumber further oxidation. The one-wave two-electron oxidation at the third/fourth potential indicated that the tricationic/tetracationic species of **2a** prefer the extended geometry due to the increased Coulombic repulsion(Table 1). The chain-length dependency shown above is consistent with the redox properties of the precedential twinned electrophores: the "n = 3 rule"[40] is often valid as in the present study, and the longer chain is less suitable for the π-π stacking.

In this connection the behavior of twin donor **2b** (n = 4) is interesting. It shows stepwise one-electron oxidation processes into the corresponding cation radical and dication diradical, whereas the next oxidation potential is not anodically shifted, suggesting that cation radical of **2b** is the pimer with the stacked geometry, whereas dication diradical of **2b** adopts the extended form as in its neutral/tricationic/tetra-cationic species. These considerations are strongly supported by the results of the spectral changes upon constant-current oxidation of these dimers(Scheme 7).[41]

Scheme 7 | Redox schemes of twin BIC-donors **2a**–**2c** showing the predominant/major conformer at each redox state. The species in the bracket have negligible steady-state concentration under the voltammetric conditions.

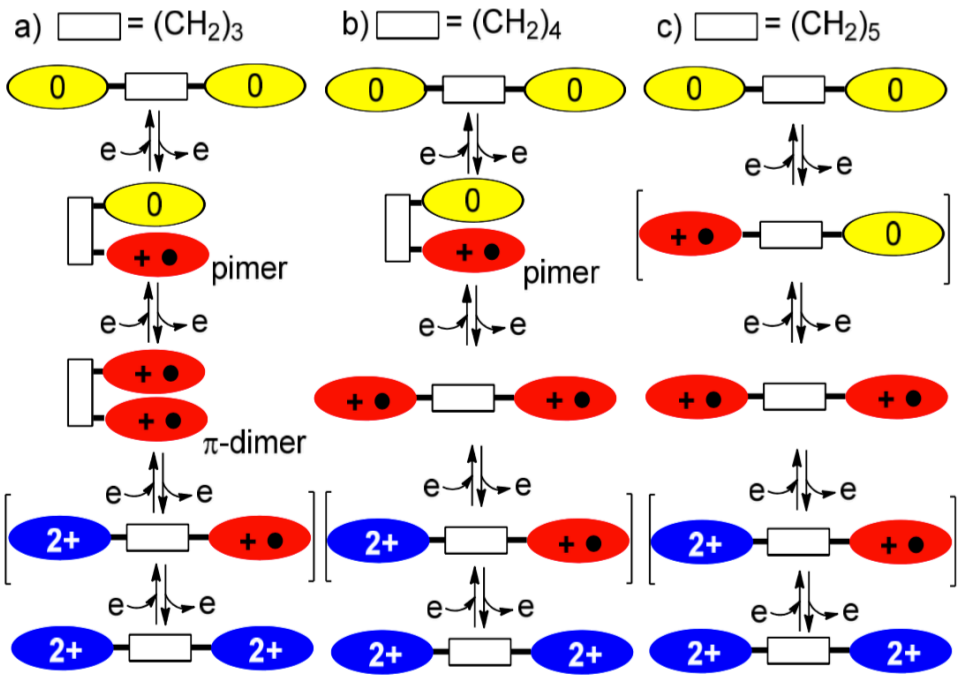

2-7. Spectroelectrograms of 2a, 2b, 2c

The electrochromic systems that exhibit drastic changes in the NIR absorption are rare but attracting recent attention. As shown in Figures 10-12, the twin-BIC donors **2a**, **2b**, **2c** work as electrochromic materials that exhibit changes in the UV-Vis-NIR region, as in the cases of monomeric BIC. It is well known that the pimers and π-dimers exhibit the absorption in the further longer-wavelength region, in addition to those of unstacked cation radicals. So that, new bands would be appeared upon electrochemical oxidation of **2a** and **2b**. In fact, along with the absorption at 750 nm which is in common with the cation radical of monomeric BIC, a new absorption shoulder around 800 nm appeared during the oxidation of **2a**, which is absent in the cation radical of **1c** measured under the similar conditions. This peak is attributed to the pimer with the stacked geometry, and similar behavior was also observed upon electrolysis of the dimer **2b** with a tetramethylene chain (*n* =4). As the electrochemical oxidation of **2a** was further continued, a new absorption band near 1100 nm was observed, which is attributable to the π-dimer with the stacked dication diradical. In this way, the author succeeded in observing the absorption bands characteristic to the pimer and the π-dimer of BIC.

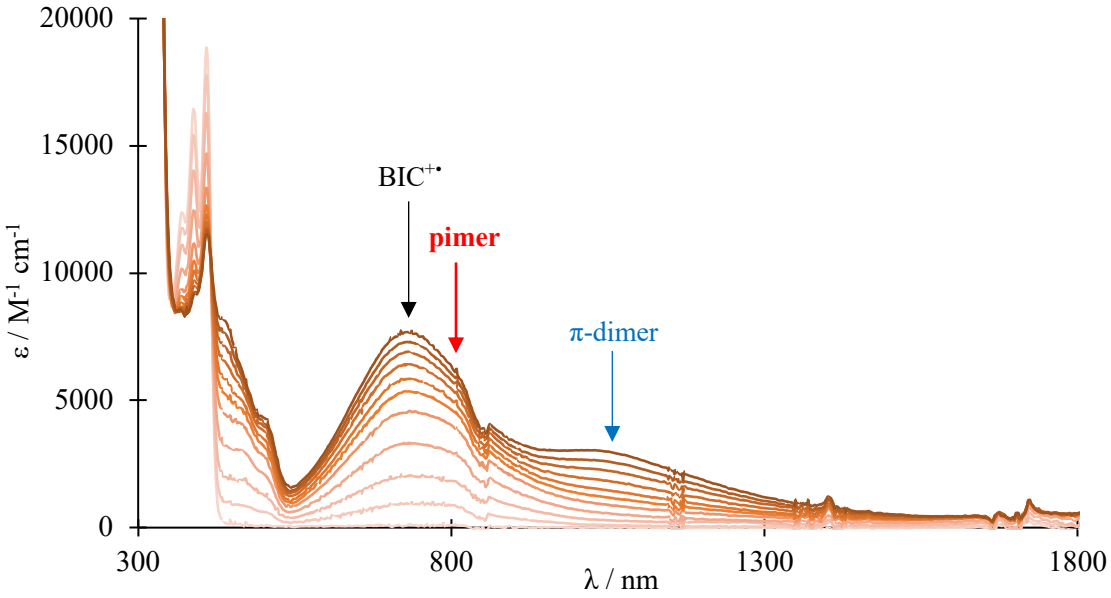

Figure 10 | A continuous change in UV/Vis/NIR spectrum upon constant current electrochemical oxidation of **2a** (20 μA, every 8 min) in 1,1,2-trichloroethane that contained 0.05 M Bu_4NPF_6 as the electrolyte.

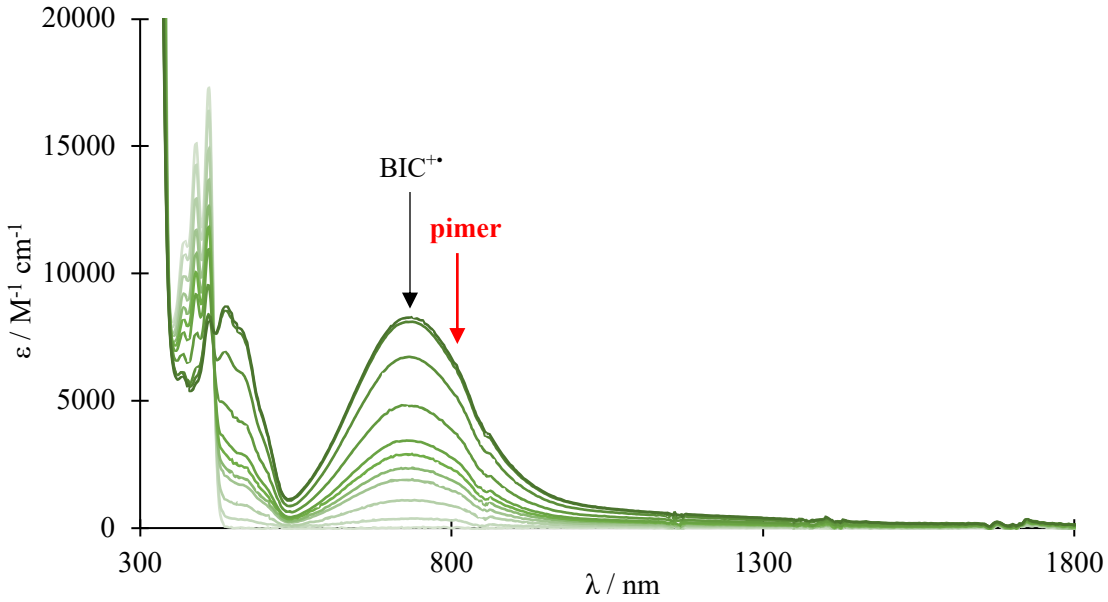

Figure 11 | A continuous change in UV/Vis/NIR spectrum upon constant current electrochemical oxidation of **2b** (20 μA, every 8 min) in 1,1,2-trichloroethane that contained 0.05 M Bu_4NPF_6 as the electrolyte.

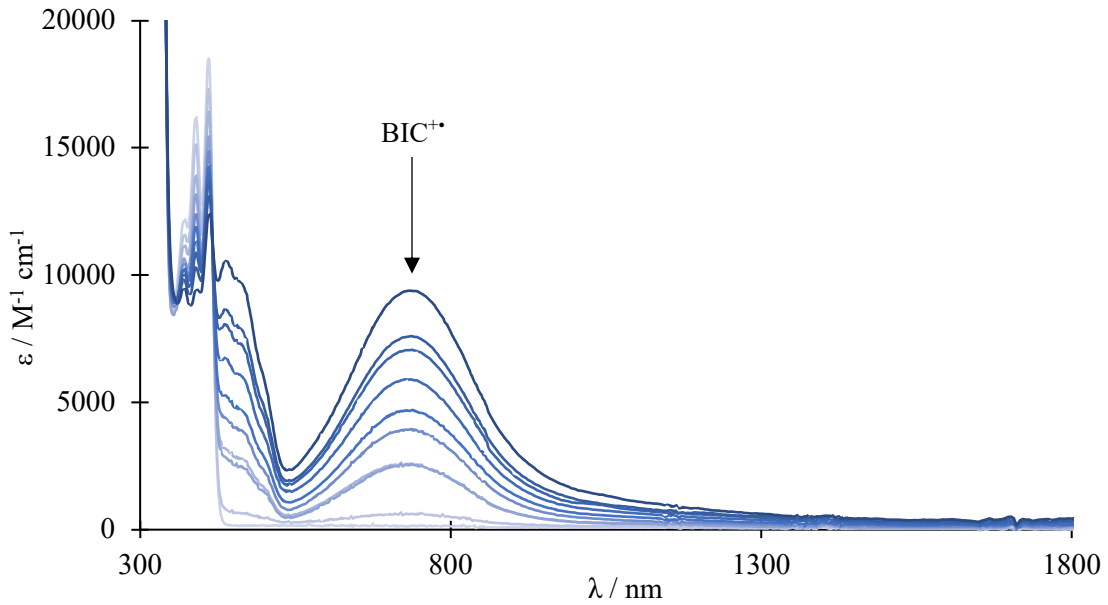

Figure 12 | A continuous change in UV/Vis/NIR spectrum upon constant current electrochemical oxidation of **2c** (20 μA, every 8 min) in 1,1,2-trichloroethane that contained 0.05 M Bu_4NPF_6 as the electrolyte.

2-8. Preparation of BIC dimers with a xylylene spacer (*o*-, *m*-, *p*-)

Based on the study on twin-BIC donors with an alkylene chain, investigations on the dimers were continued by designing other dimers with a xylylene spacer which has more rigid spatial configuration. By the reaction of the monobutylated-BIC with NaH, followed by *o*-, *m*- or *p*-xylylene dibromide in DMF, the desired BIC-dimers **2d**, **2e** and **2f** were prepared in good to high yields.

Scheme 8 | Preparation of twin-BIC donors **2d**-**2f** with an *o*-, *m*-, or *p*-xylylene spacer.

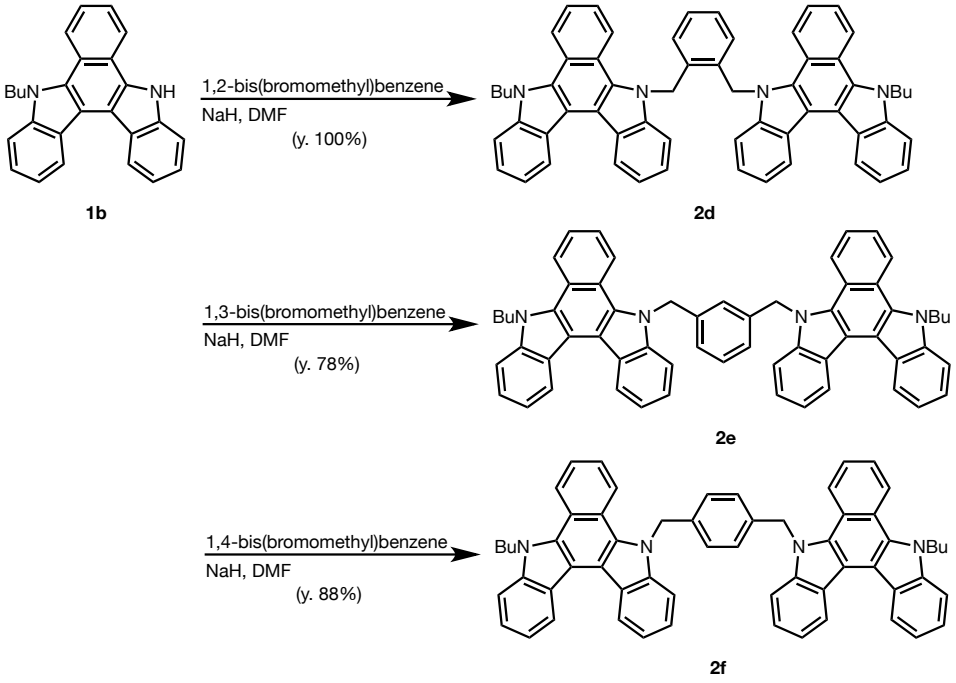

In terms of improving solubility, the dimers with an *o*-xylylene and *m*-xylylene spacer were also prepared having two units of mono-octylated-BIC. *N*-octyl derivatives **10b** was obtained upon treatment of benzocarbazole **9** with NaH and 1-bromooctane in DMF. Exposure of **10b** to the nitrene insertion conditions at 160 °C in 1,2-dichloro-bezene provided monooctylated-BIC **1b**. Using the similar conditions to those for preparation of di-butylated-dimers, the twin-BIC donors **2d'** and **2e'** were obtained.

Scheme 9 | Preparation of mono-octylated-BIC **1b**.

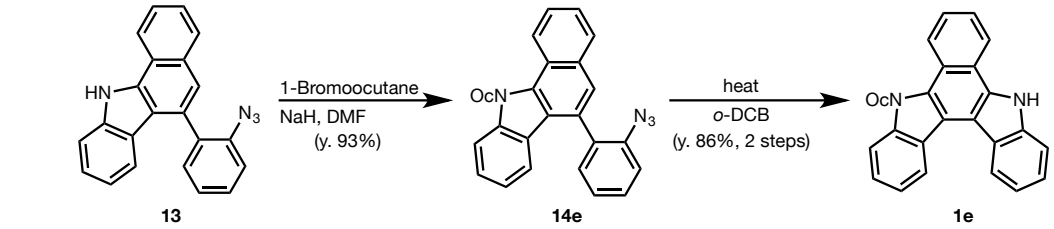

Scheme 10 | Preparation of twin-BIC donors **2d'** and **2e'** with an *o*- or *m*-xylylene spacer.

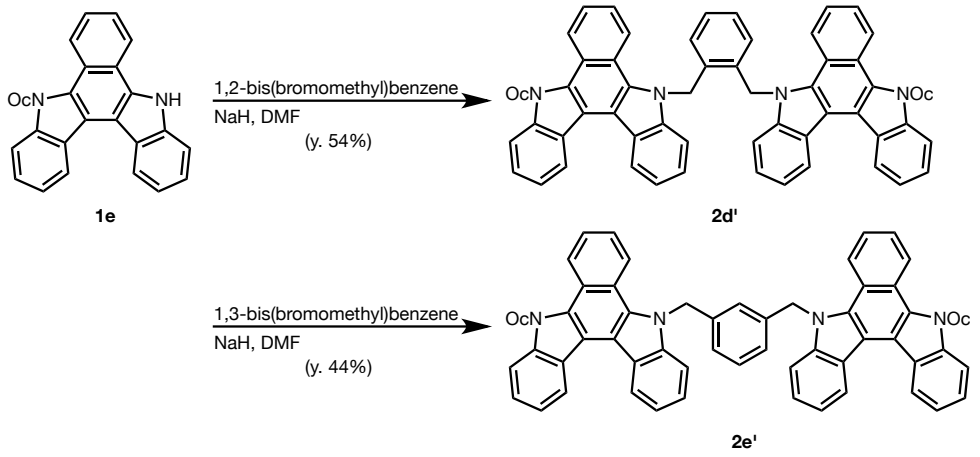

2-9. Cyclic and differential pulse voltammograms of 2d, 2e, 2f

According to the voltammetric analyses in 1,1,2,2-tetrachlorothenae, **2d** with an *o*-xylylene spacer undergoes two-stage two-electron oxidation as in monomeric BIC **1c**. This is in sharp contrast to the precedential twin donors with the same spacer, which form pimers (stacked cation radicals) and π-dimers (stacked dication diradicals). Thus, the disk-shaped π-system of BIC is too large to adopt the stacked form when connected by an *o*-xylylene spacer. On the contrary, the voltammogram of **2e** with a *m*-xylylene unit are nearly identical to that of **2b** (n = 4), showing that cation radical of **2e** is the pimer with the stacked geometry.

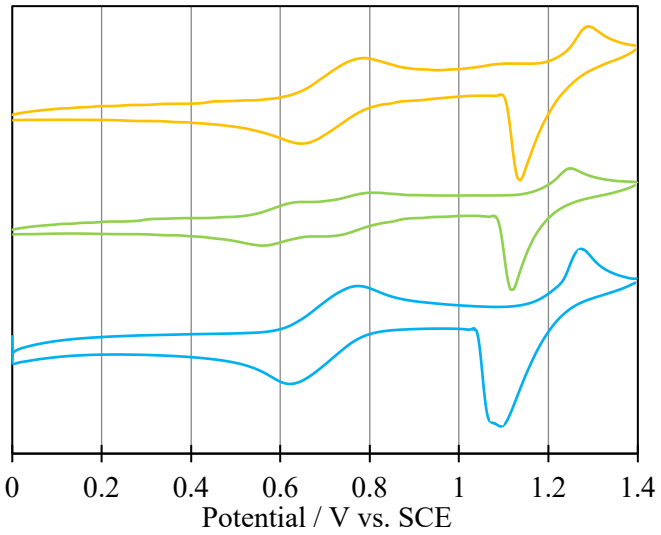

Figure 13 | Cyclic voltammograms of **2d**–**2f** measured in 1,1,2,2-tetrachloroethane (0.1 M Bu_4NPF_6, E/V vs. SCE, Pt electrode, 100 mVs^{-1}).

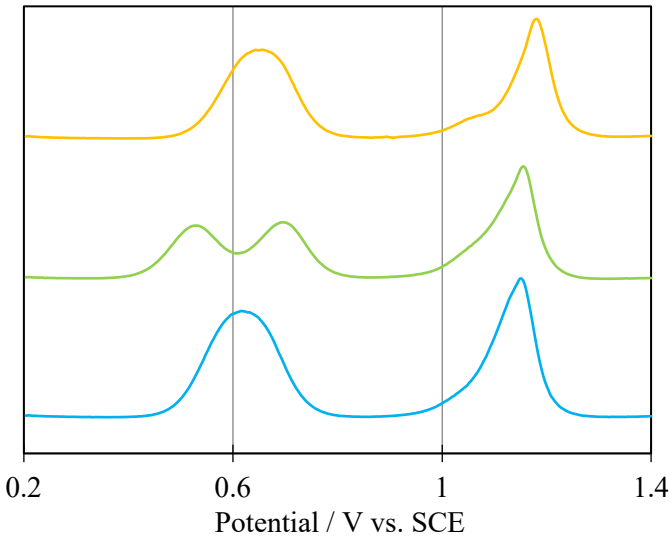

Figure 14 | Differential pulse voltammograms of **2d**–**2f** measured in 1,1,2,2-tetrachloroethane (0.1 M Bu_4NPF_6, E/V vs. SCE, Pt electrode, 100 mVs^{-1}).

This finding is quite unique for the BIC electrophores because there have been no reports that show superior π-π stacking of the *m*-xylylene-bridged electrophores compared to the corresponding *o*-xylylene-bridged counterparts. The large π-system of BIC would enable to realize partial but enough π-π overlap even though the two electrophores are arranged at a certain distance. In this way, the present work has revealed that the suitable spacer for the effective π-π overlap differs depending on the electrophores according to their bulkiness and the π-area to be overlapped. As expected, **2f** with a *p*-xylylene spacer behave similarly to monomer BIC **1c**.

The twin-BIC donors **2d'** and **2e'** with two octyl groups showed the identical redox behavior to those of **2d** and **2e**, respectively. They are more suitable for spectroscopic measurements due to higher solubility and were used to obtain spectroelectrograms as shown in the next section.

2-10. Spectroelectrograms of 2d' and 2e'

Figure 15 shows the tracking the spectral changes upon constant current oxidation of the twin-BIC donors **2d'** and **2e'** measured in 1,1,2-trichloroethane. The dimer **2d'** with an *o*-xylylene spacer exhibits essentially the same behavior to **2c** (n = 5) or monomeric BIC, whereas the dimer **2e'** with a *m*-xylylene spacer shows the absorption shoulder which is also observed for the dimers **2a** and **2b**. This shoulder could be attributed to the pimer formation with the stacked form, so the spectroelectrograms also supported the consideration that the cation radical of **2e'** adopts a stacked geometry. The absorption band at 1100 nm characteristic to π-dimer formation, which appeared upon electrolysis of the dimer **2a** with a trimethylene chain, was not observed upon electrolysis of **2e'**, so it is shown that **2e'** can form a pimer in the cation radical state but cannot form the π-dimer in the dication diradical state.

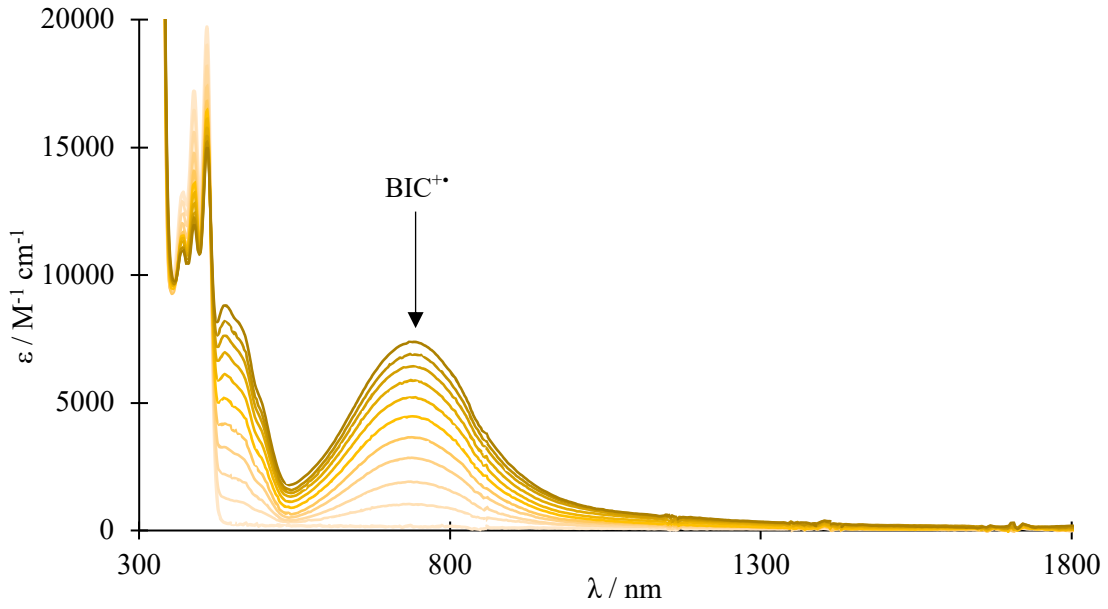

Figure 15 | A continuous change in UV/Vis/NIR spectrum upon constant current electrochemical oxidation of **2d'** (20 μA, every 8 min) in 1,1,2-trichloroethane that contained 0.05 M Bu_4NPF_6 as the electrolyte.

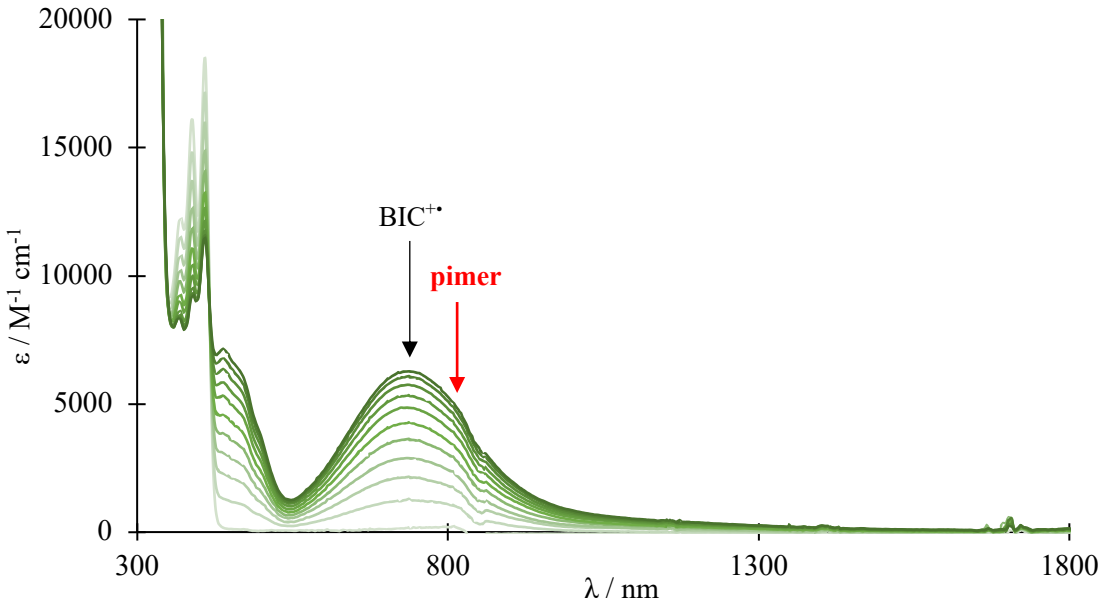

Figure 16 | A continuous change in UV/Vis/NIR spectrum upon constant current electrochemical oxidation of **2e'** (20 μA, every 8 min) in 1,1,2-trichloroethane that contained 0.05 M Bu_4NPF_6 as the electrolyte.

2-11. Preparation of BIC dimers with another aromatic spacer

To further investigate the effectiveness of a spacer for the formation of a folded structure in the oxidized states, three twin-BIC donors with a (naphthalene-1,8-diyl)bis(methylene) spacer (**2i**), (biphenyl-2,2'-diyl)bis(methylene) (**2g**), and (1,1'-binaphthyl-2,2'-diyl)bis(methylene) (**2h**) were designed and prepared. By the reaction of **1b** with NaH followed by the corresponding spacer in DMF, the desired dimers **2g**, **2h** and **2i** were obtained.

Scheme 11 | Preparation of twin-BIC donors **2g**-**2i** with an arylene spacer.

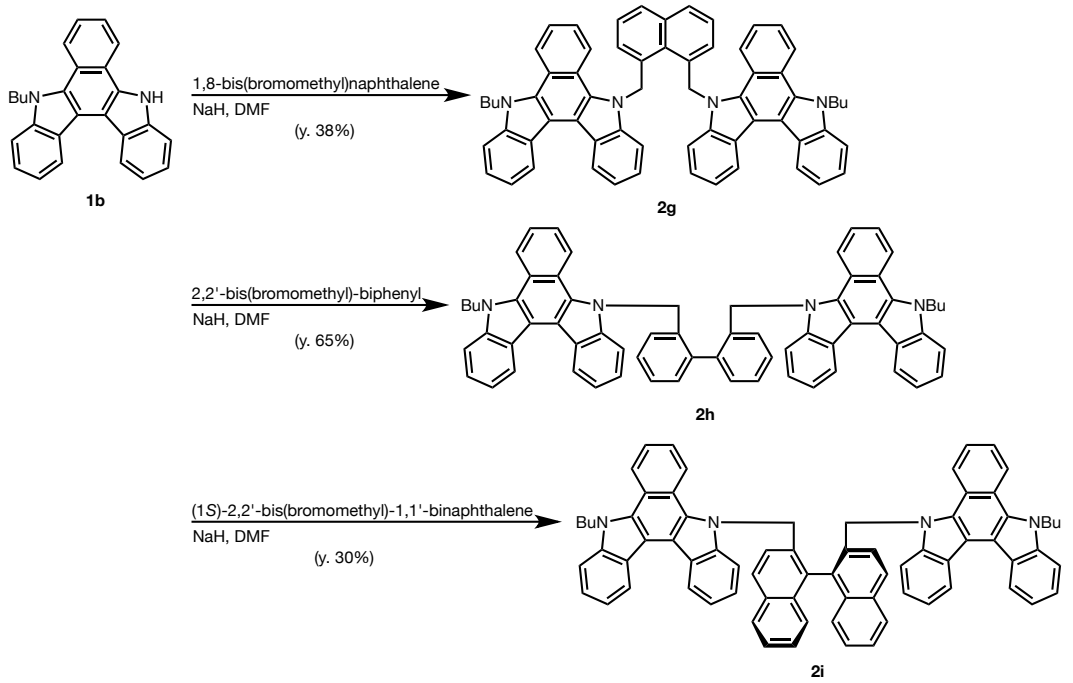

2-12. Cyclic and differential pulse voltammograms of 2g, 2h, 2i

According to the voltammetric analyses, all of the three compounds gave the similar voltammograms as monomeric BIC **1c** or pentamethylene compound **2c**, showing that the two units of BIC in **2g**, **2h** and **2i** are not interacting to each other in the cation radical state or in the dication diradical state, and so that there are almost no signs that suggest geometrical change of the unfolded structure.

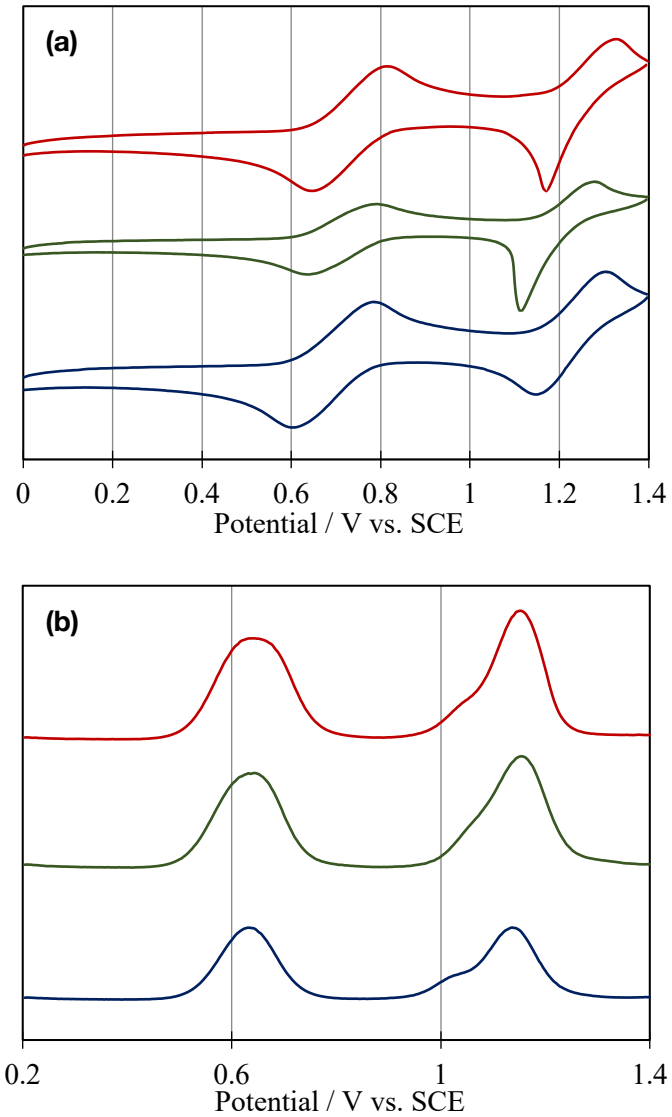

Figure 17 | (a) Cyclic and (b) differential pulse voltammograms of **2g**–**2i** measured in 1,1,2,2-tetrachloroethane (0.1 M Bu_4NPF_6, E/V vs. SCE, Pt electrode, 100 mVs^{-1}**).**

2-13. Consideration on the distance between the connecting sites

To investigate the relationship between the distance between the connecting sites of the spacer for the two BIC units and the stacked-geometry formation, the author calculated the distance between two methyl groups of *o*-, *m*-, *p*-xylene and 1,8-dimethylnaphthalene by density functional theory (DFT) calculation (B3LYP/6-31G*). It is suggested that certain distance between two BIC electrophores is required. The appropriate stacking distance (ca. 3.4 Å) is determined on the balance of attracting force and the Coulombic repulsion between the two units. To realize the ideal stacking geometry without severe angle/torsional strain the distance between the connecting sites is the important factor. The distance for the two methyl groups of *m*-xylene is 5.06 Å, which is approximately 2 Å larger than that of *o*-xylene. In addition, the distance of 1,8-dimethylnaphthalene is 2.98 Å, which is the same value to that of *o*-xylene. The fact that only *m*-xylene unit is favored among these four, the distance for the connecting sites should be around 5 Å for the BIC dimers.

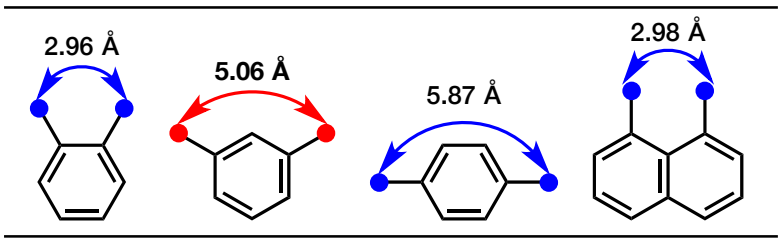

Figure 18 | The distance between the connecting sites of the spacer for the two BIC chromophores.

2-14. Pimer formation of *m*-xylylene-bridged BIC

It is interesting that the twin-BIC donors exhibit different preference from other twin-type redox systems in term of the isomeric xylylene spacers. In the bis(paraquat) systems, the one with an *o*-xylylene spacer forms stacked pimer upon one-electron reduction whereas the corresponding *m*-isomer does not. This is in line with the bis(dimethoxytoluene)-type electron donor.[8] In contrast, twin-BIC donors with a *m*-xylylene spacer forms pimer with the stacked geometry, but the dimer with an *o*-xylylene spacer does not. When the two X-ray structures of the pimers were compared, the author found the key difference that can account for the different preference of xylylene spacer as postulated below.

In the case of the dimer with a dimethoxytoluene unit, the dihedral angle of C_1-C_2-C_3-C_4 is 90°. Thus, the two chromophores are stacked in a head-to-head fusion as shown in Figure 20a. In contrast, BIC dimer cannot form the conformation in which the dihedral angle of C_1-C_2-C_3-N = 90 ° because the steric hindrance occurs between the annulated benzo- moiety in BIC and the benzene moiety in xylylene spacer. So that, BIC dimer with a *m*-xylylene spacer forms the conformation in which the dihedral angle of C_1-C_2-C_3-N = 180 °, and thus the two BIC units are stacked in a head-to-tail manner.

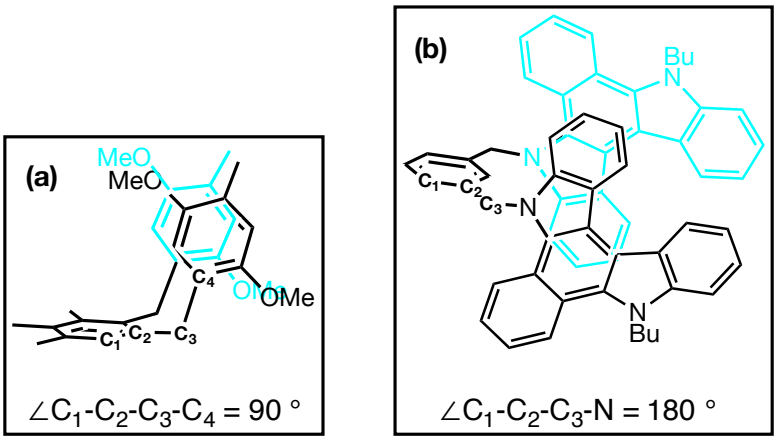

Figure 19 | The torsion angle of **(a)** C_1-C_2-C_3-C_4 for the dimer with a dimethoxytoluene units and **(b)** C_1-C_2-C_3-N for the dimer with two units of BIC.

In this conformation, with the angle of C_2-C_3-N of 109 °, the ideal value for sp^3 carbon, the two units of BIC are stacked to each other with an effective overlap of the large pi-face. When the BIC dimer with an *o*-xylylene spacer adopts the similar conformation, the angle of C_2-C_3-N should be widened to 145°, and such a large angular distortion is unfavored.

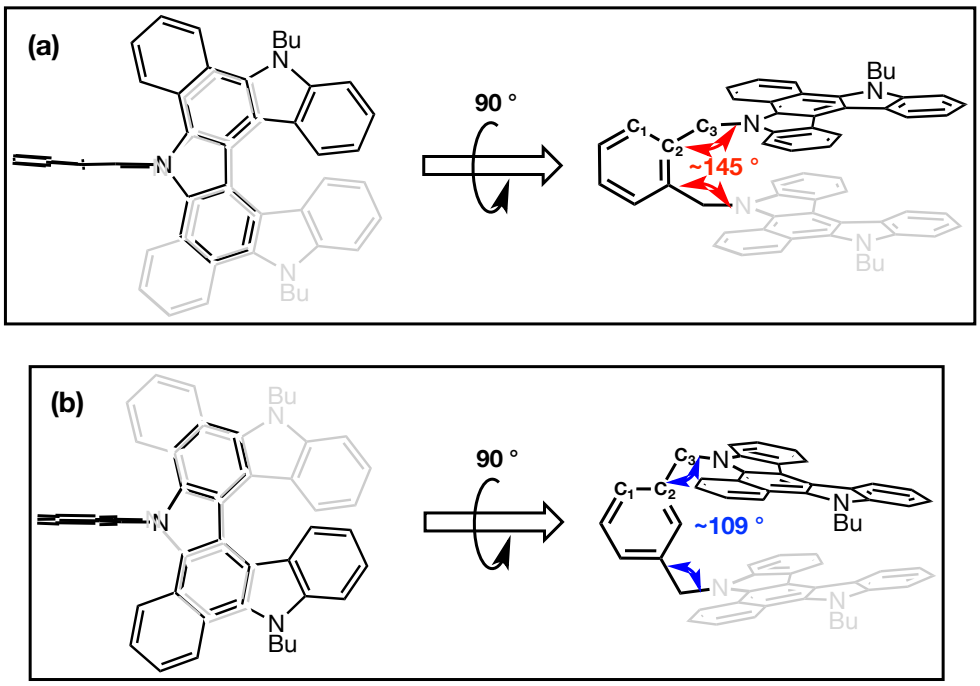

Figure 20 | The comparison of the angle of C_2-C_3-N for the twin-BIC donor with **(a)** an *o*-xylylene spacer and **(b)** a *m*-xylylene spacer.

2-15. Determination of the spacer structure for oligomers

As a result of the study on the structure of spacer in the dimer described in the previous section, it was found that the dimer **2a**, **2b**, **2e** with trimethylene (n = 3), tetramethylene (n = 4), and *m*-xylylene respectively, could form pimer with a stacked geometry. It is noteworthy that the author found the pimer formation in the meta-bridged-electrophores. It is a quite unique behavior for the BIC electrophores since there have been no reports that indicates superior π-π stacking of *m*-bridged-electrophores to *o*-bridged counterpart. Based on this finding, the author was able to demonstrate his own hypothesis.

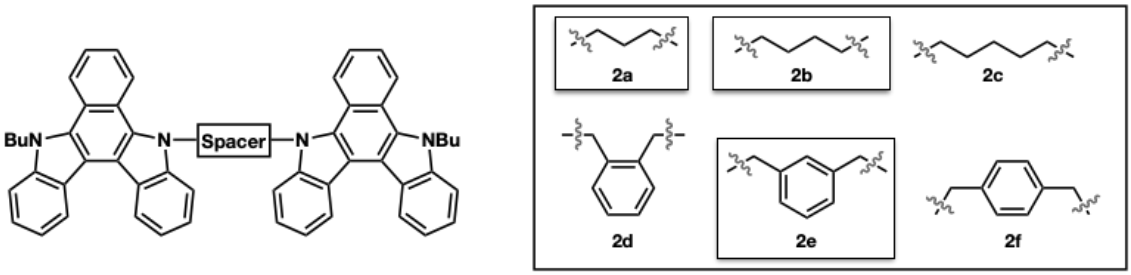

Figure 21 | BIC dimers **2a**-**2f** with alkylene (n = 3, 4, 5) and xylylene (*o*-, *m*-, *p*-) spacer.

For creating mixed-valence oligomer selectively, **2a** with trimethylene chain is not suitable, since this dimer forms not only pimer (0 and +1), but also π-dimer (+1 and +1). Since there is a concern that the solubility of the compound decreases rapidly when oligomerized, tetramethylene chain in **2b** is not suitable. For the same reason, the author used a *m*-xylylene with improved solubility by introducing a *tert*-butyl group at the 5-position (*m*-XY') as the spacer in this study. For the same reason, *n*-butyl groups were also attached at the termini of the oligomers, and thus *N*-butyl-substituted BIC (**1b**) was used as a starting monomer unit. These are the key features of our molecular design for oligo(aromatic diamine)s **2**–**6** with 2–6 BIC units (Figure **21**).

In addition to the fully conjugated MV state, the half-filled polycations could adopt another electronic/geometric structure, which is a cluster of pimers (Scheme 2b). Thus, dimerized pimer units are formed, which do not interact with each other. Such half-filled polycations would be generated from the independently designed four-chromophoric systems (**7** and **8**, Figure 22), in which interaction between the pimers would be prevented in their half-filled dication diradicals by incorporation of an inappropriate spacer such as *o*-xylylene or *p*-xylylene in the center of tetramers.

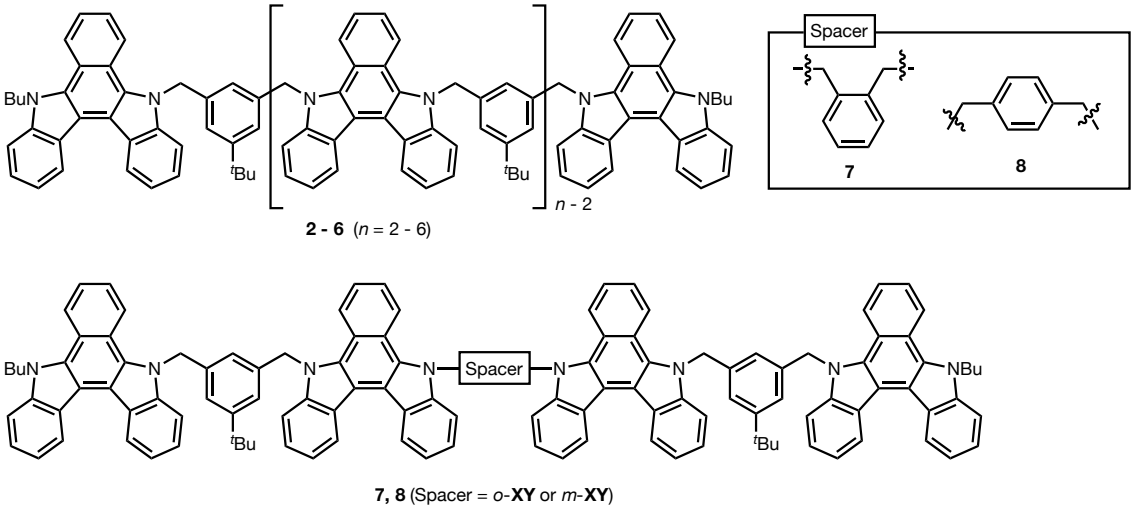

Figure 22 | BIC oligomers **2** - **8** with *m*-xylylene spacer.

2-16. Preparation of BIC oligomers (2 ~ 8)

Convergent syntheses of **2** – **8** were conducted based on S_N2 reactions of the corresponding carbazoles and benzyl/xylylene halides in the presence of NaH in DMF (Scheme 12). Thus, the reaction of monomer **1b** with 0.5 eq. of *m*-XY'Br_2 gave dimer **2**. When the reaction was conducted with an excess amount of *m*-XY'Br_2, 1:1 adduct **15** was obtained, from which trimer **3** was generated upon treatment with 0.5 eq. of parent BIC **1e**.

On the other hand, benzocarbazoles with a phenylazide group could be converted to BIC derivatives upon exposure to nitrene insertion conditions (160 °C in 1,2-dichlorobenzene), and thus were used as precursors for the selective formation of unsymmetrically substituted BICs, as in monomer **1b** from **14b**.

Scheme 12

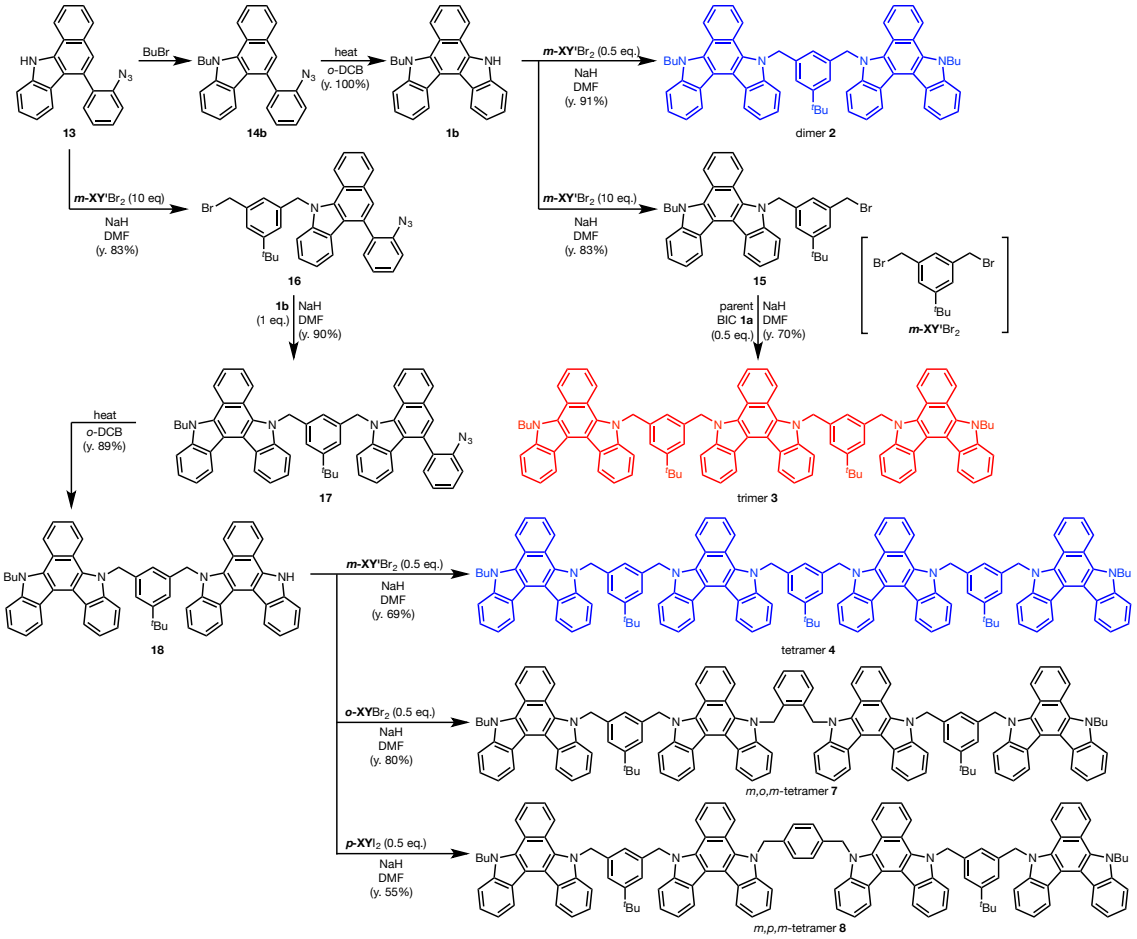

Thus, the unsymmetrically substituted dimer **18** was derived in a stepwise manner from **13** via **16** and **17**, from which tetramer **4** was obtained by the reaction with 0.5 equivalents of *m*-XY'Br_2. Pentamer **5** and hexamer **6** were also prepared from the key synthon **18**. Pentamer **5** was prepared upon treatment with **18** and **19**, which was generated by the reaction with **1a** and excess amount of *m*-XY'Br_2. With the isomers of xylylene dihalide, tetramers **7** and **8** were prepared from **18**, each of which has an *o*-xylylene and a *p*-xylylene spacer in the center of the tetrameric structure, respectively. The unsymmetrically substituted trimer **20** was derived stepwise manner from **18** via **19**, from which hexamer **6** was obtained by the reaction with 0.5 eq. of *m*-XY'Br_2 same as the preparation of tetramer **4**.

Scheme 13

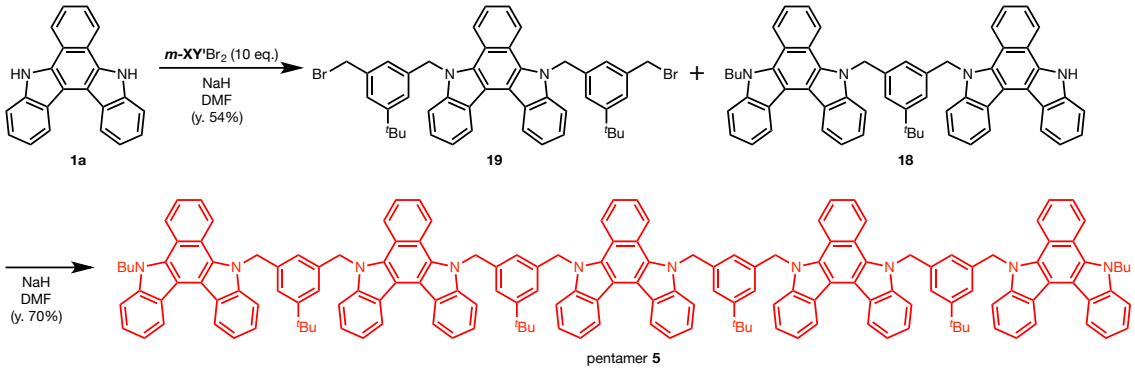

Scheme 14

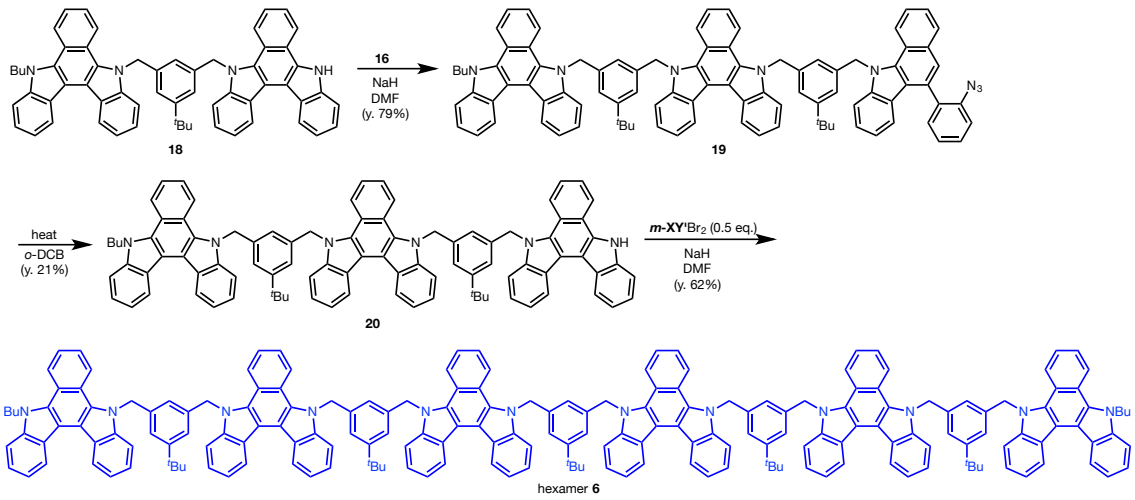

All of the oligomers are pale-yellow crystalline solids, and their strongly fluorescent nature is inherited from BIC **1**.[24,25] The absorption maxima, emission maxima, and quantum yields of fluorescence of **2**-**8** are similar to those of monomeric BIC **1d**, and thus it is highly likely that neutral **2**-**8** prefer non-folded geometries without electronic communication among BIC units in solution (Figures 23 and 24 ;Table 2).

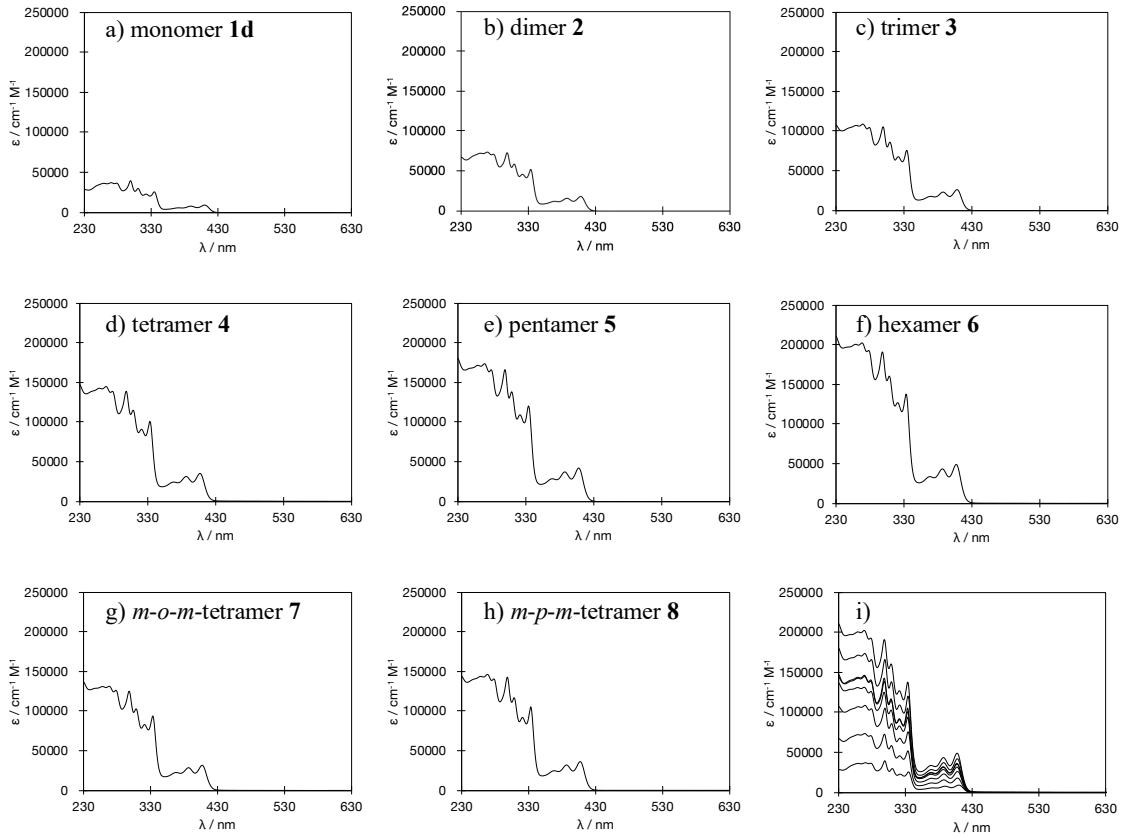

Figure 23 | UV spectra of BIC derivatives (a) **1d**, (b) **2**, (c) **3**, (d) **4**, (e) **5**, (f) **6**, (g) **7,** and (h) **8**, measured in CH_2Cl_2. (i) shows the spectra of **1d**, and **2** – **6**.

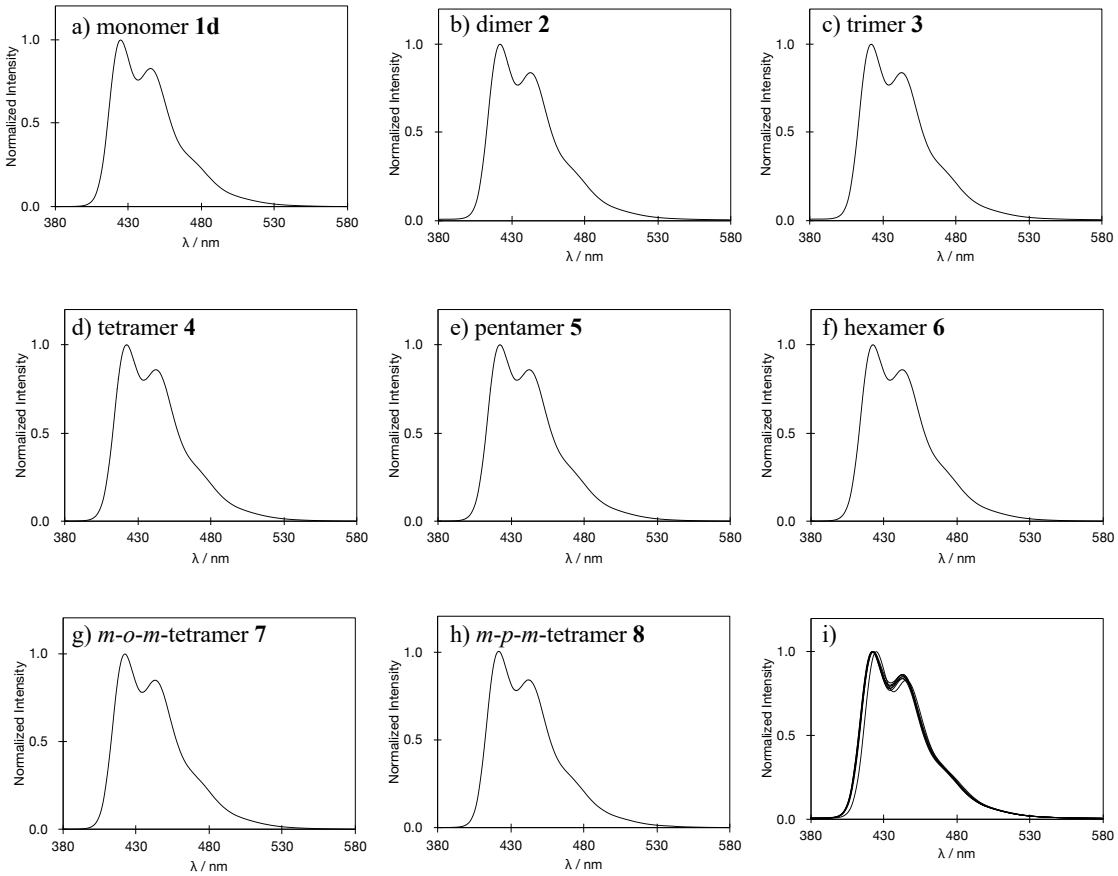

Figure 24 | Fluorescence spectra of BIC derivatives (a) **1d**, (b) **2**, (c) **3**, (d) **4**, (e) **5**, (f) **6**, (g) **7,** and (h) **8**, measured in CH_2Cl_2. (i) shows the spectra of **1d**, and **2** – **6**.

Table 2 | UV-Vis and fluorescence spectral data of **1d** and **2** – **6** in CH_2Cl_2.

compd.	λ_{abs} (nm)[a]	$\varepsilon(M^{-1}\,cm^{-1})$	λ_{em}[b](nm)	Φ_F[c]
1d (monomer)	410	9400	445	0.37
2 (*m*-dimer)	409	18000	443	0.47
3 (all-*m*-trimer)	408	26400	443	0.40
4 (all-*m*-tetramer)	407	33100	443	0.39
5 (all-*m*-pentamer)	408	42200	444	0.47
6 (all-*m*-hexamer)	408	47000	443	0.40
7 (*m*-*o*-*m*-tetramer)	407	31600	443	0.33
8 (*m*-*p*-*m* tetramer)	407	36200	442	0.37

[a] The wavelengths for the longest absorption peaks are given. [b] Excitation wavelength: 360 nm. [c] Fluorescence quantum yields were determined using 9,10-diphenylanthracene as an external standard.

2-17. Electrochemical properties of BIC oligomers

Cyclic and differential pulse voltammetric (CV and DPV) analyses showed that dimer **2** with an *m*-**XY'** spacer undergoes selective one-electron oxidation to form a singly charged cation radical. Thus, two sequential 1e oxidations occur at different potentials (ΔE = 0.17 V in CH_2Cl_2) to form $\mathbf{2}^{+\bullet}$ and then $\mathbf{2}^{2+2\bullet}$. By additional one-wave two-electron (2e) oxidation to $\mathbf{2}^{4+}$, both units of BIC become dicationic. The separation of the first and second 1e oxidation potentials clearly shows that cation radical $\mathbf{2}^{+\bullet}$ is a stabilized MV species, and thus further oxidation of $\mathbf{2}^{+\bullet}$ into $\mathbf{2}^{2+2\bullet}$ is inhibited. Actually, $\mathbf{2}^{+\bullet}$ was isolated in 64% yield as a stable borate salt upon preparative oxidation of **2** with 1 equivalent of $(4\text{-}BrC_6H_4)_3N^{+\bullet}BARF^-$[42] (BARF = $[3,5\text{-}(CF_3)_2C_6H_3]_4B$).

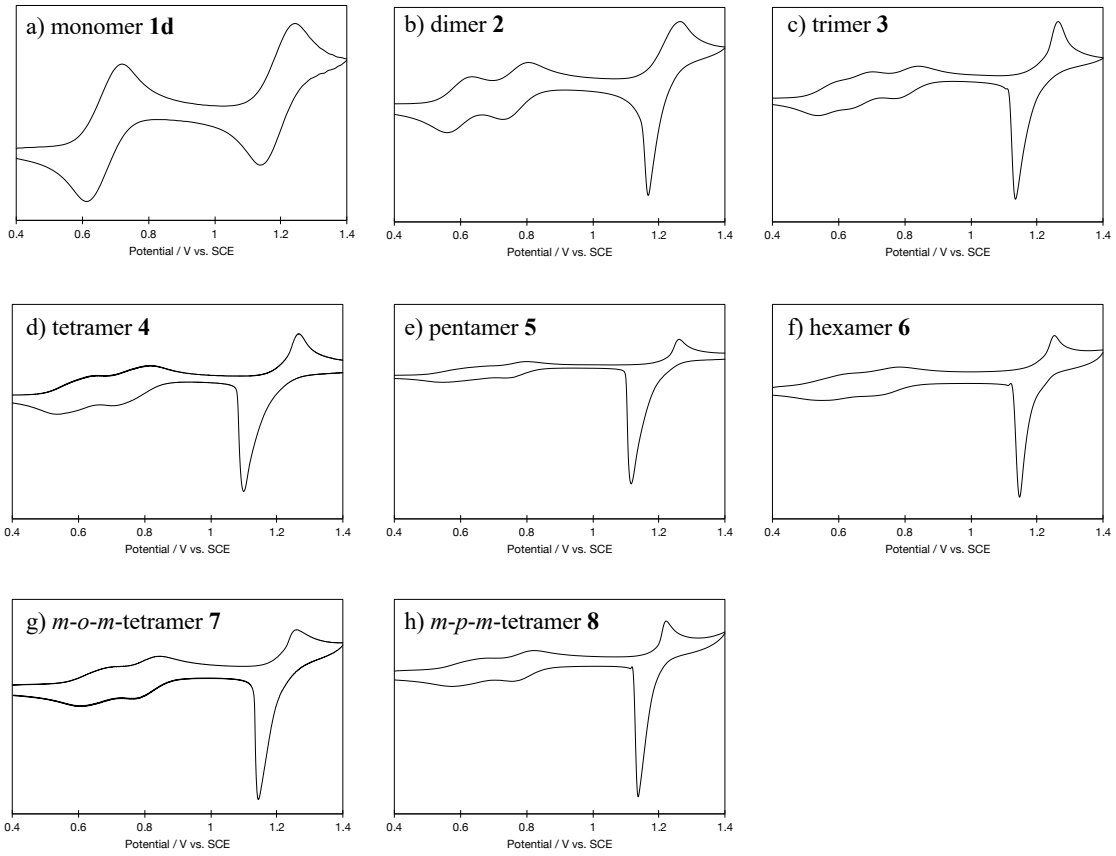

Figure 25 | Cyclic voltammograms of **1d**, and **2** - **8** measured in CH_2Cl_2 (*E*/V vs SCE, 0.1 M Bu_4NPF_6 as a supporting electrolyte, Pt electrode, scan rate 100 mV/s). Vertical axes indicate the electric current. The sharp return peaks can be rationalized by considering that the 2*n*-oxidized states of *n*-mers are adsorbed on the working electrode.

The third 2e oxidation potential of **2** corresponding to conversion of $\mathbf{2}^{2+2\bullet}$ to $\mathbf{2}^{4+}$ is nearly identical to that for the process of $\mathbf{1d}^{+\bullet}$ to $\mathbf{1d}^{2+}$, indicating that two units of $BIC^{+\bullet}$ in $\mathbf{2}^{2+2\bullet}$ do not interact with each other, and thus $\mathbf{2}^{2+2\bullet}$ is not a π-dimer in solution. This behavior of **2** affording a pimer but not a π-dimer is similar to that of **2e** without *tert*-butyl group on the *m*-xylylene spacer (Figures 25 and 26 ;Table 3).

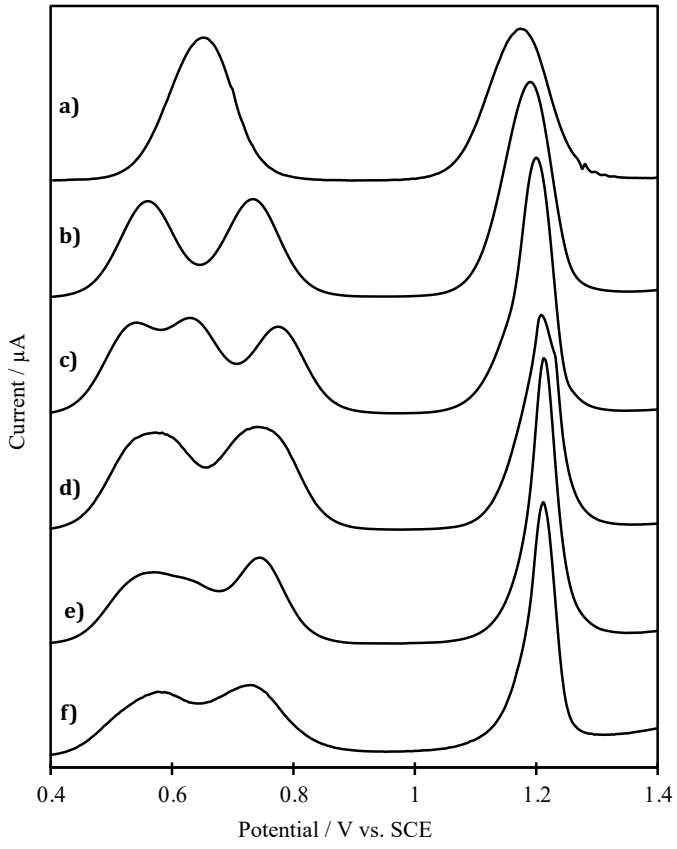

Figure 26 | Differential pulse voltammograms of (a) **1d**, (b) **2**, (c) **3**, (d) **4**, (e) **5**, and (f) **6** measured in CH_2Cl_2 (*E*/V vs SCE, Pt electrode, 0.1 M Bu_4NPF_6).

CV and DPV of tetramer (**4**) showed that it undergoes selective 2e oxidation to the dication diradical ($\mathbf{4}^{2+2\bullet}$). Thus, two sequential 2e oxidation processes occur followed by an additional one-wave 4e oxidation. Similarly, CV and DPV of hexamer (**6**) showed two sequential 3e oxidation processes followed by an additional one-wave 6e oxidation, confirming that trication triradical ($\mathbf{6}^{3+3\bullet}$) can be generated selectively. Actually, upon oxidation of hexamer **6** with 3 equivalents of magic blue [MB, $(4\text{-}BrC_6H_4)_3N^{+\bullet}SbCl_6^-$], $6^{3+3\bullet}(SbCl_6^-)_3$ was isolated as a stable salt in 57% yield. Similarly, upon oxidation of tetramer **4** with 2 equivalents of MB, $\mathbf{4}^{2+2\bullet}(SbCl_6^-)_2$ was obtained in 93% yield. The voltammetric analyses and preparative-scale oxidation experiments clearly show that half-filled (*n*/2-charged) cationic species are generated selectively from the dimer (**2**), tetramer (**4**), and hexamer (**6**) connected by the *m*-**XY'** spacer.

Table 3 | Oxidation potentials of **1d**, **2**-**8** and **2d**, **2e**, **2f** measured by DPV method in CH_2Cl_2.

compd.	E^{ox}	
1d (monomer)	+0.65 (1e),	+1.17 (1e)
2 (*m*-dimer)	+0.56 (1e), +0.73 (1e),	+1.19 (2e)
3 (all-*m*-trimer)	+0.54 (1e), +0.63 (1e), +0.78 (1e),	+1.20 (3e)
4 (all-*m*-tetramer)	+0.57 (2e), +0.74 (2e),	+1.21 (4e)
5 (all-*m*-pentamer)	+0.57 (2e), +0.64 (1e), +0.74 (2e),	+1.21 (5e)
6 (all-*m*-hexamer)	+0.58 (3e), +0.73 (3e),	+1.21 (6e)
7 (*m*-*o*-*m*-tetramer)	+0.63 (2e), +0.79 (2e),	+1.21 (4e)
8 (*m*-*p*-*m* tetramer)	+0.60 (2e), +0.77 (2e),	+1.19 (4e)
2d (*o*-dimer)[b]	+0.64 (2e),	+1.18 (2e)
2e (*m*-dimer)[b]	+0.53 (1e), +0.70 (1e),	+1.16 (2e)
2f (*p*-dimer)[b]	+0.62 (2e),	+1.15 (2e)

[a] E/V vs SCE, Pt electrode, 0.1 M Bu_4NPF_6. [b] Due to low solubility in CH_2Cl_2, measurements were done in 1,1,2,2-tetrachloroethane.

2-18. Spectroscopic analyses of BIC oligomers

In the electronic spectrum of $\mathbf{2}^{+\bullet}$, strong absorption was observed in the NIR region similar to the case of the monomeric $\mathbf{1c}^{+\bullet}$ salt (λ_{max} = 702 nm in MeCN),[24,25] but the absorption consists of two bands with a new shoulder in the longer wavelength region [$\mathbf{2}^{+\bullet}BARF^{-}$:$\lambda_{max}$ = 721 and 780 (sh) nm in MeCN]. Such modification of the NIR absorption in $\mathbf{2}^{+\bullet}$ would be induced by π-π interactions through the folded geometry in $\mathbf{2}^{+\bullet}$, and thus it is concluded that $\mathbf{2}^{+\bullet}$ is the pimer of the MV state. Broadening and splitting of the NIR absorption causes a large peak width (full width at half maximum, FWHM)[43] of $\mathbf{2}^{+\bullet}$, whereas the NIR absorptions of $\mathbf{4}^{2+2\bullet}$ and $\mathbf{6}^{3+3\bullet}$ would have a larger FWHM owing to the extended π–π interaction through the fully delocalized long-range MV state.

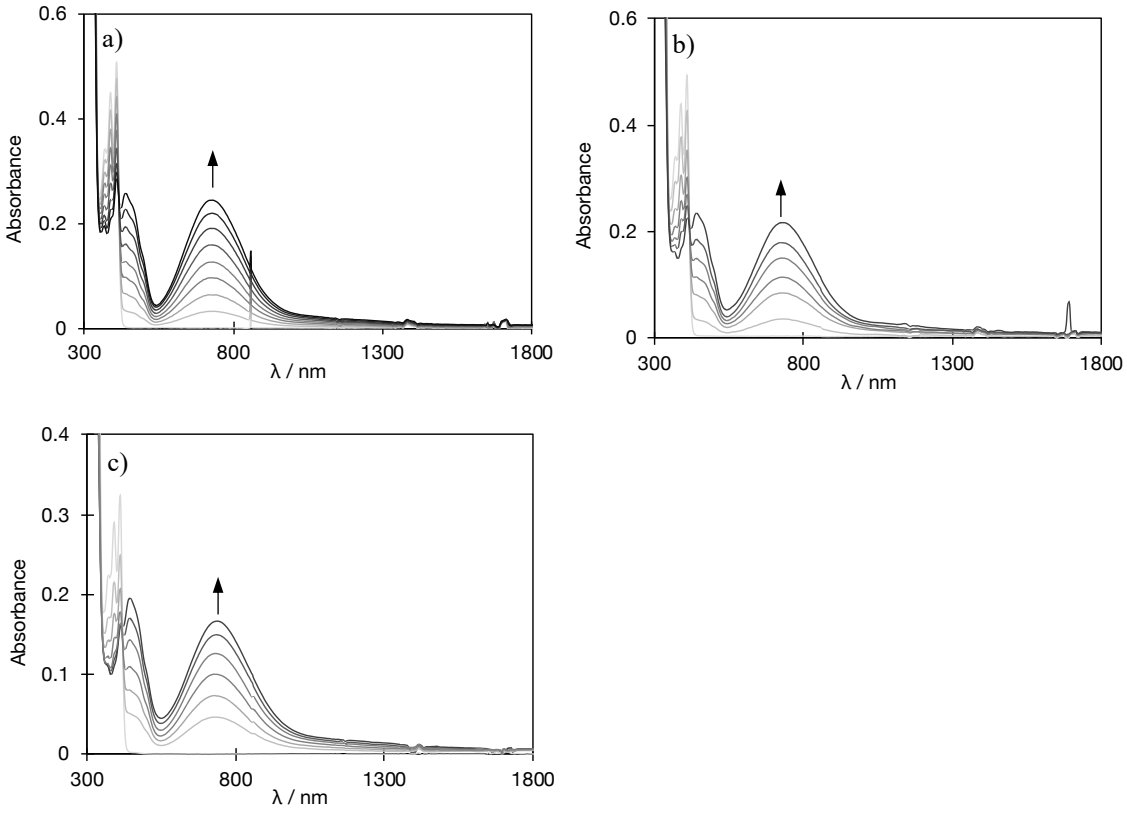

Figure 27 | A continuous change in UV-Vis-NIR spectrum upon constant current electrochemical oxidation of a) **2** (2.8×10^{-5} M, 20 μA, every 2 min), b) **4** (1.4×10^{-5} M, 20 μA, every 4 min), c) **6** (6.7×10^{-4} M, 20 μA, every 8 min) in CH_2Cl_2 containing 0.05 M Bu_4NPF_6 as a supporting electrolyte.

Thus, a detailed examination of FWHM was conducted by titration experiments of **1c**, **2**, **4**, and **6** with MB in CH_2Cl_2 (Figure 28). Greater FWHM values were obtained until the formation of half-filled cationic species ($\mathbf{2}^{+\bullet}$, $\mathbf{4}^{2+2\bullet\bullet}$, and $\mathbf{6}^{3+3\bullet}$) with the addition of up to 1, 2, and 3 equivalents of MB. The resulting FWHM values for **2** (240 nm with 1 eq.), **4** (244 nm with 2 eq.), and **6** (248 nm with 3 eq.) are larger than that for monomer **1c** (219 nm with 0.5 eq.). The larger values for the longer oligomers show that $\mathbf{4}^{2+2\bullet}$ and $\mathbf{6}^{3+3\bullet}$ are in a fully delocalized long-range MV state with the formation of a 1D columnar stack. Further addition of MB caused a decrease in FWHM [**2** (229 nm with 2 eq.), **4** (235 nm with 4 eq.), and **6** (235 nm with 6 eq.)], confirming that an increase in FWHM is characteristic only for the half-filled cations of the MV state.

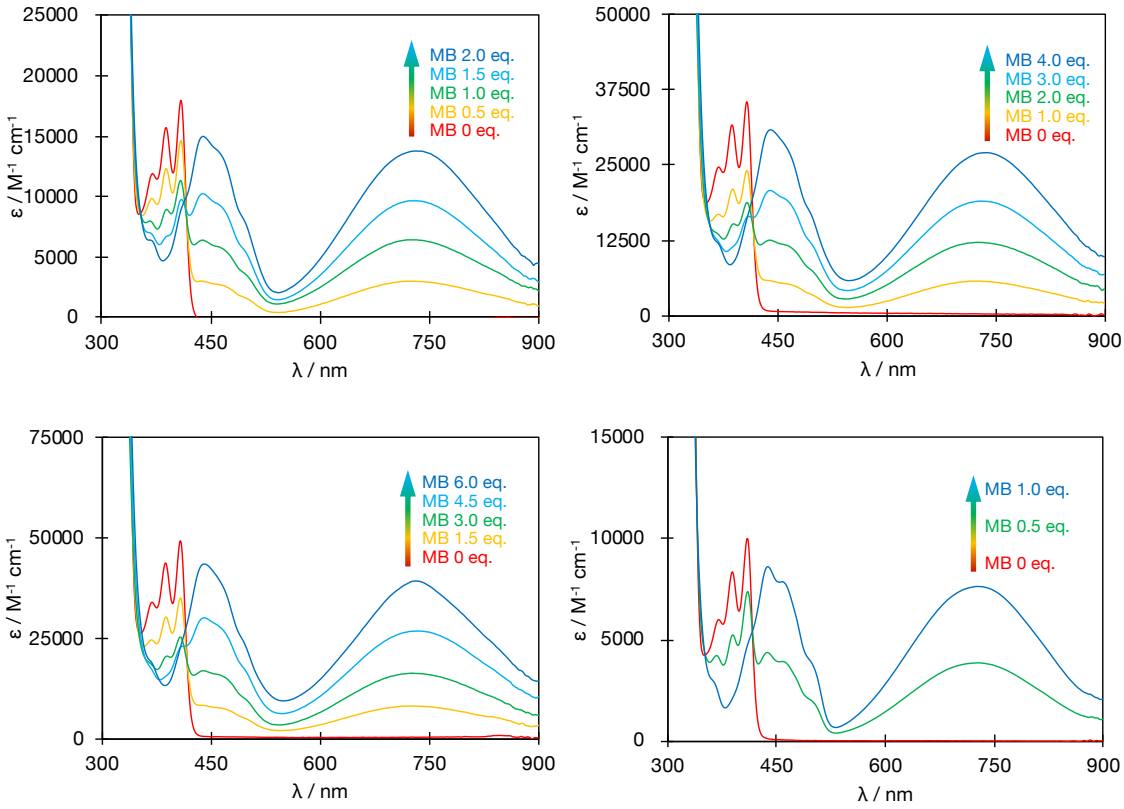

Figure 28 | Change in UV-Vis-NIR spectra of (a) **1c**, (b) **2**, (c) **4**, and (d) **6** upon addition of several aliquots of MB in CH_2Cl_2.

In contrast to **4**, other tetramers **7** and **8** could not generate the fully delocalized long-range MV state upon 2e oxidation because of the presence of an *o*-xylylene or *p*-xylylene spacer in the center. Thus, $\mathbf{7}^{2+2\bullet}$ and $\mathbf{8}^{2+2\bullet}$ cannot form a 1D columnar structure, and the two pimer units are electronically separated by *o*-xylylene or *p*-xylylene. The FWHM values obtained upon treatment with 2 equivalents of **7** (237 nm) and **8** (238 nm) are similar to that of pimer $\mathbf{2}^{+\bullet}$ but smaller than that of fully delocalized $\mathbf{4}^{2+2\bullet}$. This proves that $\mathbf{7}^{2+2\bullet}$ and $\mathbf{8}^{2+2\bullet}$ are half-filled polycations with a double-pimer structure, where two pimer units do not interact with each other (Scheme 2b).

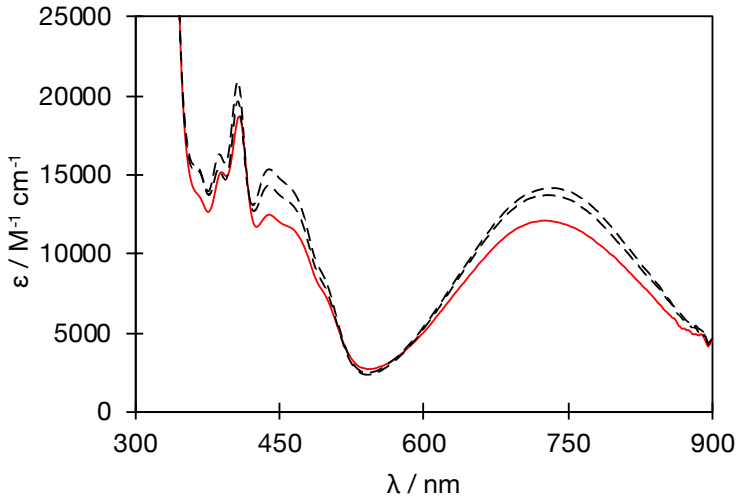

Figure 29 | UV-Vis-NIR spectra of **4, 7, 8** upon addition of two equivalent of MB in CH_2Cl_2.

2-19. X-ray crystallography of dication diradical of tetramer 4

Finally, the 1D columnar stack structure of $\mathbf{4}^{2+2\bullet}$ was confirmed by successful X-ray analysis of the $\mathbf{4}^{2+2\bullet}(SbCl_6^-)_2$ salt. As shown in Figure 30, the four disk-shaped units are stacked in a face-to-face manner. In the three kinds of overlap, the shortest C---C contacts are 3.41, 3.32, and 3.27 Å for overlap -1, -2, -3, respectively, all of which are close to the sum of the van der Waal radii (3.40 Å). Their arrangements are suitable for the interaction of the HOMO of BIC and SOMO of $BIC^{+\bullet}$, especially for the first two overlaps of pseudo-C_2 symmetry. It is highly likely that the two positive charges and two unpaired electrons are delocalized over the four BIC units through these overlaps in the 1D stack structure.

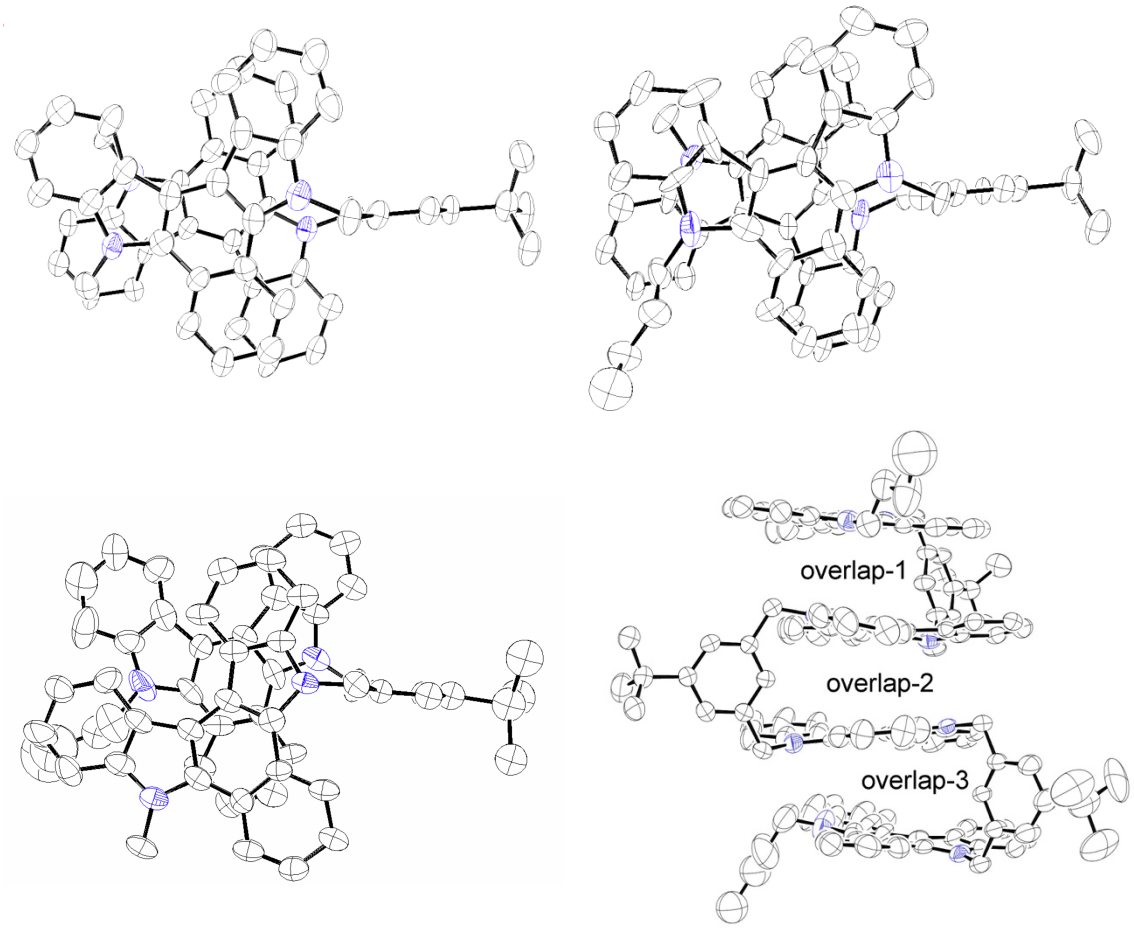

Figure 30 | Three kinds of π-π overlap in dication diradical salt of **4** [$\mathbf{4}^{2+2\bullet}(SbCl_6^-)_2(MeCN)_{0.5}(toluene)_{1.5}$] determined by X-ray analysis: (a) overlap-1, (b) overlap-2, and (c) overlap-3. (d) Side view of 1D stacking structure.

In fact, the C–C bonds connecting two five-membered rings (C_{14b} –C_{14c}) in the four BIC units are 1.411(9), 1.402(8), 1.420(9), and 1.402(10) Å, respectively. Its bond length is the most sensitive to the charge on the BIC unit [1.429(2) Å for neutral **1c** and 1.358(7) Å for **1c**$^{+\bullet}$(BF_4^-)]. The intermediary values in the **4**$^{2+2\bullet}$($SbCl_6^-$)$_2$ salt indicates that each BIC unit has nearly half positive charge although further discussion would be inappropriate on considering the large esd values for the bond length.

2-20. Even–odd dependency of half-filled MV states

The present oligomers with *n* BIC units (*n* = even) connected by *m*-XY' undergo selective *n*/2-electron oxidation to give the corresponding half-filled (*n*/2-charged) polycations with a fully delocalized MV state. Based on the above results, the odd-numbered oligomers must also be stabilized by forming 1D stacked MV states upon oxidation, where oxidation states of (*n*–1)/2 and (*n*+1)/2 can both be considered a half-filled state (Figure 31). Accordingly, trimer **3** and pentamer **5** would each have two stable MV states (**3**$^{+\bullet}$ and **3**$^{2+2\bullet}$; **5**$^{2+2\bullet}$ and **5**$^{3+3\bullet}$), which was supported by the DPV measurement (Figure 3 and Table 2). After the sequential generation of three oxidation states [(*n*–1)/2+, (*n*+1)/2+, and *n*+], an additional one-wave *n*-electron oxidation occurs to generate 2*n*+ oxidized states.

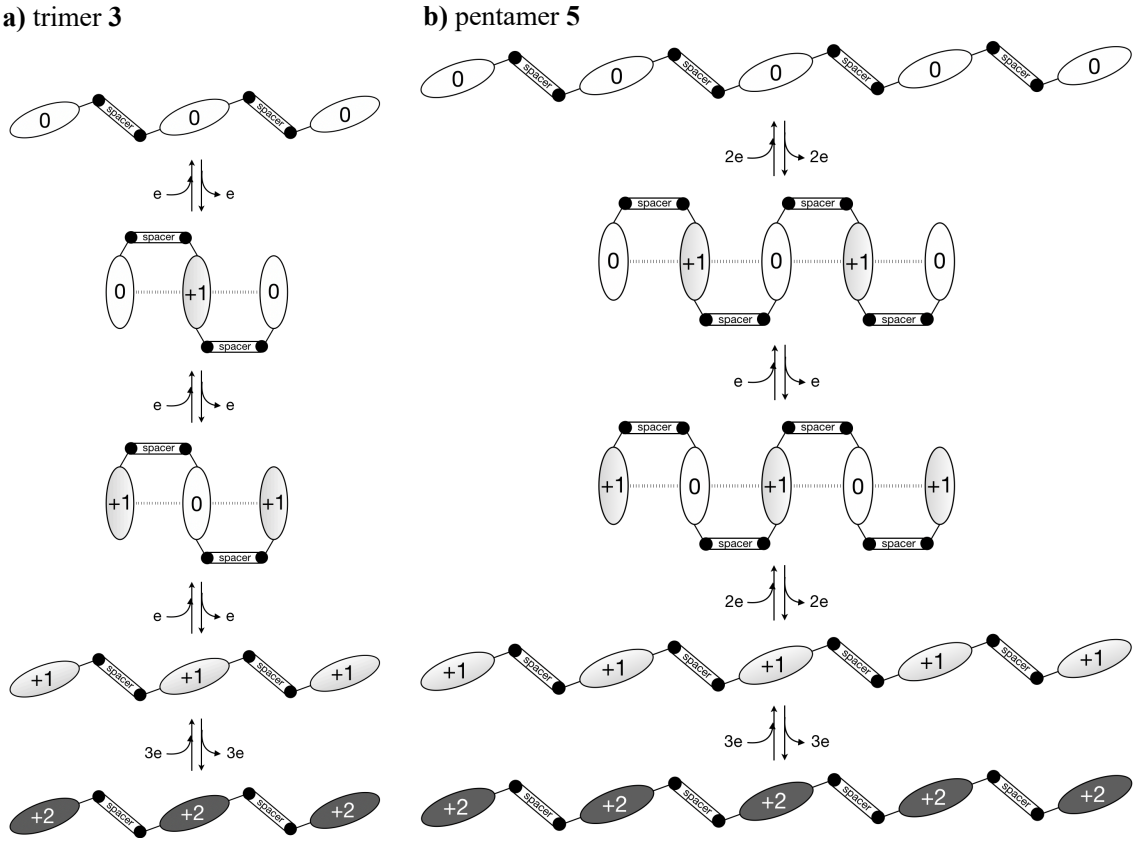

Figure 31 | Plausible redox schemes for odd-numbered oligomers **3** and **5** with two half-filled redox stages.

2-21. Conclusion for the linear BIC oligomers

In this way, the author could confirm the validity of the proposal for the generation of a novel MV state from organic linear oligomers based on the combination of a given chromophore and the best-matched spacer. Further studies of this novel protocol are then examine by using dendrimeric analogues to find new functions by using the change in geometry of the oligomers from a non-folded form into compact 1D columnar stacked geometry.

2-22. The dendrimeric BIC with multiple *m*-xylylene structure

In this section, the author designed BIC triad and tetrad using an appropriate spacer, which was selected based on the study on the BIC dimers. Thus, the author prepared triad **3** and tetrad **4** with multiple *m*-xylylene connectivity in the molecule. Their redox behaviors were investigated by the voltammetric analyses.

By the reaction of **1e**, which has an octyl group for higher solubility, with NaH followed by 1,3,5-tris(bromomethyl)benzene or 1,2,4,5-tetrakis(bromomethyl)benzene respectively, the desired molecule **3a** and **4a** were obtained (Scheme 15). When the latter reaction was conducted with *N*-butylated BIC **1b**, the desired tetrad was not obtained due to the precipitation of the intermediates before completion of the four-time S_N2 reaction.

Scheme 15 | Preparation of BIC triad **3a** and tetrad **4a.**

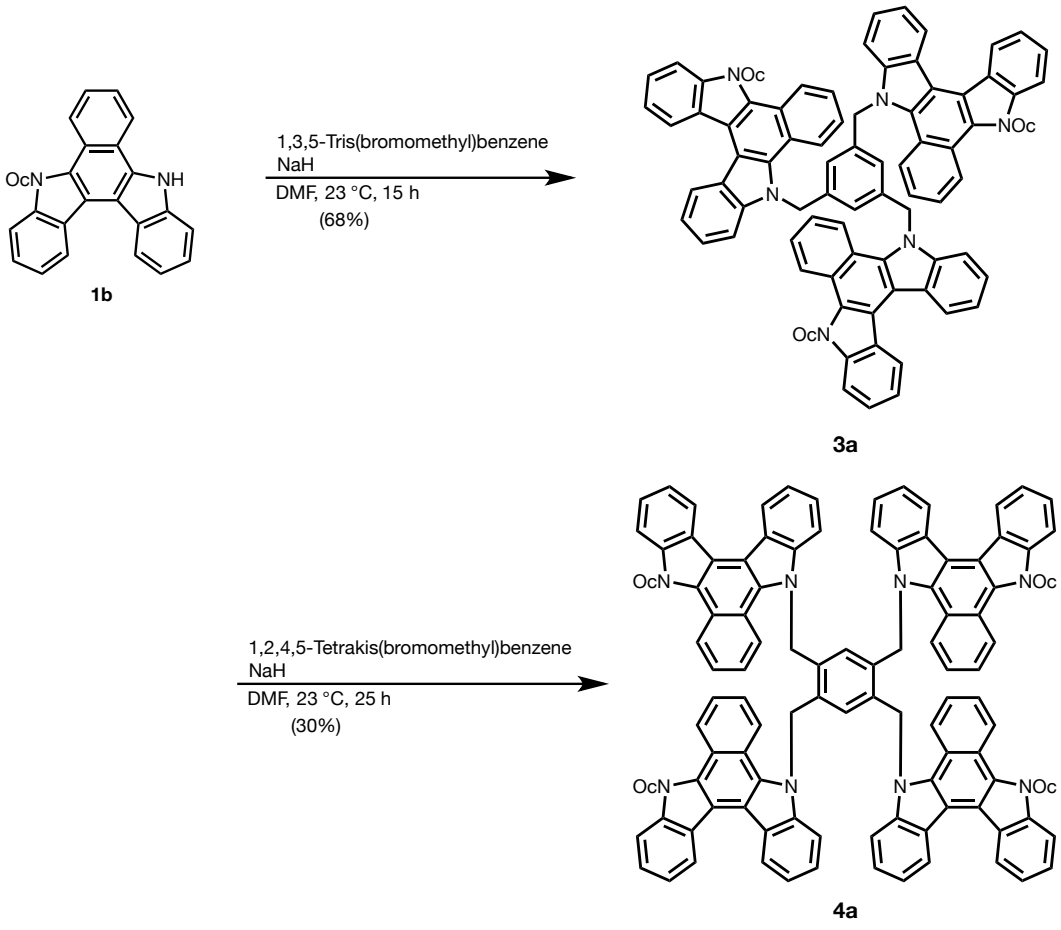

2-23. CV and DPV measurements of BIC triad and tetrad

According to the voltammetric analysis of triad **3a** (Figure 32), the potential corresponding to the process where each BIC units was oxidized from neutral to cation radical state was separated into two, with a current ratio of 1:2. There is a potential separation after one-electron oxidation, which shows that the one-electron oxidized state is stabilized by the formation of pimer with stacked geometry. The cation radical of **3a** generated upon one-electron oxidation has two neutral units and one cation radical unit. So that, strong stabilization would come from the formation of "dynamic pimer" shown int Scheme 16.

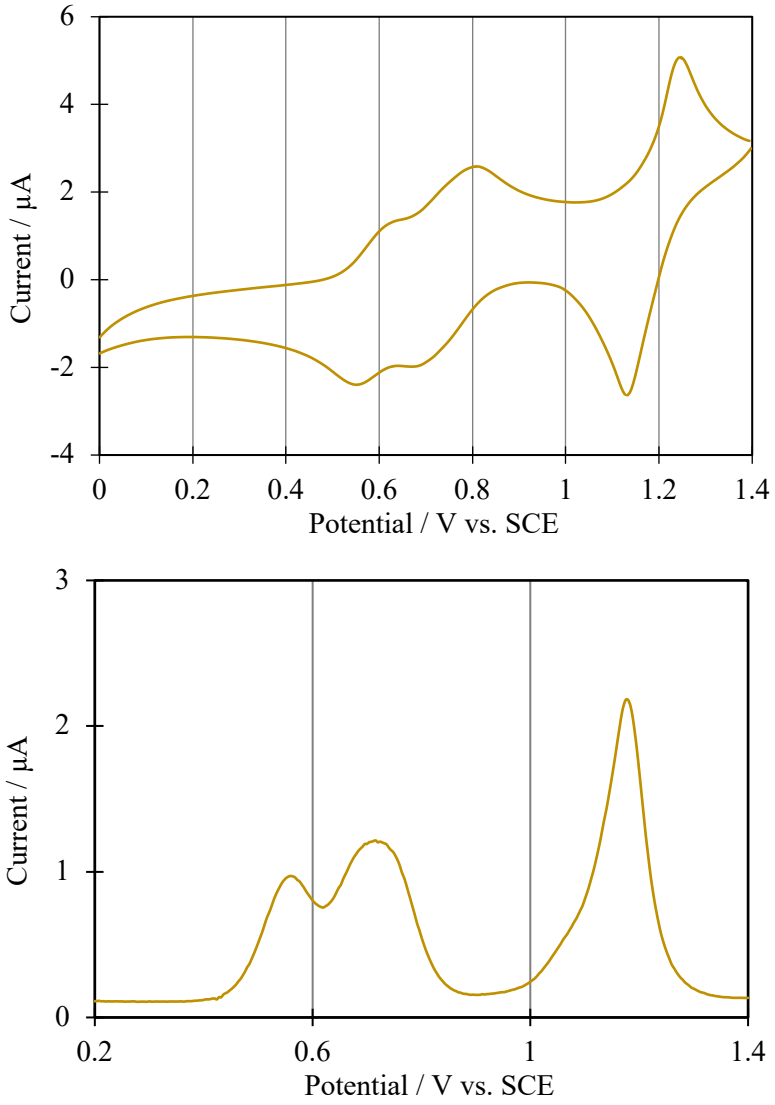

Figure 32 | (a) Cyclic and (b) differential pulse voltammograms of **3a** measured in 1,1,2,2-tetrachloroethane (0.1 M Bu_4NPF_6, E/V vs. SCE, Pt electrode, 100 mVs^{-1}).

Scheme 16 | Plausible redox scheme of BIC triad **3a**.

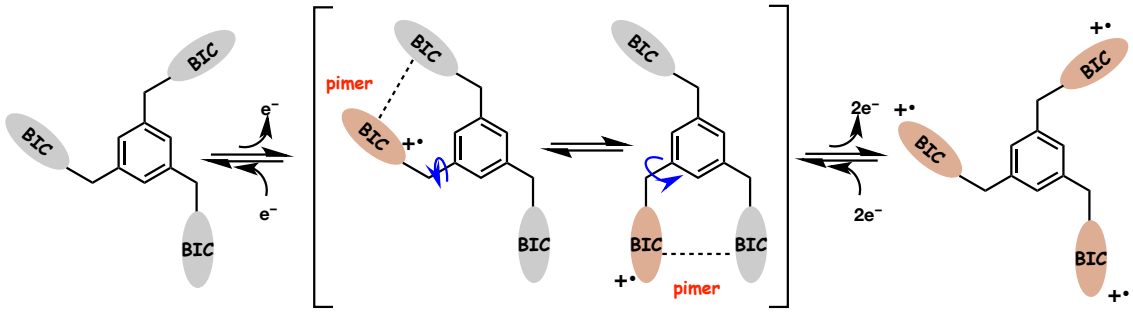

In the voltammograms of 1,2,4,5-tetra-substitued tetrad **4a**, the voltammogram is very close to those of the even-number oligomers (n = 2, 4, 6) (Figure 34). There is a potential separation after two-electron oxidation, which suggests that the two-electron oxidized state is stabilized by the pimer formation with the stacked geometry. It is highly likely that, in the two-electron oxidized species of **4a**, each of two cation radical units are stabilized by stacking with two neutral units through the formation of the "double pimer" shown in Scheme 17. In this way, the author could demonstrate his idea on the novel approach to the MV-state of half-filled charged state first by the linear oligomer up to hexamer and then by the dendrimeric oligomer up to tetrad.

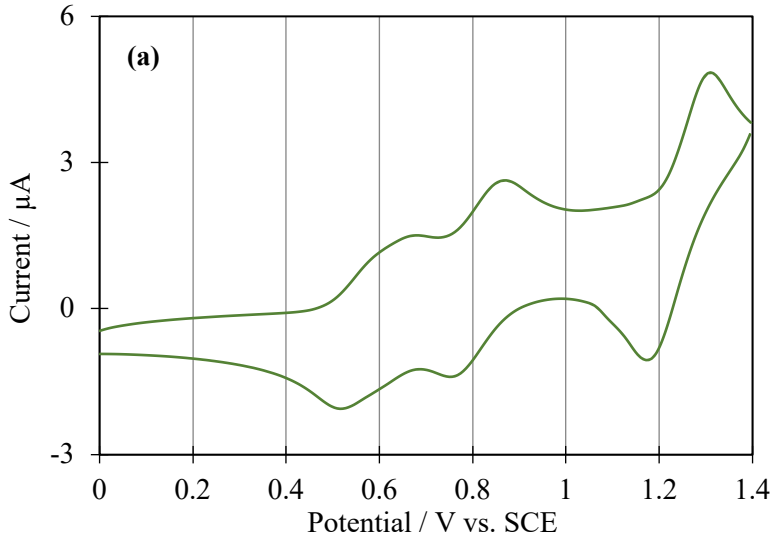

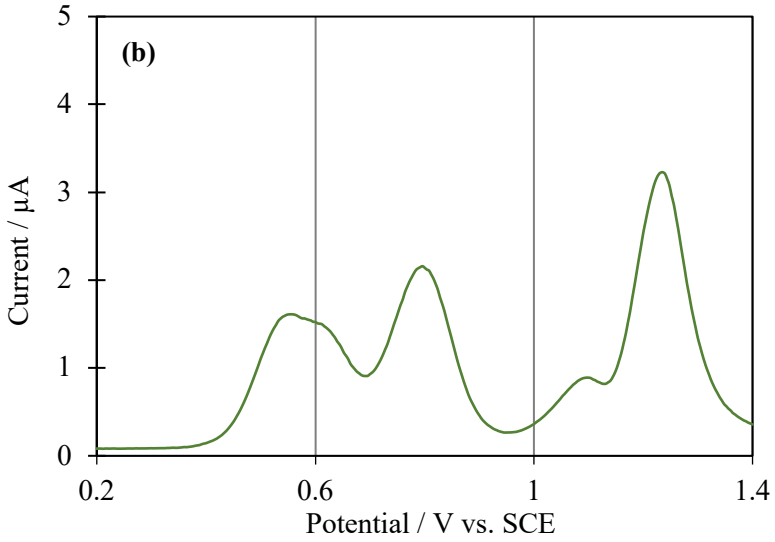

Figure 34 | (a) Cyclic and **(b)** differential pulse voltammograms of **4a** measured in 1,1,2,2-tetrachloroethane (0.1 M Bu_4NPF_6, E/V vs. SCE, Pt electrode, 100 mVs^{-1}).

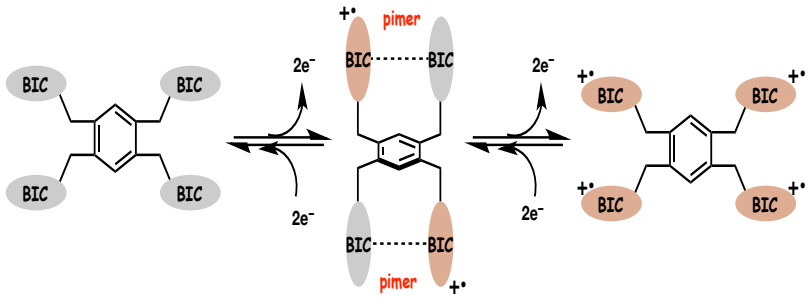

Scheme 17 | Plausible redox scheme of BIC tetrad **4a**.

Experimental section

General

^{1}H NMR spectra were recorded on Bruker AVANCE III HD (400 MHz). IR spectra were taken on a JEOL JIR-WINSPEC100 FT/IR spectrophotometer. Mass Spectra were recorded on JEOL JMS-T100GCV spectrometer in FD/FI, EI mode (GC-MS & NMR Laboratory, Graduate School of Agriculture, Hokkaido University). Column chromatography was performed on silica gel I-6-40 (YMC) of particle size 40-63 μm. Melting points were measured on Yamato MP-21 or Yanagimoto micro melting point apparatus and reported uncorrected. UV/Vis/NIR spectra were recorded on a Hitachi U-3500 spectrophotometer or PerkinElmer Lambda 900S at the Open Facility of Hokkaido University. CD spectra were measured on a JASCO J-820 spectropolarimeter. Fluorescence spectra were measured on a Hitachi F-7000 fluorescence spectrophotometer. All commercially available compounds were used without further purification. Solvents were purified prior to use.

<Preparation of BIC monomer 1b>

1) Preparation of 2-(2'-bromophenyl)indole **9**

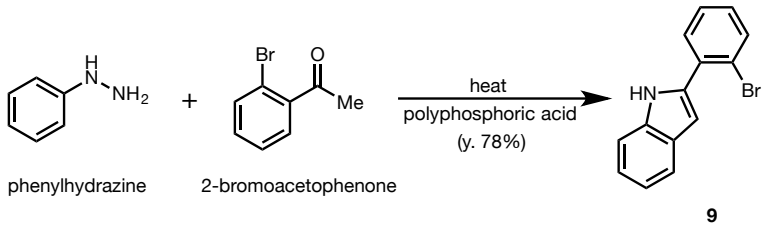

2-Bromoacetophenone (15.0 g, 75.4 mmol) and phenylhydrazine (12.2 g, 113 mmol) were mixed with polyphosphoric acid (230 g), and the mixture was heated with stirring. The temperature of the reaction mixture was kept at 100-110 °C for 4 h. The mixture was poured into ice water and extracted with EtOAc. The combined extracts were dried over anhydrous Na_2SO_4. The dried extracts were concentrated, and the crude product was chromatographed on silica gel (hexane/CH_2Cl_2 = 6/1) to afford **9** (16.1 g, 78%). The spectral data of **9** were identical to those previously described.

2) Preparation of 2-[2'-(2"-trimethylsilylethynyl)phenyl]-1*H*-indole **10**

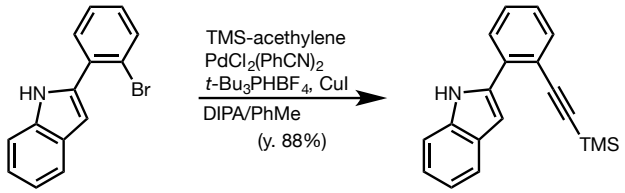

9 **10**

To a stirred suspension of indole **9** (16.1 g, 59.0 mmol), $PdCl_2(PhCN)_2$ (905 mg, 2.36 mmol) and tri(*tert*-butyl)phosphine (1.37 g, 4.72 mmol) in toluene (320 mL) and DIPA (80 mL) under argon were added CuI (449 mg, 2.36 mmol) and trimethylsilylacetylene (12.2 mL, 88.5 mmol). After stirring for 4 h at 80 °C, the mixture was diluted with Et_2O and filtered through a pad of Celite. The filtrate was concentrated in vacuo and the residue was chromatographed on silica gel (hexane/CH_2Cl_2 = 10/1) to afford silylalkyne **10** (15.0 g, 88%). The spectral data of **10** were identical to those previously described.

3) Preparation of 2-(2'-ethylphenyl)-1*H*-indole **11**

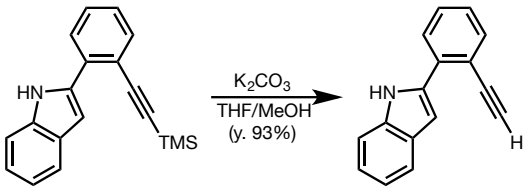

10 **11**

To a mixture of silylalkyne **11** (15.0 g, 51.4 mmol) in MeOH (120 mL) and THF (120 mL) was added K_2CO_3 (2.15 g, 15.6 mmol). After stirring for 2.5 h at 22 °C, the mixture was diluted with water and extracted with EtOAc three times. The combined organic layer was washed with brine, dried over anhydrous $MgSO_4$, and concentrated in vacuo. The residue was chromatographed on silica gel (hexane/CH_2Cl_2 = 10/1) to afford **11** (10.5 g, 93%). The spectral data of **11** were identical to those previously described.

4) Preparation of 2-{2'-[2"-(2"'-azidophenyl)ethynyl]phenyl}-1*H*-indole **12**

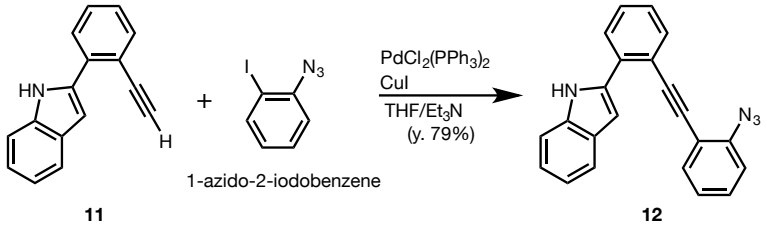

11 **12**

To a stirred suspension of alkyne **11** (10.5 g, 48.5 mmol), $PdCl_2(PPh_3)_2$ (851 mg, 1.21 mmol) and CuI (230 mg, 1.21 mmol) in dry THF (170 mL) and TEA (70 mL) under argon was added 1-azido-2-iodobenzene (14.3 g, 58.2 mmol). After stirring for 9 h at 23 °C, the mixture was diluted with Et_2O and filtered through a pad of Celite. The filtrate was concentrated in vacuo and the residue was chromatographed on silica gel (hexane/CH_2Cl_2 = 4/1) to afford **12** (12.7 g, 79%). The spectral data of **12** were identical to those previously described.

5) Preparation of 6-(2'-azidophenyl)-11*H*-benzo[*a*]carbazole **13**

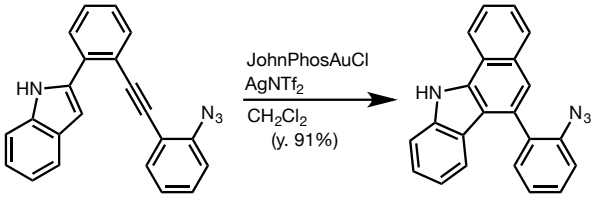

12 **13**

A solution of indole **12** (2.64 g, 7.89 mmol), JohnPhosAuCl (105 mg, 0.197 mmol) and $AgNTf_2$ (76.4 mg, 0.197 mmol) in dry CH_2Cl_2 (80 mL) was stirred for 4 h at 23 °C. Then, the mixture was concentrated in vacuo and the residue was chromate-graphed on silica gel (hexane/CH_2Cl_2 = 5/2) to afford **13** (2.53 g, 96%). The spectral data of **13** were identical to those previously described.

6) Preparation of 6-(2-azidophenyl)-11-butyl-benzo[*a*]carbazole **10a**

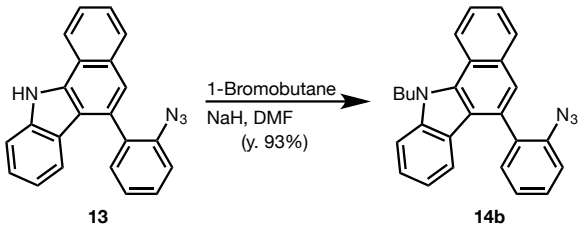

13 **14b**

To a stirred solution of azide **13** (500 mg, 1.50 mmol) in dry DMF (15 mL) under argon was added NaH (120 mg, 3.00 mmol, 60% in mineral oil) at room temperature. After stirring for 10 min at room temperature, 1-bromobutane (322 μL, 3.00 mmol) was added to the mixture. After stirring for 2 h at room temperature, the mixture was diluted with water and extracted with Et_2O three times. The combined organic layer was washed with brine, dried over anhydrous $MgSO_4$, and concentrated in vacuo. The residue was chromatographed on silica gel (hexane/CH_2Cl_2 = 6/1) to give **14b** (544 mg, 93%) as a yellow solid.

Mp 47-49 °C; IR (KBr) ν /cm^{-1} : 3050, 2956, 2928, 2870, 2116, 1574, 1488, 1467, 1453, 1432, 1398, 1367, 1333, 1300, 1244, 1186, 1164, 1136, 1126, 1095, 1030, 740 ; ^{1}H NMR (400 MHz, $CDCl_3$) δ/ppm : 8.55 (d, *J* = 8.5 Hz, 1H), 8.03 (ddd, *J* = 8.0, 1.5 Hz, 1H), 7.63 (ddd, *J* = 7.5, 1.5 Hz, 1H), 7.54-7.61 (m, 3H), 7.47-7.49 (m, 2H), 7.41 (ddd, *J* = 6.5, 1.5 Hz, 1H), 7.39 (ddd, *J* = 8.0, 1.5 Hz, 1H), 7.33 (ddd, *J* = 7.5, 1.5 Hz, 1H), 6.99-7.04 (m, 2H), 4.84 (d, *J* = 7.5 Hz, 1H), 4.82 (d, *J* = 7.5 Hz, 1H), 2.13 (qn, *J* = 7.5 Hz, 2H), 1.62 (sext, *J* = 7.5 Hz, 2H),1.07 (t, *J* = 7.5 Hz. 3H); HR-MS (FD) calcd. for $C_{26}H_{22}N_4$: 390.1845; found: 390.1848.

7) Preparation of 5-butyl-5,10-dihydrobenzo[*a*]indolo[2,3-*c*]carbazole **1b**

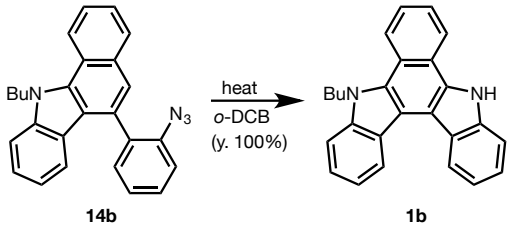

14b **1b**

A solution of azide **14b** (490 mg, 1.25 mmol) in 1,2-dichlorobenzene (65 mL) under argon was stirred for 10 h at 160 °C. After cooling to room temperature, the reaction mixture was concentrated in vacuo and the residue was chromatographed on silica gel (hexane/CH_2Cl_2 = 2/1) to afford **1b** (453.1 mg, 100%) as a pale yellow solid.

Mp 205-206 °C; IR (KBr) ν /cm^{-1} : 3412 , 3047, 2955, ,2928, 2854, 1482, 1467, 1434, 1405, ,1378, 1361, 1338, 1286, 1253, 1240, 1224, 1189, 1175, 1152, 1135, 1091, 1032, 920, 753, 731; ^{1}H NMR (400 MHz, DMSO-d_6) δ/ppm : 12.27 (s, 1H), 8.86 (d, *J* = 8.0 Hz, 1H), 8.80 (d, *J* = 8.0 Hz, 1H), 8.73-8.76 (m, 2H), 7.89 (d, *J* = 8.0 Hz, 1H), 7.73-7.78 (m, 3H), 7.54 (dd, *J* = 7.5, 7.5 Hz, 1H), 7.47 (dd, *J* = 7.5, 7.5 Hz, 1H), 7.41 (dd, *J* = 7.5, 7.5 Hz, 1H), 7.36 (dd, *J* = 7.5, 7.5 Hz, 1H), 4.96 (t, *J* = 7.5 Hz, 2H), 1.95 (q, *J* = 7.5 Hz, 2H), 1.46 (sext, *J* = 7.5 Hz, 2H),0.95 (t, *J* = 7.5 Hz, 3H); HR-MS (FD) calcd. for $C_{26}H_{22}N_2$: 362.1783; found: 362.1782.

<Preparation of BIC dimers 2a – 2f>

8) Preparation of 10,10'-(1,3-propanediyl)bis(5-butyl-5,10-dihydrobenzo[*a*]indolo [2,3-*c*]carbazole) **2a**

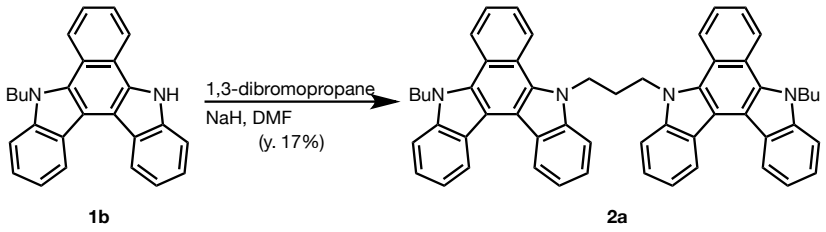

1b **2a**

To a stirred solution of **1b** (200 mg, 0.55 mmol) in dry DMF (3 mL) under argon was added NaH (44.2 mg, 1,10 mmol, 60% in mineral oil) at room temperature. After stirring for 10 min at room temperature, 1,3-dibromopropane (28.3 μL, 0.28 mmol) was added to the mixture. After stirring for 1 h at room temperature, the mixture was diluted with water was extracted with EtOAc three times. The combined organic layer was washed with brine, and the precipitates formed in the organic layer were filtered. The residue was washed with hexane, EtOAc, and water to give pure **2a** (36.1 mg, 17%) as a pale yellow solid.

Mp 243-244 °C; IR (KBr) ν /cm^{-1} : 3049, 2955, 2927, 2870, 1607, 1478, 1466, 1425, 1402, 1361, 1341, 1263, 1231, 1212, 1156, 1140, 1104, 1032, 920, 728 ; ^{1}H NMR (400 MHz, DMSO-d_6) δ/ppm : 8.88 (d, J = 8.3 Hz, 2H), 8.87 (d, J = 8.3 Hz, 2H), 8.68 (d, J = 8.3 Hz, 2H), 8.47 (d, J = 8.3 Hz, 2H), 7.88 (d, J = 8.3 Hz, 2H), 7.47-7.56 (m, 6H), 7.40 (dd, J = 7.5, 7.5 Hz, 4H), 7.10 (dd, J = 7.5, 7.5 Hz, 2H), 5.15 (t, J = 7.0 Hz, 4H), 4.89 (t, J = 7.5 Hz, 4H), 2.70-2.74 (m, 2H), 1.86 (qn, J = 7.5 Hz, 4H), 1.38 (sext, J = 7.5 Hz, 4H), 0.89 (t, J = 7.5 Hz, 6H); HR-MS (FD) calcd. for $C_{55}H_{48}N_4$: 764.3879; found: 764.3884.

9) Preparation of 10,10'-(1,4-butanediyl)bis(5-butyl-5,10-dihydrobenzo[*a*]indolo [2,3-*c*]carbazole) **2b**

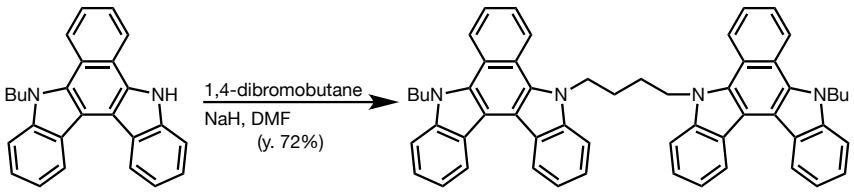

1b **2b**

To a stirred solution of **1b** (200 mg, 0.55 mmol) in dry DMF (3 mL) under argon was added NaH (44.2 mg, 1.10 mmol, 60% in mineral oil) at room temperature. After stirring for 10 min at room temperature, 1,4-dibromobutane (32.7 μL, 0.28 mmol) was added to the mixture. After stirring for 1 h at room temperature, the mixture was diluted with water and extracted with EtOAc three times. The combined organic layer was washed with brine, and the precipitates formed in organic layer were filtered. The residue was washed with hexane, EtOAc, and water to afford **2b** (154 mg, 72%) as a pale yellow solid.

Mp 276-278 °C; IR (KBr) ν /cm^{-1} : 3051, 2956, 2927, 2871, 1678, 1672, 1607, 1480, 1466, 1425, 1405, 1361, 1341, 1297, 1253, 1225, 1195, 1166, 1153, 1136, 1103, 1038, 1016, 909, 752, 726, 602; ^{1}H NMR (400 MHz, temp DMSO-d_6, 393 K) δ/ppm : 8.81 (d, J = 8.2 Hz, 2H), 8.79 (d, J = 8.2 Hz, 2H), 8.68 (d, J = 8.2 Hz, 2H), 8.58 (d, J = 8.2 Hz, 2H), 7.77 (d, J = 8.2 Hz, 2H), 7.67 (d, J = 8.2 Hz, 2H), 7.61 (ddd, J = 7.0, 7.0, 1.0 Hz, 2H), 7.41 (ddd, J = 7.0, 7.0, 1.0 Hz, 2H), 7.48-7.53 (m, 4H), 7.37 (ddd, J = 7.0, 7.0, 1.0 Hz, 2H), 7.32 (ddd, J = 7.0, 7.0, 1.0 Hz, 2H), 4.84 (t, J = 7.5 Hz, 4H), 4.87-4.90 (m,

4H), 2.08-2.12 (m, 4H), 1.94 (qn, *J* = 7.5 Hz, 4H), 1.45 (sext, *J* = 7.5 Hz, 4H), 0.94 (t, *J* = 7.5 Hz, 6H); HR-MS (FD) calcd. for $C_{56}H_{50}N_4$: 778.4036; found: 778.4045.

10) Preparation of 10,10'-(1,5-pentanediyl)bis(5-butyl-5,10-dihydrobenzo[*a*]indolo [2,3-*c*]carbazole) **2c**

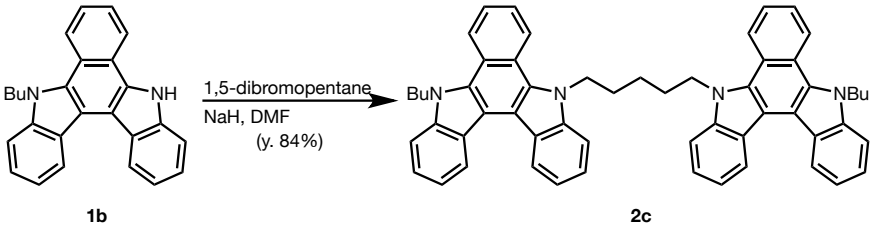

1b **2c**

To a stirred solution of **1b** (200 mg, 0.55 mmol) in dry DMF (3 mL) under argon was added NaH (44.2 mg, 1.10 mmol, 60% in mineral oil) at room temperature. After stirring for 10 min at room temperature, 1,5-dibromopentane (37.4 μL, 0.28 mmol) was added to the mixture. After stirring for 1 h at room temperature, the mixture was diluted with water and extracted with EtOAc three times. The combined organic layer was washed with brine, and the precipitates formed in the organic layer were filtered. The residue was washed with hexane, EtOAc, and water to afford **2c** (183 mg, 84%) as a pale yellow solid.

Mp 192-194 °C; IR (KBr) ν /cm^{-1} : 3049, 2957, 2928, 2869, 1608, 1479, 1467, 1424, 1401, 1361, 1341, 1285, 1265, 1230, 1159, 1143, 1107, 1033, 918, 730; ^{1}H NMR (400 MHz, DMSO-d_6) δ/ppm : 8.86-8.88 (m, 4H), 8.77 (d, *J* = 8.5 Hz, 2H), 8.73 (d, *J* = 8.5 Hz, 2H), 7.88 (d, *J* = 8.3 Hz, 2H), 7.81 (d, *J* = 8.3 Hz, 2H), 7.72 (dd, *J* = 7.6. 7.6 Hz, 2H), 7.66 (dd, *J* = 7.6, 7.6 Hz, 2H), 7.54 (dd, *J* = 7.6, 7.6 Hz, 2H), 7.50 (dd, *J* = 7.6, 7.6 Hz, 2H), 7.38-7.43 (m, 4H), 4.86-4.93 (m, 8H), 2.01-2.09 (m, 4H), 1.93 (qn, *J* = 7.5 Hz, 4H), 1.57-1.64 (m, 2H), 1.42 (sext, *J* = 7.5 Hz, 4H), 0.92 (t, *J* = 7.5 Hz, 6H), ; HR-MS (FD) calcd. for $C_{57}H_{52}N_4$: 792.4192; found: 792.4182.

11) Preparation of 10,10'-{[1,2-phenylene]bis(methylene)}bis(5-butyl-5,10-dihydrobenzo[*a*]indolo[2,3-*c*]carbazole) **2d**

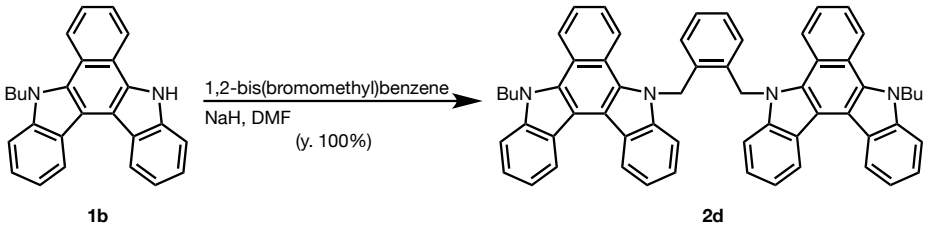

1b **2d**

To a stirred solution of **1b** (200 mg, 0.55 mmol) in dry DMF (3 mL) under argon was added NaH (44.2 mg, 1.10 mmol, 60% in mineral oil) at room temperature. After stirring for 10 min at room temperature, a solution of 1,2-bis(bromomethyl)benzene (72.0 mg, 0.28 mmol) in DMF (3 mL) was added to the mixture through a cannula. After stirring for 1 h at room temperature, the mixture was diluted with water and the precipitates were filtered. The residue was washed with $CHCl_3$ and water to afford **2d** (228 mg, 100%) as a pale yellow solid.

Mp > 300 °C; IR (KBr) ν /cm^{-1} : 3049, 2955, 2927, 2869, 1607, 1468, 1424, 1400, 1339, 1276, 1233, 1203, 1173, 1157, 1139, 1106, 1031, 916, 730; ^{1}H NMR (400 MHz, DMSO-d_6, 393 K) δ/ppm : 8.97 (dd, J = 8.5 Hz, 2H), 8.93 (dd, J = 8.5 Hz, 2H), 8.80 (dd, J = 8.5 Hz, 2H), 8.59 (dd, J = 8.5 Hz, 2H), 7.83 (dd, J = 8.5 Hz, 2H), 7.81 (dd, J = 8.5 Hz, 2H), 7.74 (ddd, J = 8.0, 7.0, 1.0 Hz, 2H), 7.53-7.64 (m, 6H), 7.49 (ddd, J = 8.0, 7.0, 1.0 Hz, 2H), 7.43 (ddd, J = 8.0, 7.0, 1.0 Hz, 2H), 7.05 (dd, J = 5.9, 3.4 Hz, 2H), 6.87 (dd, J = 5.9, 3.4 Hz, 2H), 6.40 (s, 4H), 4.93 (t, J = 7.5 Hz, 4H), 1.99 (qn, J = 7.5 Hz, 4H), 1.48 (sext, J = 7.5 Hz, 4H), 0.96 (t, 6H, J = 7.5 Hz, 6H) ; HR-MS (FD) calcd. for $C_{60}H_{50}N_4$: 826.4036; found: 826.4050.

12) Preparation of 10,10'-{[1,3-phenylene]bis(methylene)}bis(5-butyl-5,10-dihydrobenzo[*a*]indolo[2,3-*c*]carbazole) **2e**

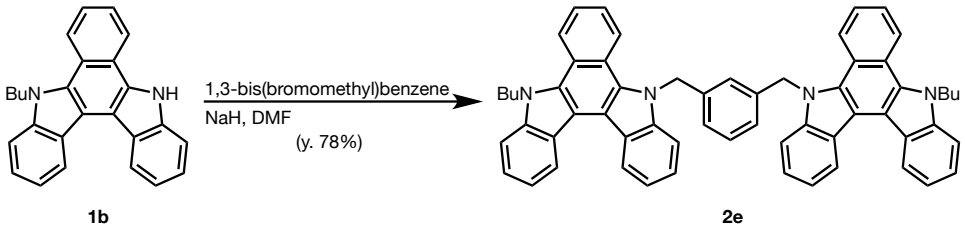

1b **2e**

To a stirred solution of **1b** (200 mg, 0.55 mmol) in dry DMF (3 mL) under argon was added NaH (44.2 mg, 1.10 mmol, 60% in mineral oil) at room temperature. After stirring for 10 min at room temperature, a solution of 1,3-bis(bromomethyl)benzene (72.9 mg, 0.28 mmol) in DMF (3 mL) was added to the mixture through a cannula. After stirring for 2 h at room temperature, the mixture was diluted with water and the precipitates were filtered. The residue was washed with $CHCl_3$ and water to afford **2e** (178 mg, 78%) as a pale yellow solid

Mp. 253-254 °C; IR (KBr) ν /cm^{-1} : 3047, 2955, 2928, 2869, 2856, 1674, 1652, 1608, 1468, 1424, 1399, 1340, 1292, 1269, 1234, 1203, 1174, 1157, 1140, 1106, 1041, 1030, 919, 736; ^{1}H NMR (400 MHz, DMSO-d_6) δ/ppm : 8.88 (d, J = 8.5 Hz, 2H), 8.86 (d, J = 8.5 Hz, 2H), 8.67 (d, J = 8.5 Hz, 2H), 8.39 (d, J = 8.5 Hz, 2H), 7.89 (d, J = 8.5 Hz, 2H), 7.69 (d, J = 8.5 Hz, 2H), 7.55-7.61 (m, 4H), 7.38-7.49 (m, 6H), 7.28 (t, J = 7.7 Hz, 1H), 7.15-7.21 (m, 3H), 7.06 (d, J = 7.6 Hz, 2H), 6.09 (s, 4H), 4.87 (t, J = 7.5 Hz, 4H), 1.92 (qn, J = 7.5 Hz, 4H), 1.43 (sext, J = 7.5 Hz, 4H), 0.94 (t, J = 7.5 Hz, 6H); HR-MS (FD) calcd. for $C_{60}H_{50}N_4$: 826.4036; found: 826.4045.

13) Preparation of 10,10'-{[1,4-phenylene]bis(methylene)}bis(5-butyl-5,10-dihydrobenzo[*a*]indolo[2,3-*c*]carbazole) **2f**

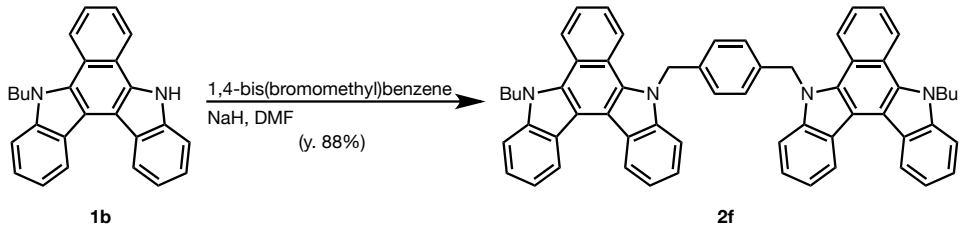

1b **2f**

To a stirred solution of **1b** (200 mg, 0.55 mmol) in dry DMF (3 mL) under argon was added NaH (44.2 mg, 1.10 mmol, 60% in mineral oil) at room temperature. After stirring for 10 min at room temperature, 1,4-bis(bromomethyl)benzene (71.3 mg, 0.28 mmol) was added to the mixture. After stirring for 1 h at room temperature, the mixture was diluted with water and the precipitates were filtered. The residue was washed with $CHCl_3$ and water to afford **2f** (200 mg, 88%) as a pale yellow solid.

Mp. 278 °C (decomp.) ; IR (KBr) ν /cm^{-1} : 3447, 3047, 2957, 2926, 2871, 2359, 1653, 1472, 1424, 1395, 1339, 1172, 1106, 726; ^{1}H NMR (400 MHz, DMSO-d_6) δ/ppm : 8.90 (dd, J = 8.5, 6.8 Hz, 4H), 8.75 (d, J = 8.5 Hz, 2H), 8.55 (d, J = 8.5 Hz,

2H), 7.84 (d, *J* = 8.5 Hz, 2H), 7.66-7.70 (m, 4H), 7.55 (ddd, 8.5, 7.6, 1.2 Hz), 7.39-7.51 (m, 8H), 7.20 (s, 4H), 6.12 (s, 4H), 4.92 (t, 7.6 Hz, 4H), 1.97 (qn, *J* = 7.5 Hz, 4H), 1.48 (sext, *J* = 7.5 Hz, 4H), 0.96 (t, *J* = 7.5 Hz, 6H); HR-MS (FD) calcd. for $C_{60}H_{50}N_4$: 826.4036; found: 826.4027.

<Preparation o BIC dimers 2d', 2e'>

14) Preparation of 5-octyl-5,10-dihydrobenzo[*a*]indolo[2,3-*c*]carbazole **1b**

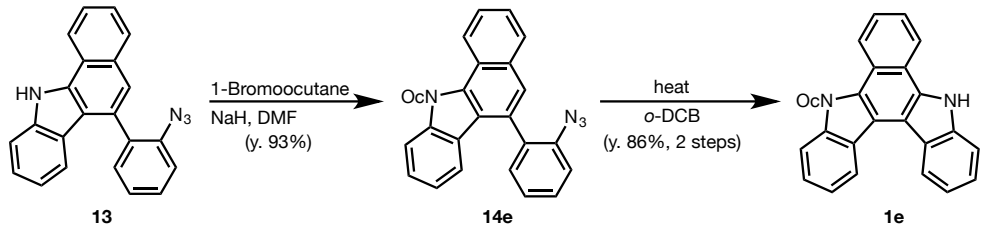

13 14e 1e

To a stirred solution of azide **13** (300 mg, 0.90 mmol) in dry DMF (10 mL) under argon was added NaH (72 mg, 1.79 mmol, 60% in mineral oil) at room temperature. After stirring for 10 min at room temperature, 1-bromooctane (232 μL, 1.34 mmol) was added to the mixture. After stirring for 3 h at room temperature, the mixture was diluted with water and extracted with Et_2O three times. The combined organic layer was washed with brine, dried over anhydrous $MgSO_4$, and concentrated in vacuo. The crude mixture was used without further purification.

A solution of azide **14e** in 1,2-dichlorobenzene (15 mL) under argon was stirred for 6 h at 160 °C. After cooling to room temperature, the reaction mixture was concentrated in vacuo and the residue was chromatographed on silica gel (hexane/CH_2Cl_2 = 2/1) to afford **1e** (324 mg, 86%, over 2 steps) as a pale yellow solid.

Mp. 141-142 °C; IR (KBr) ν /cm^{-1} : 3669, 3403, 3047, 2923, 2850, 1652, 1467, 1436, 1405, 1362, 1335, 1093, 756, 738, 482; ^{1}H NMR (400 MHz, $CDCl_3$) δ/ppm :12.27 (s, 1H), 8.86 (d, *J* = 7.8 Hz, 1H), 8.80 (d, *J* = 7.8 Hz, 1H), 8.71-8.76 (m, 2H), 7.87 (d, *J* = 8.6 Hz, 1H), 7.73-7.77 (m, 3H), 7.53 (dd, *J* = 8.6, 7.7 Hz, 1H), 7.47 (dd, *J* = 8.6, 7.7 Hz, 1H), 7.41 (dd, *J* = 8.6, 7.7 Hz, 1H), 7.36 (dd, *J* = 8.6, 7.7 Hz, 1H), 4.93 (d, *J* = 7.5 Hz, 2H), 1.95 (qn, *J* = 7.5 Hz, 2H), 1.43 (qn, *J* = 7.5 Hz, 2H), 1.32 (qn, *J* = 7.5 Hz, 2H), 1.15-1.26 (m, 6H), 0.81 (t, *J* = 6.8 Hz, 3 H); HR-MS (FD) calcd. for $C_{30}H_{30}N_2$: 418.2409; found: 418.2392.

15) Preparation of 10,10'-{[1,2-phenylene]bis(methylene)}bis(5-octyl-5,10-dihydrobenzo[*a*]indolo[2,3-*c*]carbazole) **2d'**

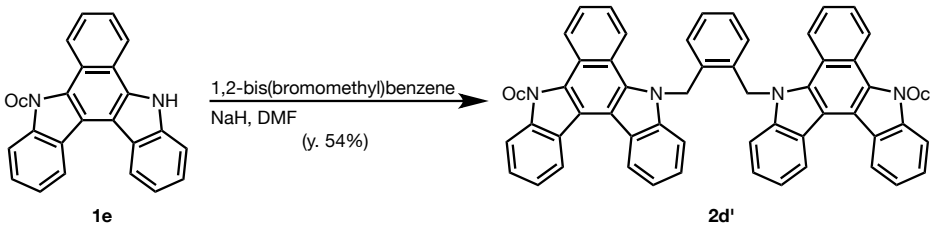

To a stirred solution of **1e** (200 mg, 0.47 mmol) in dry DMF (5 mL) under argon was added NaH (38.2 mg, 0.96 mmol, 60% in mineral oil) at room temperature. After stirring for 10 min at room temperature, 1,2-bis(bromomethyl)benzene (63.1 mg, 0.24 mmol) was added to the mixture. After stirring for 3 h at room temperature, the mixture was diluted with water and the precipitates were filtered. The residue was washed with $CHCl_3$ and water to afford **2d'** (98.7 mg, 54%) as a pale yellow solid.

Mp. 238 °C; IR (KBr) ν /cm^{-1} : 3675, 3447, 3047, 2953, 2924, 2852, 2359, 1654, 1468, 1424, 1399, 1340, 1164, 1105, 732; ^{1}H NMR (400 MHz, $CDCl_3$) δ/ppm :8.98 (d, *J* = 8.0 Hz, 2H), 8.94 (d, *J* = 8.0 Hz, 2H), 8.80 (d, *J* = 8.4 Hz, 2H), 8.60 (d, *J* = 8.4 Hz, 2H), 7.84 (d, *J* = 8.4 Hz, 4H), 7.75 (ddd, *J* = 8.4, 7.7, 1.2 Hz, 2H), 7.63 (ddd, *J* = 8.4, 7.7, 1.2 Hz, 2H), 7.59 (ddd, *J* = 8.4, 7.7, 1.2 Hz, 2H), 7.57 (ddd, *J* = 8.4, 7.7, 1.2 Hz, 2H), 7.50 (ddd, *J* = 8.4, 7.7, 1.2 Hz, 2H), 7.50 (ddd, *J* = 8.4, 7.7, 1.2 Hz, 2H), 7.44 (ddd, *J* = 8.4, 7.7, 1.2 Hz, 2H), 7.05 (dd, *J* = 6.0, 3.3 Hz, 2H), 6.84 (dd, *J* = 6.0, 3.3 Hz, 2H), 6.43 (2,br-s, 4H), 4.93 (t, *J* = 7.7 Hz, 4H), 1.99 (qn, *J* = 7.7 Hz, 4H), 1.45 (qn, *J* = 7.7 Hz, 4H), 1.34 (qn, *J* = 7.7 Hz, 6H), 1.19-1.29 (m, 12H), 0.86 (t, *J* = 7.7 Hz, 6 H) ; HR-MS (FD) calcd. for $C_{66}H_{66}N_4$: 938.5288; found: 938.5286.

16) Preparation of 10,10'-{[1,3-phenylene]bis(methylene)}bis(5-octyl-5,10-dihydrobenzo[*a*]indolo[2,3-*c*]carbazole) **2e'**

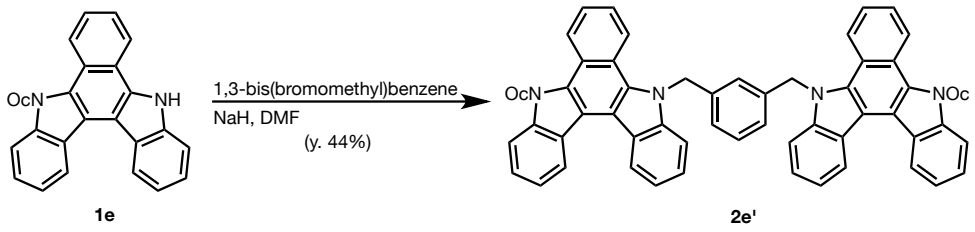

To a stirred solution of **1e** (200 mg, 0.47 mmol) in dry DMF (5 mL) under argon was added NaH (38.2 mg, 0.96 mmol, 60% in mineral oil) at room temperature. After stirring for 10 min at room temperature, a solution of 1,3-bis(bromomethyl)benzene (63.1 mg, 0.24 mmol) was added to the mixture. After stirring for 3 h at room temperature, the mixture was diluted with water and the precipitates were filtered. The residue was washed with $CHCl_3$ and water to afford **2e'** (120 mg, 44%) as a pale yellow solid.

Mp. 175 °C; IR (KBr) ν /cm^{-1} : 3447, 3048, 2923, 2852, 1652, 1608, 1471, 1424, 1400, 1340, 1167, 1141, 1107, 921, 730; ^{1}H NMR (400 MHz, $CDCl_3$) δ/ppm :8.85 (dd, *J* = 10.4, 8.7 Hz, 4H), 8.63 (d, *J* = 8.7 Hz, 2H), 8.36 (d, *J* = 8.7 Hz, 2H), 7.87 (d, *J* = 8.8 Hz, 2H), 7.67 (d, *J* = 8.8 Hz, 2H), 7.55 (ddd, *J* = 8.5, 7.2, 3.2 Hz, 4H), 7.45 (ddd, *J* = 8.5, 7.2, 3.2 Hz, 4H), 7.42 (ddd, *J* = 8.5, 7.2, 3.2 Hz, 4H), 7.39 (ddd, *J* = 8.5, 7.2, 3.2 Hz, 4H), 7.28 (dd, *J* = 8.8, 7.5 Hz, 1H), 7.15 (s, 1H), 7.11 (dd, *J* = 8.8, 7.5 Hz, 2H), 7.06 (d, *J* = 7.2 Hz, 2H), 6.06 (br-s, 4H), 4.83 (t, *J* = 7.7 Hz, 4H), 1.91 (qn, *J* = 7.7 Hz, 4H), 1.40 (qn, *J* = 7.7 Hz, 4H), 1.30 (qn, *J* = 7.7 Hz, 4H), 1.15-1.25 (m, 12H), 0.80 (t, *J* = 7.7 Hz, 6 H); HR-MS (FD) calcd. for $C_{66}H_{66}N_4$: 938.5287; found: 938.5268.

<Preparation of BIC dimers 2g – 2i>

17) Preparation of 10,10'-{[1,8-naphthalenediyl]bis(methylene)}bis(5-butyl-5,10-dihydrobenzo[*a*]indolo[2,3-*c*]carbazole) **2g**

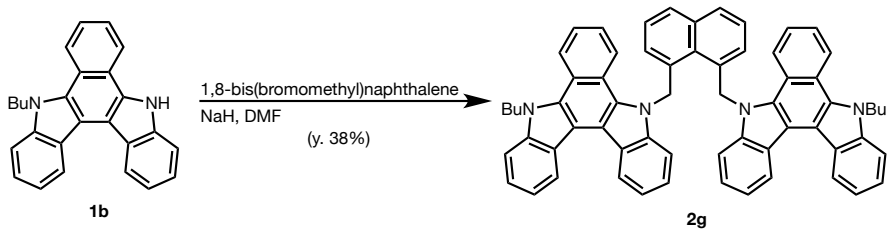

1b 2g

To a stirred solution of **1b** (100 mg, 0.28 mmol) in dry DMF (6 mL) under argon was added NaH (13 mg, 0.33 mmol, 60% in mineral oil) at room temperature. After stirring for 10 min at room temperature, a solution of 1,8-bis(bromomethyl)naphthalene (43 mg, 0.14 mmol) was added to the mixture. After stirring for 7 h at room temperature, the mixture was diluted with water and extracted with ether three times. The combined

organic layer was washed with brine, dried over anhydrous $MgSO_4$, and concentrated in vacuo. The residue was chromatographed on silica gel (hexane/CH_2Cl_2 = 2/1) to give **2g** (46 mg, 38%) as a yellow solid.

Mp. 189-190 °C; IR (KBr) ν /cm^{-1} : 3450, 3052, 2995, 2860, 1608, 1468, 1424, 1400, 1340, 1267, 1172, 1139, 1105, 917, 731; ^{1}H NMR (400 MHz, DMSO-d_6, 393 K) δ/ppm :8.99 (d, J = 8.0 Hz, 2H), 8.96 (d, J = 8.0 Hz, 2H), 8.81 (d, J = 8.7 Hz, 2H), 8.66 (d, J = 8.7 Hz, 2H), 8.03 (d, J = 7.9 Hz, 4H), 7.92 (d, J = 8.7 Hz, 2H), 7.73 (dd, J = 8.7, 7.9 Hz, 2H), 7.55-6.63 (m, 6H), 7.50 (dd, J = 8.9, 7.7 Hz, 2H), 7.45 (dd, J = 8.9, 7.7 Hz, 2H), 7.41 (dd, J = 8.9, 7.7 Hz, 2H), 7.23 (br-s, 4H), 7.10 (d, J = 7.7 Hz, 2H), 4.95 (t, J = 7.8 Hz, 4H), 1.92 (qn, J = 7.7 Hz, 4H), 1.39 (sext, J = 7.7 Hz, 4H), 0.90 (t, J = 7.7 Hz, 6H); HR-MS (FD) calcd. for $C_{64}H_{52}N_4$: 876.4192; found: 876.4182.

18) Preparation of 10,10'-{[2,2'-biphenyldiyl]bis(methylene)}bis(5-butyl-5,10-dihydrobenzo[*a*]indolo[2,3-*c*]carbazole) **2h**

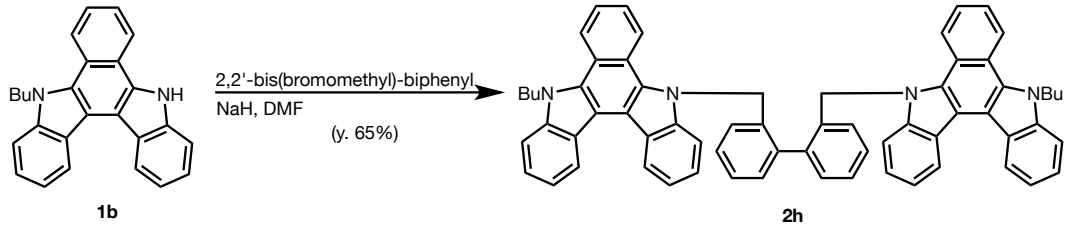

1b **2h**

To a stirred solution of **1b** (200 mg, 0.55 mmol) in dry DMF (6 mL) under argon was added NaH (44.2 mg, 1.10 mmol, 60% in mineral oil) at room temperature. After stirring for 10 min at room temperature, a solution of 2,2'-bis(bromomethyl)-biphenyl (94 mg, 0.28 mmol) was added to the mixture. After stirring for 4 h at room temperature, the mixture was diluted with water and the precipitates were filtered through *Kiriyama* funnel. The residue was chromatographed on silica gel (hexane/CH_2Cl_2 = 2/1) followed by recrystallization (1,1,2,2-tetrachloroethane) to give **2h** (160 mg, 65%) as a pale yellow solid.

Mp. 290 °C; IR (KBr)ν/cm^{-1} : 3447, 3050, 2954, 2865, 1539, 1507, 1498, 1496, 1467, 1424, 1399, 1363, 1339, 1157, 1139, 1106, 1032, 917, 816, 733; ^{1}H NMR (400 MHz, DMSO-d_6) δ/ppm :8.94-8.99 (m, 4H), 8.77 (d, J = 8.9 Hz, 2H), 8.41 (d, J = 8.5 Hz, 2H), 7.92 (d, J = 8.5 Hz, 2H), 7.86 (d, J = 7.8 Hz, 2H), 7.77-7.80 (m, 2H), 7.56-7.64 (m, 6H),

7.44-7.50 (m, 8H), 7.34 (ddd, *J* = 8.3, 7.7, 1.2 Hz, 2H), 7.00 (d, *J* = 7.7 Hz, 2H), 6.10 (d, *J* = 18.5 Hz, 2H), 6.00 (d, *J* = 18.5 Hz, 2H), 4.95 (t, *J* = 7.5 Hz, 2H), 1.94 (qn, *J* = 7.5 Hz, 4H), 1.43 (sext, *J* = 7.5 Hz, 4H), 0.94 (t, *J* = 7.5 Hz, 6H); HR-MS (FD) calcd. for $C_{66}H_{54}N_4$: 902.4349; found: 902.4335.

19) Preparation of 10,10'-{[(*S*)-1,1'-binaphthalene-2,2'diyl]bis(methylene)}bis(5-butyl-5,10-dihydrobenzo[*a*]indolo[2,3-*c*]carbazole) **2i**

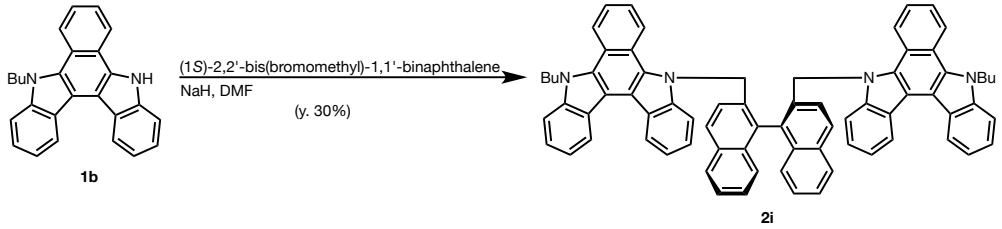

To a stirred solution of **1b** (171 mg, 0.47 mmol) in dry DMF (5 mL) under argon was added NaH (38.0 mg, 0.94 mmol, 60% in mineral oil) at room temperature. After stirring for 10 min at room temperature, (1*S*)-2,2'-bis(bromomethyl)-1,1'-binaphthalene (104 mg, 0.24 mmol) was added to the mixture. After stirring for 5 h at room temperature, the mixture was diluted with water and the precipitates were filtered. The residue was washed with $CHCl_3$ and recrystallized from 1,1,2,2-tetrachloroethane to afford **2f** (72 mg, 30%) as a pale yellow solid.

Mp. 222−224 °C; IR (KBr)ν/cm^{-1} :3447, 3052, 2955, 2926, 2865, 2353, 1699, 1635, 1559, 1467, 1424, 1399, 1340, 1176, 1105, 733; ^{1}H NMR (400 MHz, DMSO-d_6) δ/ppm :8.96 (d, *J* = 7.7 Hz, 2H), 8.92 (d, *J* = 7.7 Hz, 2H), 8.73 (d, *J* = 8.5 Hz, 2H), 8.35 (d, *J* = 8.5 Hz, 2H), 8.09 (dd, *J* = 9.6, 8.3 Hz, 4H), 7.88 (d, *J* = 8.3 Hz, 2H), 7.82 (dd, *J* = 8.8, 7.7 Hz, 2H), 7,88 (d, *J* = 7.7 Hz, 2H), 7.66 (dd, *J* = 9.6, 8.3 Hz, 2H), 7.55 (dd, *J* = 8.8, 7.7 Hz, 4H),7.52 (d, *J* = 8.3 Hz, 2H), 7.47 (d, *J* = 8.0 Hz, 2H), 7.43 (d, *J* = 8.0 Hz, 2H), 7.31-7.38 (m, 6H), 5.99 (d, *J* = 19.1 Hz, 2H), 5.75 (d, *J* = 19.1 Hz, 2H), 4.91 (t, *J* = 7.4 Hz, 2H), 1.92 (qn, *J* = 7.7 Hz, 2H), 1.41 (sext, *J* = 7.7 Hz, 2H), 0.93 (t, *J* = 7.7 Hz, 2H) ; HR-MS (FD) calcd. for $C_{74}H_{58}N_4$: 1002.4662; found: 1002.4642.

<Preparation of dimer 2>

20) Preparation of 10,10'-{[5-(*tert*-butyl)-1,3-phenylene]bis(methylene)}bis(5-butyl-5,10-dihydrobenzo[*a*]indolo[2,3-*c*]carbazole) **2**

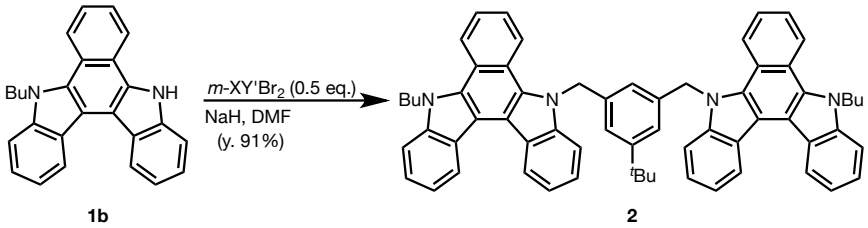

1b **2**

To a stirred solution of **1b** (150 mg, 414 μmol) and 1,3-bis(bromomethyl)-5-*tert*-butylbenzene (66 mg, 207 μmol) in dry DMF (5 mL) under argon was added NaH (33 mg, 828 μmol, 60% in mineral oil) at room temperature. After stirring for 1.5 h at room temperature, the mixture was diluted with water and extracted with EtOAc three times. The combined organic layer was washed with H_2O and brine, dried over anhydrous $MgSO_4$, and concentrated in vacuo. The residue was chromatographed on silica-gel (hexane/CH_2Cl_2 = 2.2/1) to give **2** (166 mg, 91%) as a pale-yellow solid.

Mp 129 °C (decomp.); IR (KBr) ν/cm^{-1} :3425, 3053, 2962, 2867, 2117, 1918, 1600, 1576, 1522, 1494, 1453, 1433, 1394, 1379, 1365, 1337, 1300, 1285, 1258, 1226, 1211, 1182, 1165, 1153, 1136, 1127, 1097, 1038, 990, 934, 879, 740, 707, 664, 657, 569; ^{1}H NMR (400 MHz, DMSO-*d*6) δ/ppm : 8.84 (d, 2H, *J* = 8.0 Hz), 8.78 (d, 2H, *J* = 8.0 Hz), 8.56 (d, 2H, *J* = 8.5 Hz), 8.32 (d, 2H, *J* = 8.5 Hz), 7.84 (d, 2H, *J* = 8.5 Hz), 7.58 (d, 2H, *J* = 8.0 Hz), 7.54 (dd, 2H, *J* = 7.5, 7.5 Hz), 7.48 (dd, 2H, *J* = 7.5, 7.5 Hz), 7.41 (dd, 2H, *J* = 7.5, 7.5 Hz), 7.37 (dd, 2H, *J* = 7.5, 7.5 Hz), 7.32 (dd, 2H, *J* = 7.5, 7.5 Hz), 7.27 (s, 2H), 7.06 (dd, 2H, *J* = 7.5, 7.5 Hz), 6.76 (s, 1H), 5.91 (s, 2H), 4.78 (t, 4H, *J* = 7.2 Hz), 1.87 (t, qn, *J* = 7.2 Hz), 1.37 (sext, 4H, *J* = 7.2 Hz), 1.05 (s, 9H), 0.90 (t, 4H, *J* = 7.2 Hz); ^{13}C NMR (100 MHz, DMSO-*d*6) δ/ppm: 152.18, 141.78, 139.09, 131.53, 130.98, 125.04, 124.85, 124.72, 123.70, 123.18, 122.79, 122.76, 122.71, 122.03, 121.76, 121.72, 119.96, 119.67, 114.39, 114.32, 110.65, 110.50, 50.28, 45.99, 34.78, 32.03, 31.35, 19.94, 14.19; HRMS (FD, m/z) [(M+H^+)]calcd. for $C_{64}H_{58}N_4$: 882.4661; found: 882.4671.

<Preparation of trimer 3>

21) Preparation of 5-[3-(bromomethyl)-5-(*tert*-butyl)benzyl]-10-butyl-5,10-dihydrobenzo[*a*]indolo[2,3-*c*]carbazole **15**

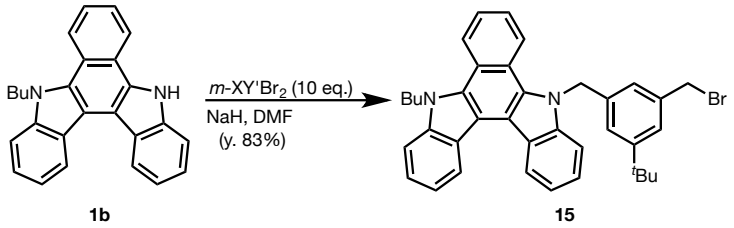

1b **15**

To a stirred solution of **1b** (200 mg, 552 μmol) in dry DMF (5 mL) under argon was added NaH (44 mg, 1.10 mmol, 60% in mineral oil) at room temperature. After stirring for 10 min at room temperature, a solution of 1,3-bis(bromomethyl)-5-*tert*-butylbenzene (177 mg, 5.52 mmol) in dry DMF (4 mL) was added dropwise over 10 min to the mixture. After stirring for 1.5 h at room temperature, the mixture was diluted with water and extracted with Et_2O three times. The combined organic layer was washed with H_2O and brine, dried over anhydrous $MgSO_4$, and concentrated in vacuo. The residue was chromatographed on silica-gel (hexane/CH_2Cl_2 = 5/1 to 3/1) to give **15** (262 mg, 83%) as a pale-yellow solid.

Mp 180 °C; IR (KBr) ν/cm^{-1} :3789, 3444, 3052, 2961, 2929, 2871, 2565, 1657, 1650, 1639, 1602, 1470, 1425, 1401, 1383, 1363, 1340, 1294, 1266, 1227, 1214, 1175, 1157, 1141, 1107, 1033, 919, 734, 727, 712, 596, 577, 479; ^{1}H NMR (400 MHz, DMSO-*d*6) δ/ppm : 8.94 (dd, 2H, *J* = 8.5, 8.5 Hz), 8.77 (d, 1H, *J* = 8.5 Hz), 8.57 (d, 1H, *J* = 8.5 Hz), 7.91 (d, 1H, *J* = 8.2 Hz), 7.77 (d, 1H, *J* = 8.2 Hz), 7.70 (dd, 1H, *J* = 7.5, 7.5 Hz), 7.38–7.56 (m, 7H), 7.27 (s, 2H), 7.04 (s, 1H), 6.13 (s, 2H), 4.93 (t, 2H, *J* = 7.3 Hz), 4.56 (s, 2H), 1.93 (qn, 2H, *J* = 7.3 Hz), 1.41 (sext, 2H, *J* = 7.3 Hz), 1.20 (s, 9H), 0.92 (t, 3H, *J* = 7.3 Hz); ^{13}C NMR (100 MHz, DMSO-*d*6) δ/ppm: 152.21, 142.06, 141.35, 139.09, 138.76, 131.83, 131.13, 125.6, 125.52, 125.24, 125.05, 124.89, 124.43, 124.07, 123.96, 123.54, 122.93, 122.81, 122.48, 122.33, 122.28, 122.12, 121.9, 120.35, 119.86, 114.55, 114.43, 110.82, 50.41, 46.12, 35.29, 34.9, 32.09, 31.41, 19.96, 14.23; HRMS (FD, m/z) [(M+H^+)]calcd. for $C_{38}H_{37}N_2Br_1$: 600.2140; found: 600.2157.

22) Preparation of 5,10-bis{3-(*tert*-butyl)-5-[(10-butylbenzo[*a*]indolo[2,3-*c*]carbazol-5(10*H*)-yl)methyl]benzyl}-5,10-dihydrobenzo[*a*]indolo[2,3-*c*]carbazole **3**

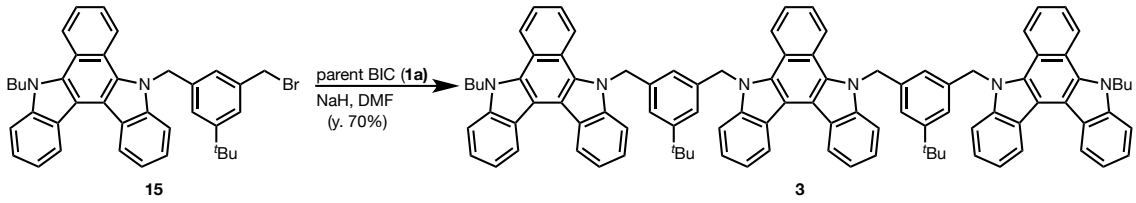

To a stirred solution of **15** (203 mg, 337 μmol) and **1a** (52 mg, 169 μmol) in dry DMF (5 mL) under argon was added NaH (30 mg, 674 μmol, 60% in mineral oil) at room temperature. After stirring for 3 h at room temperature, the mixture was diluted with water and the precipitates were filtered through *Kiriyama* funnel and washed with Et_2O, water and EtOH. The residue was chromatographed on silica-gel (hexane/CH_2Cl_2 = 3/1) to give **3** (159 mg, 70%) as a pale-yellow solid.

Mp 176 °C (decomp.); IR (KBr) ν/cm^{-1} :3448, 3050, 2958, 2921, 2872, 1605, 1470, 1424, 1399, 1362, 1339, 1268, 1201, 1171, 1140, 1107, 1041, 1032, 920, 734, 604, 477; ^{1}H NMR (400 MHz, DMSO-*d*6) δ/ppm : 8.77 (dd, 4H, *J* = 8.5, 8.5 Hz), 8.71 (d, 2H, *J* = 8.2 Hz), 8.46 (d, 2H, *J* = 8.5 Hz), 8.24 (d, 2H, *J* = 8.5 Hz), 8.08 (dd, 2H, *J* = 6.4, 3.2 Hz), 7.73 (d, 2H, *J* = 8.2 Hz), 7.58 (d, 2H, *J* = 8.2 Hz), 7.53 (d, 2H, *J* = 8.2 Hz), 7.45 (dd, 2H, *J* = 7.6, 7.6 Hz), 7.26–7.41 (m, 14H), 6.94 (dd, 2H, *J* = 7.6, 7.6 H), 6.75 (dd, 2H, *J* = 6.4, 3.2 Hz), 6.66 (s, 2H), 5.86 (s, 4H), 5.75 (s, 4H), 4.68 (t, 4H, *J* = 7.0 Hz), 1.79 (qn, 4H, *J* = 7.0 Hz), 1.29 (sext, 4H, *J* = 7.0 Hz), 1.06 (s, 18H), 0.82 (t, 6H, *J* = 7.0 Hz); ^{13}C NMR (100 MHz, DMSO-*d*6) δ/ppm: 152.20, 141.74, 141.60, 141.18, 139.09, 131.51, 131.41, 130.92, 124.95, 124.80, 124.65, 124.46, 124.17, 123.70, 123.65, 123.14, 123.11, 123.06, 122.77, 122.72, 122.69, 122.63, 122.31, 122.26, 122.13, 121.96, 121.74, 121.51, 121.47, 119.91, 119.86, 119.62, 114.30, 114.25, 114.21, 110.56, 110.48, 110.41, 110.33, 50.27, 50.02, 45.92, 34.79, 31.99, 31.37, 19.89, 14.13; HRMS (FD, m/z) [(M+H^+)]calcd. for $C_{98}H_{86}N_6$:1346.6914; found: 1346.6934.

<Preparation of tetramer 4, 7, and 8>

23) Preparation of 6-(2-azidophenyl)-11-[3-(bromomethyl)-5-(*tert*-butyl)benzyl]-11*H*-benzo[*a*]carbazole **16**

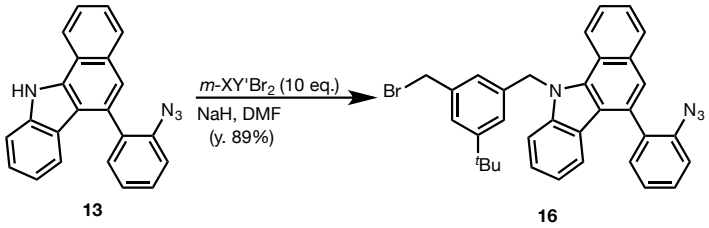

To a stirred solution of **13** (300 mg, 897 μmol) in dry DMF (10 mL) under argon was added NaH (72 mg, 1.79 mmol, 60% in mineral oil) at room temperature. After stirring for 10 min at room temperature, a solution of 1,3-bis(bromomethyl)-5-*tert*-butylbenzene (2.87 g, 8.97 mmol) in dry DMF (5 mL) was added dropwise over 10 min to the mixture. After stirring for 1.5 h at room temperature, the mixture was diluted with water and extracted with Et_2O three times. The combined organic layer was washed with H_2O and brine, dried over anhydrous $MgSO_4$, and concentrated in vacuo. The residue was chromatographed on silica-gel (hexane/CH_2Cl_2 = 5/1 to 4/1 to 3/1) to give **16** (460 mg, 89%) as a pale-yellow solid.

Mp 163–164 °C; IR (KBr) ν/cm^{-1} :3629, 2444, 3050, 2956, 2870, 1605, 1540, 1470, 1424, 1399, 1292, 1267, 1201, 1173, 1157, 1139, 1107, 1032, 1018, 986, 919, 733, 587, 477; ^{1}H NMR (400 MHz, $CDCl_3$) δ/ppm : 8.27 (d, 4H, *J* = 8.5 Hz), 8.00 (dd, 1H, *J* = 7.7, 1.5 Hz), 7.60 (ddd, 1H, *J* = 8.5, 77., 1.5 Hz), 7.33–7.54 (m, 10H), 7.11 (s, 1H), 7.07 (d, 2H, *J* = 3.7 Hz), 5.96 (d, 2H, *J* = 3.7 Hz), 4.38 (s, 2H), 1.30 (s, 9H); ^{13}C NMR (100 MHz, $CDCl_3$) δ/ppm: 152.86, 141.78, 138.76, 138.43, 138.01, 135.84, 132.97, 132.94, 131.86, 131.74, 129.46, 129.38, 125.59, 125.54, 125.17, 125.01, 123.85, 123.49, 123.14, 122.21, 122.03, 121.44, 121.24, 120.18, 118.62, 118.24, 109.42, 50.47, 34.86, 33.8, 31.29; HRMS (FD, m/z) [(M+H^+)]calcd. for $C_{34}H_{29}N_4Br_1$:572.1576; found: 572.1586.

24) Preparation of 5-{3-[(6-(2-azidophenyl)-11*H*-benzo[*a*]carbazol-11-yl)methyl]-5-(*tert*-butyl)benzyl}-10-butyl-5,10-dihydrobenzo[*a*]indolo[2,3-*c*]carbazole **17**

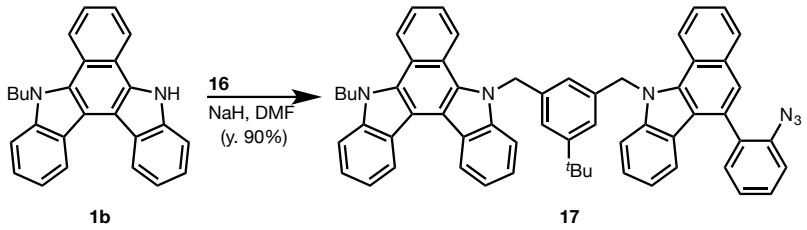

1b **17**

To a stirred solution of **1b** (100 mg, 256 μmol) and **16** (147 mg, 256 μmol) in dry DMF (4 mL) under argon was added NaH (16 mg, 384 μmol, 60% in mineral oil) at room temperature. After stirring for 5 h at room temperature, the mixture was diluted with water and the precipitates were filtered through *Kiriyama* funnel and washed with MeOH. The residue was chromatographed on silica-gel (hexane/CH_2Cl_2 = 2/1) to give **17** (197 mg, 90%) as a pale-yellow solid.

Mp 181 °C (decomp); IR (KBr) ν/cm^{-1} :3439, 3051, 2959, 2870, 2345, 2116, 2090, 1919, 1605, 1576, 1522, 1470, 1454, 1425, 1399, 1333, 1300, 1202, 1174, 1158, 1140, 1107, 1033, 933, 920, 870, 736, 709, 478; ^{1}H NMR (400 MHz, DMSO-*d*6) δ/ppm: 8.90 (ddd, 2H, *J* = 7.6, 7.6, 1.1 Hz), 8.73 (d, 1H, *J* = 8.6 Hz), 8.43 (d, 1H, *J* = 8.6 Hz), 8.31 (d, 1H, *J* = 8.6 Hz), 8.00 (d, 1H, *J* = 7.6 Hz), 7.91 (d, 1H, *J* = 8.2 Hz), 7.62–7.69 (m, 4H), 7.56 (dd, 1H, *J* = 7.6, 7.6 Hz), 7.52 (d, 1H, *J* = 8.2 Hz), 7.39–7.47 (m, 7H), 7.28 (ddd, 1H, *J* = 7.6, 7.6, 1.1 Hz), 7.24 (s, 1H), 7.21 (dd, 1H, *J* = 7.6, 7.6 Hz), 7.16 (s, 1H), 7.13 (ddd, 1H, *J* = 7.6, 7.6, 1.1 Hz), 6.97 (dd, 1H, *J* = 7.6, 7.6 Hz), 6.92 (s, 1H), 6.86 (d, 1H, *J* = 7.6 Hz), 6.01 (s, 2H), 5.97 (s, 2H), 4.92 (t, 2H, *J* = 7.4 Hz), 1.92 (qn, 2H, *J* = 7.4 Hz), 1.41 (sext, 2H, *J* = 7.3 Hz), 0.99 (s, 9H), 0.92 (t, 3H, *J* = 7.4 Hz) ; ^{13}C NMR (100 MHz, DMSO-*d*6) δ/ppm: 152.23, 142, 141.45, 141.32, 139.13, 138.9, 138.38, 135.6, 134.88, 132.9, 132.85, 131.71, 131.68, 131.09, 130.35, 129.43, 125.9, 125.76, 125.46, 125.31, 125.24, 125.04, 124.99, 124.84, 124.78, 123.89, 123.4, 122.83, 122.76, 122.68, 122.59, 122.41, 122.39, 122.18, 122.05, 121.85, 121.74, 121.44, 121.25, 120.62, 120.23, 120.18, 119.78, 117.89, 114.51, 114.44, 110.77, 110.65, 110.45, 110.4, 50.46, 49.49, 46.1, 34.72, 32.1, 31.23, 19.96, 14.23; HRMS (FD, m/z) [(M+H^+)]calcd. for $C_{60}H_{50}N_6$: 854.4097; found: 854.4079.

25) Preparation of 5-{3-[benzo[*a*]indolo[2,3-*c*]carbazol-5(10*H*)-ylmethyl]-5-(tert-butyl)benzyl}-10-butyl-5,10-dihydrobenzo[*a*]indolo[2,3-*c*]carbazole **17**

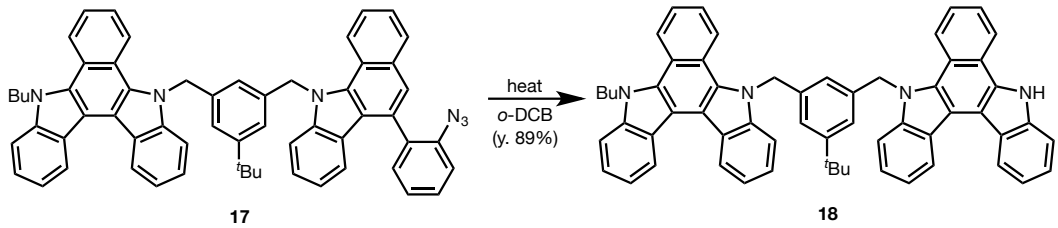

17 **18**

A solution of **17** (392 mg, 458 μmol) in 1,2-dichlorobenzene (7 mL) under argon was stirred for 18 h at 160 °C. After cooling to room temperature, the reaction mixture was reprecipitated with hexane and the precipitates were filtered through *Kiriyama* funnel. The residue was washed with MeOH to give **18** (338 mg, 89%) as a pale-yellow solid. Mp 158 °C (decomp); IR (KBr) ν/cm^{-1} :3433, 3050, 2958, 2926, 2866, 1918, 1605, 1470, 1434, 1402, 1362, 1336, 1291, 1267, 1238, 1173, 1157, 1138, 1107, 1092, 1036, 921, 734, 593, 577, 476; ^{1}H NMR (400 MHz, DMSO-*d*6) δ/ppm : 12.25 (s, 1H), 8.80 (d, 1H, *J* = 8.1 Hz), 8.85 (d, 1H, *J* = 7.7 Hz), 8.81 (dd, 1H, *J* = 8.5, 8.5 Hz), 8.65 (d, 1H, *J* = 7.7 Hz), 8.64 (d, 1H, *J* = 8.5 Hz), 8.39 (d, 1H, *J* = 8.5 Hz), 8.38 (d, 1H, *J* = 8.5 Hz), 7.76 (d, 1H, *J* = 8.1 Hz), 7.66 (d, 1H, *J* = 8.1 Hz), 7.62 (d, 1H, *J* = 7.7 Hz), 7.51–7.58 (m, 3H), 7.49 (dd, 1H, *J* = 7.7, 7.7 Hz), 7.34–7.44 (m, 6H), 7.25 (s, 1H), 7.22 (s, 1H), 7.18 (ddd, 1H, *J* = 7.7, 7.7, 1.0 Hz), 7.11 (dd, 1H, *J* = 7.7, 7.7 Hz), 6.86 (s, 1H), 6.02 (s, 2H), 5.94 (s, 2H), 4.85 (t, 2H, *J* = 7.3 Hz), 1.89 (qn, 2H, *J* = 7.3 Hz), 1.39 (sext, 2H, *J* = 7.3 Hz), 1.00 (s, 9H), 0.91 (t, 3H, *J* = 7.3 Hz); ^{13}C NMR (100 MHz, DMSO-*d*6) δ/ppm: 152.19, 141.93, 141.32, 141.27, 139.42, 139.18, 139.11, 132.13, 131.64, 131.04, 130.7, 125.28, 125.16, 125.11, 124.97, 124.78, 124.72, 124.66, 124.39, 123.8, 123.53, 123.28, 123.08, 122.93, 122.8, 122.71, 122.66, 122.64, 122.45, 122.37, 122.24, 122.16, 122.12, 121.79, 121.74, 121.69, 121, 120.09, 119.97, 119.74, 119.44, 114.76, 114.46, 114.39, 112.34, 112.04, 110.72, 110.62, 110.51, 110.39, 50.39, 49.98, 46.04, 34.73, 32.05, 31.3, 19.95, 14.21; HRMS (FD, m/z) [(M+H^{+})]calcd. for $C_{60}H_{50}N_4$:826.4035; found: 826.4036.

26) Preparation of 10,10'-{[5-(tert-butyl)-1,3-phenylene]bis(methylene)}bis{5-[3-(tert-butyl)-5-((10-butylbenzo[*a*]indolo[2,3-*c*]carbazol-5(10*H*)-yl)methyl)benzyl]-5,10-dihydrobenzo[*a*]indolo[2,3-*c*]carbazole} **4**

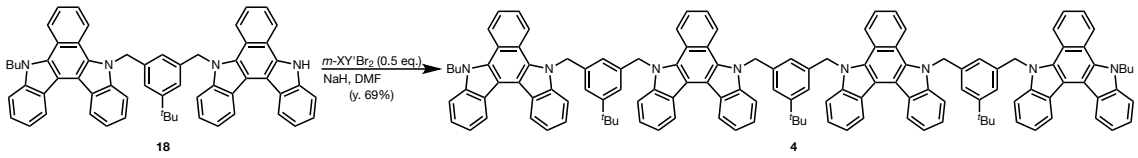

18 4

To a stirred solution of **18** (150 mg, 181 μmol) and 1,3-bis(bromomethyl)-5-*tert*-butylbenzene (29 mg, 91 μmol) in dry DMF (4 mL) under argon was added NaH (11 mg, 272 μmol, 60% in mineral oil) at room temperature. After stirring for 3 h at room temperature, the mixture was diluted with water and the precipitates were filtered through *Kiriyama* funnel and washed with MeOH. The residue was reprecipitated from CH_2Cl_2/hexane to give **4** (113 mg, 69%) as a pale-yellow solid.

Mp 174 °C (decomp); IR (KBr) ν/cm^{-1} :3744, 3442, 3050, 2956, 2926, 2869, 1918, 1653, 1605, 1540, 1471, 1424, 1399, 1362, 1339, 1292, 1269, 1218, 1200, 1171, 1157, 1140, 1107, 1032, 1018, 920, 734, 579; ^{1}H NMR (400 MHz, DMSO-*d*6) δ/ppm: 8.74 (d, 2H, *J* = 8.0 Hz), 8.69 (dd, 4H, *J* = 8.0, 8.0 Hz), 8.67 (dd, 2H, *J* = 8.0, 1.7 Hz), 8.42 (d, 2H, *J* = 8.5 Hz), 8.20 (d, 2H, *J* = 8.5 Hz), 8.08 (ddd, 4H, *J* = 6.9, 2.3, 2.3 Hz), 7.70 (d, 2H, *J* = 8.5 Hz), 7.49 (dd, 4H, *J* = 9.6, 9.6 Hz), 7.43 (dd, 4H, *J* = 8.5, 2.8 Hz), 7.20–7.36 (m, 22H), 6.94 (dd, 2H, *J* = 8.0, 8.0 Hz), 6.79 (ddd, 4H, *J* = 6.8, 2.3, 2.3 Hz), 6.66 (s, 3H), 5.79 (s, 4H), 5.73 (s, 4H), 5.72 (s, 4H), 4.66 (t, 4H, *J* = 7.4 Hz), 1.79 (qn, 4H, *J* = 7.4 Hz), 1.30 (sext, 4H, *J* = 7.4 Hz), 1.04 (s, 9H), 1.01 (s, 18H), 0.82 (t, 6H, *J* = 7.4 Hz); ^{13}C NMR (100 MHz, DMSO-*d*6) δ/ppm: 152.29, 141.88, 141.84, 141.75, 141.33, 139.04, 138.97, 131.69, 131.65, 131.14, 124.81, 124.80, 124.73, 124.72, 124.71, 124.69, 124.61, 124.60, 124.36, 124.15, 124.15, 124.13, 123.60, 123.59, 123.21, 123.20, 123.14, 123.13, 123.02, 123.01, 122.73, 122.72, 122.71, 122.65, 122.64, 122.62, 122.54, 122.48, 122.35, 122.04, 121.74, 121.73, 121.61, 119.85, 119.84, 119.82, 119.58, 119.57, 114.49, 114.39, 110.50, 110.50, 110.33, 110.29, 50.42, 50.23, 46.07, 34.75, 34.71, 31.94, 31.35, 31.32, 19.86, 14.28, 14.00; HRMS (FD, m/z) [(M+H$^+$)]calcd. for $C_{132}H_{114}N_8$: 1810.9166; found: 1810.9188.

27) Preparation of 1,2-bis{[10-(3-(*tert*-butyl)-5-((10-butylbenzo[*a*]indolo[2,3-*c*]carbazol-5(10*H*)-yl)methyl)benzyl)benzo[*a*]indolo[2,3-*c*]carbazol-5(10*H*)-yl]methyl}benzene **7**

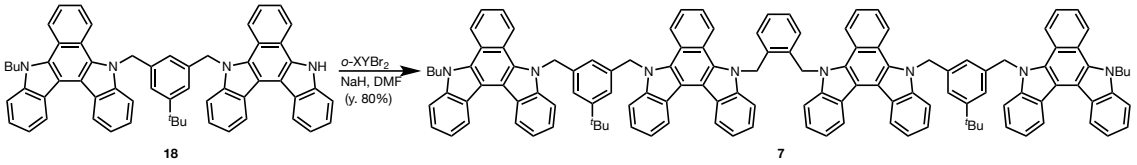

18 7

To a stirred solution of **18** (70 mg, 84 μmol) and 1,2-bis(bromomethyl)benzene (11 mg, 42 μmol) in dry DMF (2 mL) under argon was added NaH (6 mg, 127 μmol, 60% in mineral oil) at room temperature. After stirring for 2 h at room temperature, the mixture was diluted with water and the precipitates were filtered through *Kiriyama* funnel and washed with MeOH and hexane to afford **7** (59 mg, 80%) as a pale-yellow solid.

Mp 199 °C (decomp); IR (KBr) ν/cm^{-1} :3682, 3662, 3635, 3439, 3050, 2959, 2869, 1625, 1605, 1571, 1470, 1424, 1401, 1339, 1270, 1202, 1170, 1140, 1107, 1031, 918, 734, 576, 477; ^{1}H NMR (400 MHz, DMSO-*d*6) δ/ppm: 8.95 (d, 2H, *J* = 8.0 Hz), 8.85 (d, 2H, *J* = 7.5 Hz), 8.78 (d, 2H, *J* = 8.0 Hz), 8.71 (d, 2H, *J* = 8.0 Hz), 8.49 (d, 2H, *J* = 8.5 Hz), 8.37 (d, 2H, *J* = 8.5 Hz), 8.29 (d, 4H, *J* = 8.5 Hz), 7.84 (d, 2H, *J* = 8.2 Hz), 7.69 (d, 2H, *J* = 8.2 Hz), 7.63 (dd, 2H, *J* = 7.5, 7.5 Hz), 7.59 (d, 2H, *J* = 7.5 Hz), 7.54 (dd, 4H, *J* = 7.5, 7.5 Hz), 7.50 (d, 4H, *J* = 8.2 Hz), 7.43 (dd, 2H, *J* = 7.5, 7.5 Hz), 7.23–7.40 (m, 18H), 7.10 (dd, 2H, *J* = 7.5, 7.5 Hz), 7.07 (dd, 2H, *J* = 7.5, 7.5 Hz), 6.97 (dd, 2H, *J* = 5.6, 3.4 Hz), 6.78 (s, 2H), 6.68 (dd, 2H, *J* = 5.6, 3.4 Hz), 6.14 (s, 4H), 5.97 (s, 4H), 5.89 (s, 4H), 4.69 (t, 4H, *J* = 7.4 Hz), 1.81 (qn, 4H, *J* = 7.4 Hz), 1.31 (sext, 4H, *J* = 7.4 Hz), 1.09 (s, 18H), 0.82 (t, 6H, *J* = 7.4 Hz); ^{13}C NMR (100 MHz, $CDCl_3$) δ/ppm: 152.33, 141.96, 141.93, 141.73, 141.35, 139.04, 138.99, 135.11, 131.93, 131.91, 131.76, 131.23, 128.06, 128.05, 125.83, 125.82, 125.06, 124.92, 124.89, 124.8, 124.75, 124.61, 124.46, 123.76, 123.74, 123.7, 123.13, 123.09, 122.99, 122.82, 122.76, 122.74, 122.68, 122.55, 122.5, 122.4, 122.09, 122.03, 121.89, 121.84, 120.38, 120.17, 120.04, 119.86, 119.6, 114.7, 114.64, 114.55, 114.47, 110.81, 110.54, 110.51, 110.44, 50.48, 50.43, 48.11, 46.12, 34.8, 31.89, 31.39, 19.85, 13.98; HRMS (FD, m/z) [(M+H^{+})]calcd. for $C_{128}H_{106}N_8$: 1754.8540; found: 1754.8555.

28) Preparation of 1,4-bis{[10-(3-(*tert*-butyl)-5-((10-butylbenzo[*a*]indolo[2,3-*c*]carbazol-5(10*H*)-yl)methyl)benzyl)benzo[*a*]indolo[2,3-*c*]carbazol-5(10*H*)-yl]methyl}benzene **8**

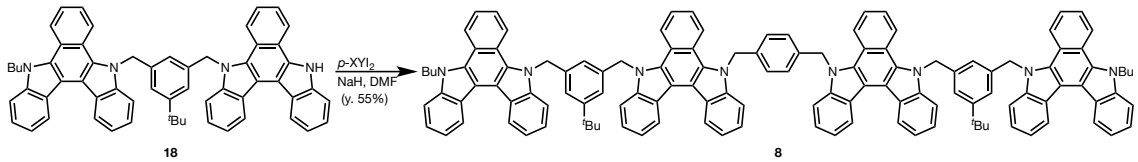

18 8

To a stirred solution of **18** (65 mg, 79 μmol) and 1,4-bis(iodomethyl)benzene (14 mg, 39 μmol) in dry DMF (1 mL) under argon was added NaH (6 mg, 157 μmol, 60% in mineral oil) at room temperature. After stirring for 4 h at room temperature, the mixture was diluted with water and the precipitates were filtered through *Kiriyama* funnel and washed with MeOH and hexane. The residue was chromatographed on silica-gel (hexane/CH_2Cl_2 = 8/5) to afford **8** (38 mg, 55%) as a pale-yellow solid.
Mp 209 °C (decomp); IR (KBr) ν/cm^{-1} :3439, 3049, 2957, 2869, 2348, 2284, 1692, 1665, 1605, 1546, 1536, 1524, 1513, 1470, 1423, 1400, 1338, 1293, 1268, 1201, 1169, 1157, 1139, 1106, 1031, 1018, 976, 918, 868, 806, 782, 733, 577; ^{1}H NMR (400 MHz, DMSO-*d*6) δ/ppm: 8.86 (d, 2H, *J* = 8.2 Hz), 8.82 (d, 2H, *J* = 8.2 Hz), 8.76 (dd, 4H, *J* = 8.3, 8.3 Hz), 8.52 (d, 2H, *J* = 8.6 Hz), 8.33 (d, 2H, *J* = 8.6 Hz), 8.28 (d, 4H, *J* = 8.6 Hz), 7.82 (d, 2H, *J* = 8.3 Hz), 7.69 (d, 2H, *J* = 8.2 Hz), 7.58 (dd, 4H, *J* = 8.6, 8.6 Hz), 7.53 (d, 2H, *J* = 5.8 Hz), 7.28–7.50 (m, 18H), 7.25 (s, 2H), 7.18 (dd, 2H, *J* = 7.7, 7.7 Hz), 7.10 (s, 4H), 7.02 (dd, 2H, *J* = 7.7, 7.7 Hz), 6.96 (dd, 2H, *J* = 7.7, 7.7 Hz) 6.73 (s, 2H), 6.01 (s, 4H), 5.93 (s, 4H), 5.89 (s, 4H), 4.75 (t, 4H, *J* = 7.4 Hz), 1.81 (qn, 4H, *J* = 7.4 Hz), 1.31 (sext, 4H, *J* = 7.4 Hz), 1.03 (s, 18H), 0.82 (t, 6H, *J* = 7.4 Hz); HRMS (FD, m/z) [(M+H^+)]calcd. for $C_{128}H_{106}N_8$: 1754.8540; found: 1754.8561.

<Preparation of pentamer 5>

29) Preparation of 5,10-bis[3-(bromomethyl)-5-(*tert*-butyl)benzyl]-5,10-dihydrobenzo[*a*]indolo[2,3-*c*]carbazole **19**

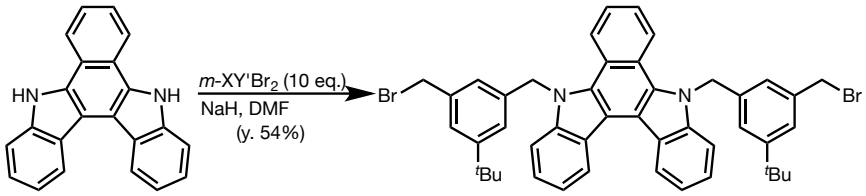

1a **19**

To a stirred solution of parent BIC **1a** (150 mg, 490 μmol) in dry DMF (5 mL) under argon was added NaH (78 mg, 1.96 mmol, 60% in mineral oil) at room temperature. To a stirred solution of 1,3-bis(bromomethyl)-5-*tert*-butylbenzene (1.57 g, 4.90 mmol, 10 eq.) in dry DMF (10mL) under argon wad added the above mixture over 10 min at room temperature. After stirring for 3 h at room temperature, the mixture was diluted with water and the precipitates were filtered through *Kiriyama* funnel. The residue was chromatographed on silica gel (hexane/CH_2Cl_2 = 3/1) to give **19** (209 mg, 54%) as a pale yellow solid, which was labile and decomposed slowly in solution.

Thus, **19** was used without further purification after confirming its identity by ^{1}H NMR [^{1}H NMR (400 MHz, DMSO-*d*6) δ/ppm: 8.99 (d, 2H, *J* = 8.0 Hz), 8.54 (d, 2H, *J* = 8.0 Hz), 7.79 (d, 2H, *J* = 8.0 Hz), 7.57 (dd, 2H, *J* = 7.5, 7.5 Hz), 7.50 (dd, 2H, *J* = 7.5, 7.5 Hz), 7.46 (dd, 2H, *J* = 7.5 Hz), 7.46 (s, 2H), 7.39 (s, 2H), 7.02 (s, 2H), 6.15 (s, 4H), 4.55 (s, 4H), 1.21 (s, 18H)].

30) Preparation of 5,10-bis{3-(*tert*-butyl)-5-[(10-(3-(*tert*-butyl)-5-((10-butylbenzo[*a*]indolo[2,3-*c*]carbazol-5(10*H*)-yl)methyl)benzyl)benzo[*a*]indolo[2,3-*c*]carbazol-5(10*H*)-yl)methyl]benzyl}-5,10-dihydrobenzo[*a*]indolo[2,3-*c*]carbazole **5**

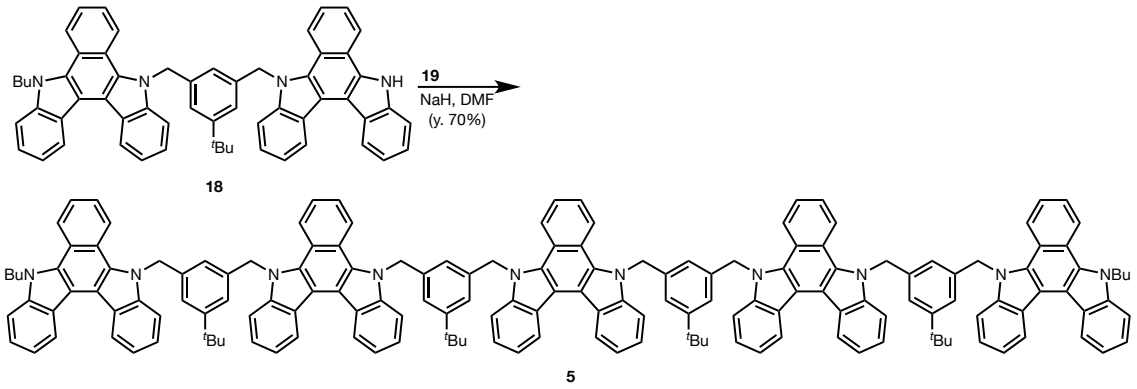

To a stirred solution of **18** (90 mg, 109 μmol, 2.8 eq.) and **19** (14 mg, 39 μmol) in dry DMF (3 mL) under argon was added NaH (8 mg, 170 μmol, 60% in mineral oil) at room temperature. After stirring for 5 h at room temperature, the mixture was diluted with water and the precipitates were filtered through *Kiriyama* funnel and washed with MeOH and hexane to afford **5** (96 mg, 77%) as a pale yellow solid.

Mp 216 °C (decomp); IR (KBr) ν/cm^{-1}:3444, 3050, 2960, 2870, 1662, 1605, 1471, 1424, 1400, 1363, 1339, 1291, 1200, 1171, 1158, 1141, 1108, 1043, 1031, 1018, 920, 868, 734, 714, 580, 477; ^{1}H NMR (400 MHz, DMSO-*d*6) δ/ppm: 8.76 (d, 2H, *J* = 8.2 Hz), 8.69 (d, 8H, *J* = 7.7 Hz), 8.46 (d, 2H, *J* = 8.5 Hz), 8.24 (d, 2H, *J* = 8.5 Hz), 8.11 (dd, 3H, *J* = 6.5, 6.5 Hz), 8.10 (dd, 3H, *J* = 6.5, 6.5 Hz), 7.70 (d, 2H, *J* = 8.2 Hz), 7.38–7.48 (m, 10H), 7.21–7.37 (m, 20H), 7.19 (s, 4H), 7.18 (s, 4H), 7.02 (dd, 2H, *J* = 7.7, 7.7 Hz), 6.84 (dd, 3H, *J* = 6.5, 6.5 Hz), 6.83 (dd, 3H, *J* = 6.5, 6.5 Hz), 6.69 (s, 4H), 5.81 (s, 4H), 5.73 (s, 8H), 5.71 (s, 4H), 4.70 (t, 4H, *J* = 7.4 Hz), 1.84 (qn, 4H, *J* = 7.4 Hz), 1.36 (sext, 4H, *J* = 7.4 Hz), 1.03 (s, 18H), 1.02 (s, 18H), 0.87 (t, 6H, *J* = 7.4 Hz); ^{13}C NMR (100 MHz, DMSO-*d*6) δ/ppm: 152.43, 142.1, 142.03, 142.02, 141.97, 141.58, 141.57, 138.96, 138.95, 138.93, 138.92, 138.91, 131.96, 131.94, 131.93, 131.90, 131.90, 131.46, 131.45, 131.44, 124.69, 124.66, 124.66, 124.63, 124.62, 124.61, 124.58, 124.34, 124.30, 124.30, 124.08, 124.07, 124.06, 123.61, 123.21, 123.19, 123.18, 123.15, 123.14, 123.03, 123.03, 122.81, 122.76, 122.72, 122.71, 122.65, 122.64, 122.62, 122.61, 122.20, 121.93, 121.85, 121.83, 121.78, 121.76, 119.82, 119.8, 119.79, 119.77, 119.55, 114.75, 114.68, 114.63, 110.47, 110.33, 110.29, 110.27, 50.61, 50.50, 50.45, 50.43, 46.26, 34.70, 34.68, 31.91, 31.29, 31.28, 19.82, 13.84; HRMS (FD, m/z) [(M+H^{+})]calcd. for $C_{169}H_{142}N_{10}$: 2275.1419; found: 2275.1419.

<Preparation of hexamer 6>

30) Preparation of 5-{3-[(6-(2-azidophenyl)-11H-benzo[*a*]carbazol-11-yl)methyl]-5-(*tert*-butyl)benzyl}-10-{3-(*tert*-butyl)-5-[(10-butylbenzo[*a*]indolo[2,3-*c*]carbazol-5(10*H*)-yl)methyl]benzyl}-5,10-dihydrobenzo[*a*]indolo[2,3-*c*]carbazole **20**

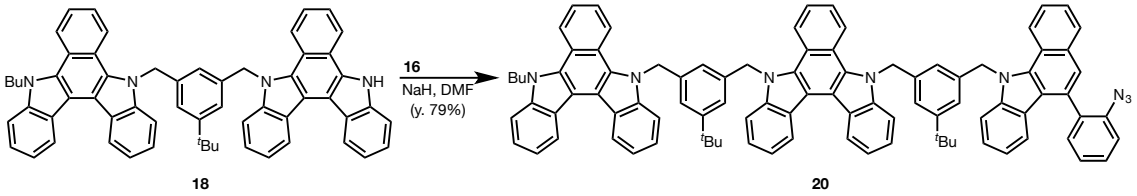

18 20

To a stirred solution of **18** (250 mg, 302 μmol) and **16** (173 mg, 302 μmol) in dry DMF (6 mL) under argon was added NaH (18 mg, 453 μmol, 60% in mineral oil) at room temperature. After stirring for 2 h at room temperature, the mixture was diluted with water and the precipitates were filtered through *Kiriyama* funnel and washed with MeOH and hexane. The residue was chromatographed on silica gel (hexane/CH_2Cl_2 = 3/1) to give **20** (197 mg, 90%) as a pale yellow solid.

Mp 175 °C (decomp); IR (KBr) ν/cm^{-1} : 3440, 3050, 2959, 2867, 2116, 1825, 1793, 1751, 1685, 1604, 1576, 1522, 1470, 1424, 1399, 1362, 1332, 1299, 1201, 1171, 1140, 1108, 1031, 933, 920, 870, 736, 712; ^{1}H NMR (400 MHz, DMSO-*d*6) δ/ppm: 8.76–8.82 (m, 3H), 8.70 (d, 1H, *J* = 8.7 Hz),8.50 (d, 1H, *J* = 8.7 Hz), 8.26 (dd, 2H, *J* = 8.7, 8.7 Hz), 8.21 (dd, 1H, *J* = 6.6, 3.2 Hz), 8.15 (dd, 1H, *J* = 6.6, 3.2 Hz), 7.92 (d, 1H, *J* = 7.6 Hz), 7.76 (d, 1H, *J* = 8.3 Hz), 7.64 (ddd, 1H, *J* = 7.6, 7.6, 1.7 Hz), 7.53–7.55 (m, 3H), 7.46–7.50 (m, 3H), 7.21–7.42 (m, 15H), 7.17 (s, 1H), 7.14 (s, 1H), 7.09 (dd, 1H, *J* = 7.6, 7.6 Hz), 7.03 (dd, 1H, *J* = 7.6, 7.6 Hz), 6.86–6.96 (m, 4H), 6.83 (s, 1H), 6.72 (s, 1H), 5.95 (s, 2H), 5.88 (s, 2H), 5.87 (s, 2H), 5.71 (s, 2H), 4.73 (t, 2H, *J* = 7.4 Hz), 1.84 (qn, 2H, *J* = 7.4 Hz), 1.35 (sext, 2H, *J* = 7.4 Hz), 1.06 (s, 9H), 0.98 (s, 9H), 0.86 (t, 3H, *J* = 7.4 Hz); ^{13}C NMR (100 MHz, DMSO-*d*6) δ/ppm: 152.33, 152.30, 141.92, 141.81, 141.77, 141.45, 141.39, 141.33, 139.06, 139.00, 138.98, 138.76, 138.40, 138.36, 134.98, 133.07, 132.88, 132.87, 131.72, 131.72, 131.68, 131.63, 131.13, 130.27, 130.26, 129.42, 129.37, 129.37, 125.84, 125.83, 125.68, 125.67, 125.37, 125.16, 124.92, 124.91, 124.90, 124.88, 124.79, 124.76, 124.66, 124.45, 124.44, 124.41,

124.33, 124.32, 124.31, 123.66, 123.63, 123.62, 123.59, 123.31, 123.28, 123.09, 123.08, 122.76, 122.74, 122.68, 122.63, 122.55, 122.54, 122.53, 122.46, 122.45, 122.42, 122.33, 122.07, 122.06, 121.76, 121.66, 121.65, 121.28, 120.65, 120.18, 120.00, 119.88, 119.81, 119.80, 119.62, 119.60, 117.99, 114.46, 114.42, 114.41, 110.56, 110.36, 110.25, 50.35, 49.57, 46.08, 34.76, 34.66, 31.97, 31.35, 31.21, 22.44, 19.89, 14.31, 14.06; HRMS (FD, m/z) [(M+H$^+$)]calcd. for $C_{94}H_{78}N_8$: 1318.6349; found: 1318.6333.

31) Preparation of 5-{3-[benzo[*a*]indolo[2,3-*c*]carbazol-5(10*H*)-yl-methyl]-5-(*tert*-butyl)benzyl}-10-{3-(*tert*-butyl)-5-[(10-butylbenzo[*a*]indolo[2,3-*c*]carbazol-5(10*H*)-yl)methyl]benzyl}-5,10-dihydrobenzo[*a*]indolo[2,3-*c*]carbazole **21**

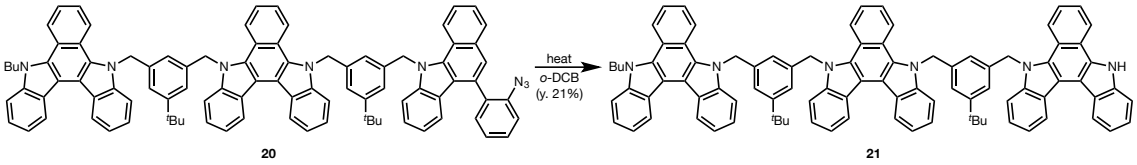

20 **21**

A solution of **20** (308 mg, 233 μmol) in 1,2-dichlorobenzene (5 mL) under argon was stirred for 21 h at 160 °C. After cooling to room temperature, the reaction mixture was diluted with hexane and the precipitates were filtered through *Kiriyama* funnel and washed with MeOH. The residue was chromatographed on silica gel (hexane/CH_2Cl_2 = 1/1) and recrystallized from toluene to give **21** (64 mg, 21%) as a pale yellow solid. Mp 143 °C (decomp); IR (KBr) ν/cm^{-1} : 3432, 3049, 2959, 2869, 2349, 1718, 1700, 1676, 1669, 1663, 1653, 1635, 1604, 1559, 1540, 1470, 1435, 1424, 1401, 1362, 1335, 1291, 1270, 1238, 1201, 1171, 1157, 1139, 1108, 1092, 1032, 1017, 921, 734, 581, 477; ^{1}H NMR (400 MHz, DMSO-*d*6) δ/ppm: 12.26 (s, 1H), 8.81 (d, 2H, *J* = 8.0 Hz), 8.77 (d, 2H, *J* = 8.0 Hz), 8.68 (d, 1H, *J* = 8.0 Hz), 8.65 (d, 1H, *J* = 8.0 Hz), 8.48 (d, 1H, *J* = 8.5 Hz), 8.37 (d, 1H, *J* = 8.5 Hz), 8.27 (d, 1H, *J* = 8.5 Hz), 8.16 (ddd, 2H, *J* = 8.0, 8.0, 4.5 Hz), 7.75 (dd, 2H, *J* = 8.0, 2.8 Hz), 7.23–7.64 (m, 22H), 7.17 (s, 1H), 7.14 (d, 1H, *J* = 7.6 Hz), 6.98 (dd, 1H, *J* = 7.6, 7.6 Hz), 6.84 (s, 1H), 6.82 (s, 2H), 6.68 (s, 1H), 5.99 (s, 2H), 5.87 (s, 4H), 5.73 (s, 2H), 4.71 (t, 2H, *J* = 7.3 Hz), 1.80 (qn, 2H, *J* = 7.3 Hz), 1.28 (sext, 2H, *J* = 7.3 Hz), 1.07 (s, 9H), 0.99 (s, 9H), 0.82 (t, 3H, *J* = 7.3 Hz); ^{13}C NMR (100 MHz, DMSO-*d*6) δ/ppm: 152.21, 152.20, 141.80, 141.76, 141.71, 141.62, 141.32, 141.21, 139.43, 139.42, 139.39, 139.17, 139.13, 139.09, 139.08, 132.15, 131.57,

131.56, 131.50, 131.48, 130.93, 130.74, 129.36, 128.67, 125.29, 125.28, 125.12, 125.11, 124.99, 124.97, 124.89, 124.80, 124.79, 124.76, 124.71, 124.70, 124.66, 124.49, 124.48, 124.39, 124.33, 124.31, 123.67, 123.54, 123.49, 123.27, 123.10, 122.94, 122.83, 122.78, 122.75, 122.69, 122.68, 122.53, 122.50, 122.37, 122.30, 122.23, 122.15, 121.99, 121.70, 121.67, 121.56, 121.01, 119.99, 119.9, 119.63, 119.44, 114.77, 114.30, 114.28, 112.39, 112.36, 112.05, 110.60, 110.45, 110.41, 110.39, 50.25, 50.13, 49.99, 45.94, 34.80, 34.72, 31.99, 31.38, 31.30, 22.53, 19.91, 14.15; HRMS (FD, m/z) [(M+H$^+$)]calcd. for $C_{94}H_{78}N_6$: 1296.6288; found: 1296.6299.

32) Preparation of 10,10'-{[5-(*tert*-butyl)-1,3-phenylene]bis(methylene)}bis{5-[3-(*tert*-butyl)-5-((10-(3-(*tert*-butyl)-5-((10-butylbenzo[*a*]indolo[2,3-*c*]carbazol-5(10*H*)-yl)methyl)benzyl)benzo[*a*]indolo[2,3-*c*]carbazol-5(10*H*)-yl)methyl)benzyl]-5,10-dihydrobenzo[a]indolo[2,3-c]carbazole} **6**

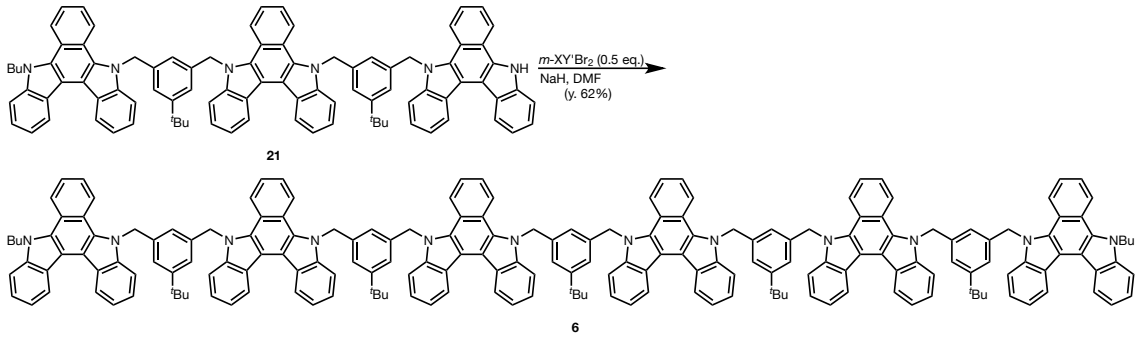

To a stirred solution of **21** (37 mg, 29 μmol) and 1,3-bis(bromomethyl)-5-*tert*-butylbenzene (5 mg, 14 μmol, 0.5 eq.) in dry DMF (1 mL) under argon was added NaH (4 mg, 57 μmol, 60% in mineral oil) at room temperature. After stirring for 3 h at room temperature, the mixture was diluted with water and the precipitates were filtered through *Kiriyama* funnel and washed with MeOH. The residue was chromatographed on silica gel (hexane/CH_2Cl_2 = 4/3) to give **6** (24 mg, 62%) as a pale yellow solid.

Mp 214 °C (decomp); IR (KBr) ν/cm^{-1} : 3442, 3050, 2961, 2869, 1652, 1647, 1603, 1569, 1472, 1421, 1400, 1363, 1339, 1261, 1218, 1200, 1170, 1158, 1139, 1107, 1030, 919, 734, 712; ^{1}H NMR (400 MHz, DMSO-*d*6) δ/ppm: 8.73 (d, 3H, *J* = 8.2 Hz), 8.65 (d, 9H, *J* = 7.6 Hz), 8.43 (d, 2H, *J* = 8.6 Hz), 8.22 (d, 2H, *J* = 8.2 Hz), 8.05–8.07 (m, 8H), 7.65 (d, 3H, *J* = 8.2 Hz), 7.15–7.45 (m, 47H), 6.99 (dd, 3H, *J* = 7.6, 7.6 Hz), 6.79–6.81 (m, 8H), 6.65 (s, 4H), 5.77 (s, 4H), 5.67 (s, 10H), 5.66 (s, 4H), 4.67 (t, 4H, *J* = 7.4

Hz), 1.81 (qn, 4H, J = 7.4 Hz), 1.33 (sext, 4H, J = 7.4 Hz), 0.98 (s, 18H), 0.98 (s, 18H), 0.97 (s, 9H), 0.83 (t, 6H, J = 7.4 Hz); ^{13}C NMR could not be measured due to low solubility; HRMS (FD, m/z) [(M+H$^+$)]calcd. for $C_{200}H_{170}N_{12}$: 2739.3671; found: 2739.3702.

<Preparation of cationic salts>

33) Preparation of 5-butyl-10-{3-(*tert*-butyl)-5-[(10-butylbenzo[*a*]indolo[2,3-*c*]carbazol-5(10*H*)-yl)methyl]benzyl}-5,10-dihydrobenzo[*a*]indolo[2,3-*c*]carbazolium tetrakis[3,5-bis(trifluoromethyl)phenyl]borate **2**$^{+\bullet}$BAr$_4^-$

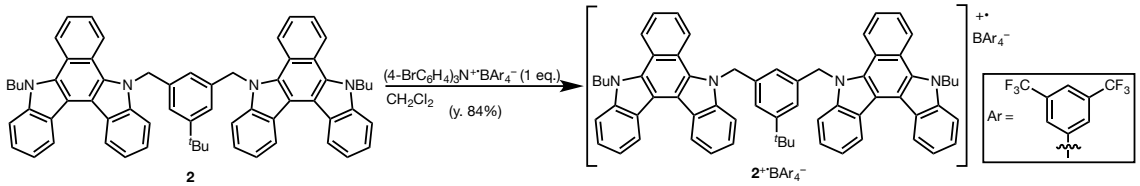

A solution of **2** (20 mg, 22 μmol) and tris(4-bromophenyl)aminium tetrakis(3,5-bis(trifluoromethyl)phenyl)borate (30 mg, 22 μmol, 1 eq.) in dry CH_2Cl_2 (1 mL) under argon was stirred at room temperature. After stirring for 9 h at room temperature, the solvent was removed and the residue was washed with hexane to give **2**$^{+\bullet}$BAr$_4^-$ (25 mg, 64%) as a green solid.

Mp 110 °C; IR (KBr) ν/cm^{-1} : 3442, 3072, 2961, 2872, 1603, 1565, 1548, 1507, 1479, 1463, 1440, 1383, 1343, 1326, 1293, 1249, 1200, 1159, 1118, 1105, 1034, 922, 905, 864, 787, 744, 708, 580, 560; Anal. calcd. (%) for $C_{64}H_{58}N_4Cl_{12}Sb_2$: C 66.02, H 4.04, N 3.21. Found: C 65.69, H 4.30, N 3.27.

34) Preparation of 10,10'-{[5-(*tert*-butyl)-1,3-phenylene]bis(methylene)}bis(5-butyl-5,10-dihydrobenzo[*a*]indolo[2,3-*c*]carbazolium) bis(hexachloroantimonate) $\mathbf{2}^{2+2\bullet}(SbCl_6^-)_2$

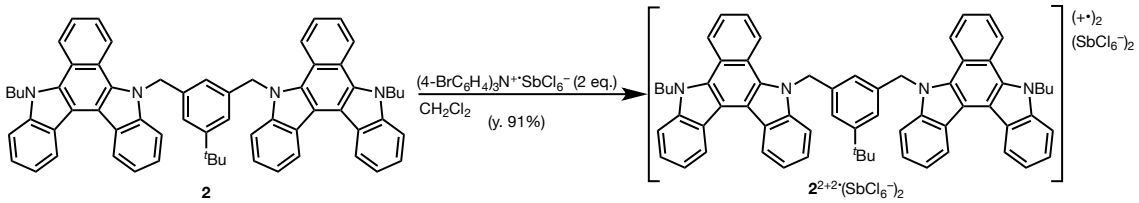

2 **2**$^{2+2\bullet}(SbCl_6^-)_2$

A solution of **2** (50 mg, 57 μmol) and tris(4-bromophenyl)aminium hexachloroantimonate (**MB**) (92.4 mg, 113 μmol, 2 eq.) in dry CH_2Cl_2 (6 mL) under argon was stirred at room temperature. After stirring for 4.5 h at room temperature, the mixture was diluted with dry ether and the precipitates were filtered through *Kiriyama* funnel and washed with dry ether to give $\mathbf{2}^{2+2\bullet}(SbCl_6^-)_2$ (84 mg, 96%) as a dark blue solid.

Mp 163 °C; IR (KBr) ν/cm^{-1} : 3442, 3072, 2961, 2872, 1603, 1565, 1548, 1507, 1479, 1463, 1440, 1383, 1343, 1326, 1293, 1249, 1200, 1159, 1118, 1105, 1034, 922, 905, 864, 787, 744, 708, 580, 560; Anal. calcd. (%) for $C_{64}H_{58}N_4Cl_{12}Sb_2$: C 49.53, H 3.77, N 3.61. Found: C 49.49, H 3.59, N 3.50.

35) Preparation of 10,10'-{[5-(*tert*-butyl)-1,3-phenylene]bis(methylene)}bis{5-[3-(*tert*-butyl)-5-((10-butylbenzo[*a*]indolo[2,3-*c*]carbazol-5(10*H*)-yl)methyl)benzyl]-5,10-dihydrobenzo[*a*]indolo[2,3-*c*]carbazolium} bis(hexachloroantimonate) $\mathbf{4}^{2+2\bullet}(SbCl_6^-)_2$

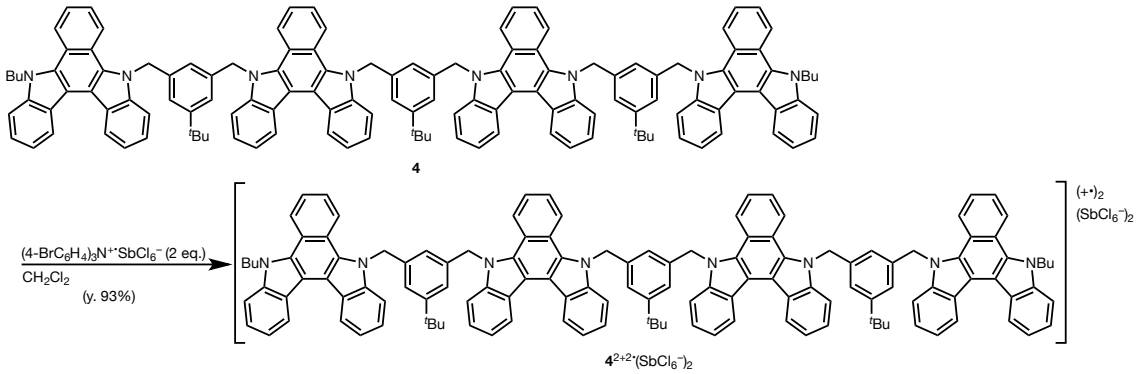

4 **4**$^{2+2\bullet}(SbCl_6^-)_2$

A solution of **4** (45 mg, 25 μmol) and tris(4-bromophenyl)aminium hexachloroantimonate (**MB**) (40 mg, 49 μmol, 2 eq.) in dry CH_2Cl_2 (2 mL) under argon was stirred at room temperature. After stirring for 1.5 h at room temperature, the mixture was diluted with dry ether and the precipitates were filtered through *Kiriyama* funnel and washed with dry ether to give $\mathbf{4}^{2+2\bullet}(SbCl_6^-)_2$ (57 mg, 93%) as a green solid. The same salt was obtained in 48% yield based on **4** when only 1 eq. of **MB** was used.

Mp 159 °C; IR (KBr) ν/cm^{-1} : 3854, 3439, 3052, 2960, 2870, 1734, 1603, 1551, 1508, 1463, 1438, 1382, 1364, 1339, 1292, 1251, 1201, 1169, 1158, 1129, 1105, 1030, 993, 919, 864, 737, 707, 687, 583; Anal. Caldc. (%) for $C_{132}H_{114}N_8Cl_{12}Sb_2$ + 0.5 CH_2Cl_2: C 63.06, H 4.59, N 4.44. Found: C 63.20, H 4.56, N 4.30.

36) Preparation of 10,10'-{[5-(*tert*-butyl)-1,3-phenylene]bis(methylene)}bis{5-[3-(*tert*-butyl)-5-((10-butylbenzo[*a*]indolo[2,3-*c*]carbazol-5(10*H*)-yl)methyl)benzyl]-5,10-dihydrobenzo[*a*]indolo[2,3-*c*]carbazolium} bis(tetrafluoroborate) $\mathbf{4}^{2+2\bullet}(BF_4^-)_2$

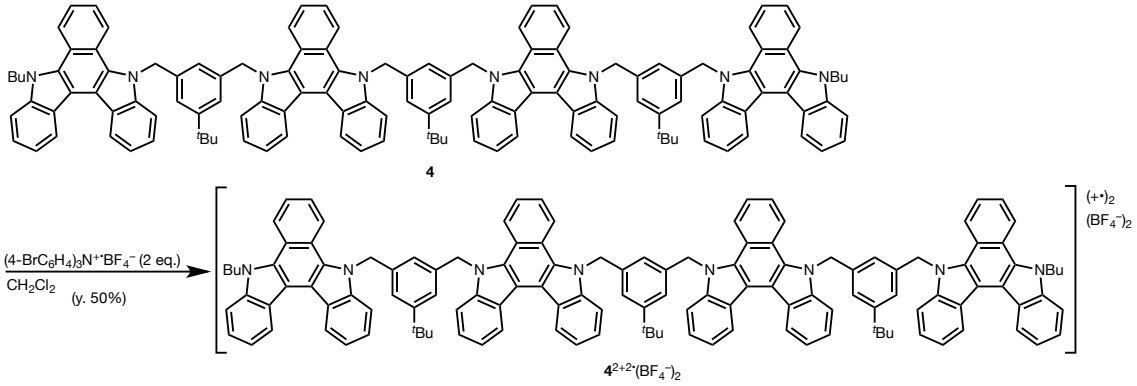

A solution of **4** (40 mg, 22 μmol) and tris(4-bromophenyl)aminium tetrafluoroborate (**MB**) (25 mg, 44 μmol, 2 eq.) in dry CH_2Cl_2 (2 mL) under argon was stirred at room temperature. After stirring for 3 h at room temperature, the mixture was diluted with dry ether and the precipitates were filtered through *Kiriyama* funnel and washed with dry ether to give $\mathbf{4}^{2+2\bullet}(BF_4^-)_2$ (22 mg, 50%) as a green solid.

Mp 169 °C; IR (KBr) ν/cm^{-1} : 3489, 2957, 2865, 1727, 1702, 1693, 1681, 1649, 1602, 1563, 1547, 1510, 1466, 1438, 1382, 1364, 1339, 1291, 1253, 1201, 1169, 1106, 1056, 919, 866, 737, 579, 556, 520; Anal. calcd. (%) for $C_{132}H_{114}N_8B_2F_8$ + 0.75 CH_2Cl_2: C 77.79, H 5.68, N 5.47. Found: C 77.89, H 5.63, N 5.43.

37) Preparation of 10,10'-{[5-(*tert*-butyl)-1,3-phenylene]bis(methylene)}bis{5-[3-(*tert*-butyl)-5-((10-(3-(*tert*-butyl)-5-((10-butylbenzo[*a*]indolo[2,3-*c*]carbazol-5(10*H*)-yl)methyl)benzyl)benzo[*a*]indolo[2,3-*c*]carbazol-5(10*H*)-yl)methyl)benzyl]-5,10-dihydrobenzo[a]indolo[2,3-c]carbazolium} tris(hexachloroantimonate) $\mathbf{6}^{3+3\bullet}(SbCl_6^-)_3$

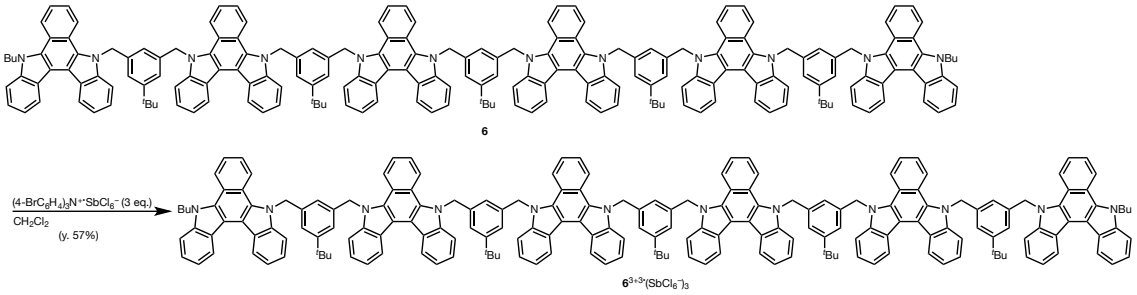

A solution of **6** (56 mg, 20 μmol) and tris(4-bromophenyl)aminium hexachloroantimonate (**MB**) (50 mg, 61 μmol, 3 eq.) in dry CH_2Cl_2 (2 mL) under argon was stirred at room temperature. After stirring for 3 h at room temperature, the precipitates were filtered through *Kiriyama* funnel and washed with dry CH_2Cl_2 to give $\mathbf{6}^{3+3\bullet}(SbCl_6^-)_3$ (43 mg, 57%) as a green solid.

Mp 140 °C (decomp); IR (KBr) ν/cm^{-1} : 3424, 2961, 2869, 1697, 1603, 1550, 1508, 1464, 1438, 1381, 1339, 1292, 1252, 1201, 1158, 1129, 1105, 1030, 994, 920, 865, 739, 710, 582, 553, 530; Anal. calcd. (%) for $C_{200}H_{170}N_{12}Cl_{18}Sb_3 + 4CH_2Cl_2$: C 59.99, H 4.39, N 4.11. Found: C 60.02, H 4.19, N 4.11.

<Preparation of dendrimeric triad 3a>

38) Preparation of 10,10',10''-[(1,3,5-benzene)tris(methylene)]tris(5-octyl-5,10-dihydrobenzo[a]indolo[2,3-c]carbazole) **3a**

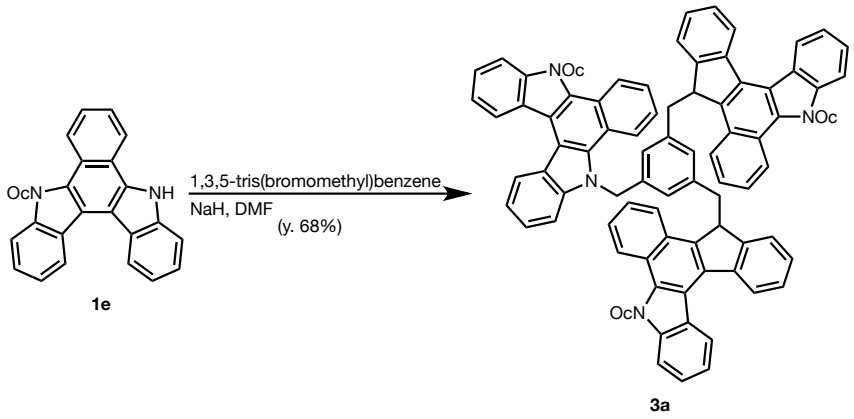

To a stirred solution of **1e** (88.7 mg, 212 μmol) in DMF (4 mL) under argon was added NaH (25.0 mg, 0.70 mmol, 60% in mineral oil) at room temperature. After stirring for 10 min at room temperature, 1,3,5-tris(bromomethyl)benzene (25 mg, 70 μmol) was added to the mixture. After stirring for 16 h at room temperature, the mixture was diluted with water and the precipitates were filtered. The residue was washed with water, hexane, EtOH to afford **3a** (62.6 mg, 65%) as a pale yellow solid.

Mp. 116-117 °C; IR (KBr) ν /cm^{-1} :3675, 3628, 3427, 3049, 2924, 2853, 1699, 1652, 1607, 1559, 1471, 1424, 1399, 1331, 1167, 1140, 1106, 928, 732; ^{1}H NMR (400 MHz, DMSO-d_6) δ/ppm :8.75 (d, J = 7.8 Hz, 3H), 8.64 (d, J = 7.8 Hz, 3H), 8.47 (d, J = 8.3 Hz, 3H), 8.16 (d, J = 8.3 Hz, 3H), 7.76 (d, J = 7.8 Hz, 3H), 7.53 (ddd, J = 8.6, 7.7, 1.1 Hz, 3H), 7.36-7.41 (m, 9H), 7.20-7.27 (m, 6H), 7.01 (s, 3H), 6.90 (ddd, J = 8.6, 7.7, 1.1 Hz, 3H), 5,87 (s, 6H), 4.72 (t, J = 7.8 Hz, 6H), 1.91 (qn, J = 7.8 Hz, 6H), 1.43 (t, J = 7.8 Hz, 6H), 1.23-1.35 (m, 24H), 0.82 (t, J = 7.8 Hz, 6H); HR-MS (FD) calcd. for $C_{99}H_{96}N_6$: 1368.7696; found: 1368.7688.

<Preparation of dendrimeric tetrad 4a>

39) Preparation of 10,10',10",10"'-[(1,2,4,5-benzene)tetrakis(methylene)]tetrakis(5-octyl-5,10-dihydrobenzo[*a*]indolo[2,3-*c*]carbazole) **4a**

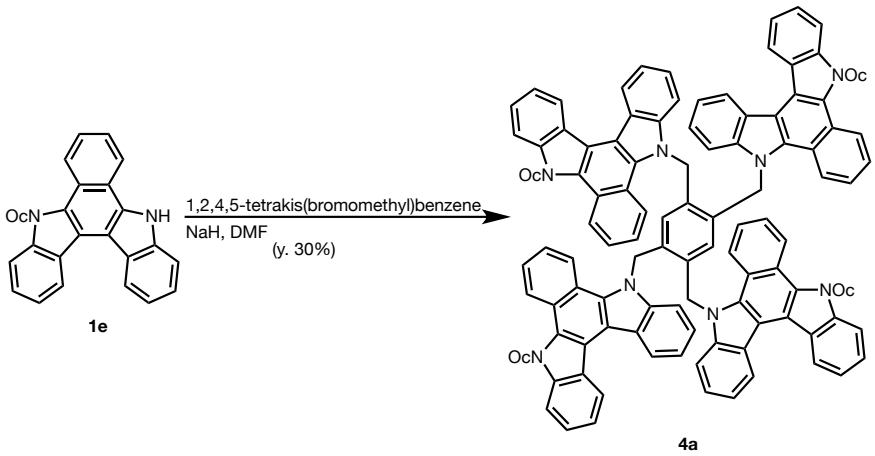

To a stirred solution of **1e** (268 mg, 640 μmol) in DMF (15 mL) under argon was added NaH (38.0 mg, 0.96 mmol, 60% in mineral oil) at room temperature. After stirring for 10 min at room temperature, 1,2,4,5-tetrakis(bromomethyl)benzene (72 mg, 16 μmol) was added to the mixture. After stirring for 23 h at room temperature, the mixture was diluted with water and the precipitates were filtered. The residue was washed with water, hexane, EtOAc to afford **4a** (178 mg, 62%) as a pale yellow solid.

Mp. 294 °C; IR (KBr) ν /cm^{-1} :3447, 3049, 2923, 2852, 1609, 1468, 1424, 1398, 1337, 1292, 1268, 1187, 1168, 1140, 1106, 922, 728; ^{1}H NMR (400 MHz, DMSO-d_6) δ/ppm : 8.41 (d, J = 7.9 Hz, 4H); 8.22 (dd, J = 10.0, 8.6 Hz, 8H), 7.97 (d, J = 8.6 Hz, 4H), 7.59 (d, J = 7.9 Hz, 4H), 7.48 (ddd, J = 8.4, 7.6, 1.0 Hz, 4H), 7.34 (ddd, J = 8.4, 7.6, 1.0 Hz, 4H), 7.22-7.26 (m, 8H), 6.97-7.08 (m, 12H), 6.22 (s, 2H), 5.96 (s, 8H), 4.45 (t, J = 7.6 Hz, 4H), 1.86 (qn, J = 7.6 Hz, 4H), 1.21-1.48 (m, 40H), 0.87 (t, J = 7.6 Hz, 12H); HR-MS (FD) calcd. for $C_{130}H_{126}N_8$: 1799.0105; found: 1799.0129.

References

[1] D. O. Cowan, C. LeVanda, J. Park, F. Kaufman, *Acc. Chem. Res.* **1973**, *6*, 1–7.

[2] J. Hankache, O. S. Wenger, *Chem. Rev.* **2011**, *111*, 5138–5178.

[3] A. Heckmann, C. Lambert, *Angew. Chem. Int. Ed Engl.* **2012**, *51*, 326–392.

[4] M. M. Hansmann, M. Melaimi, G. Bertrand, *J. Am. Chem. Soc.* **2018**, *140*, 2206–2213.

[5] X. Z. Yan, J. Pawlas, T. Goodson, J. F. Hartwig, *Journal of the American Chemical Society* **2005**, *127*, 9105–9116.

[6] S. F. Nelsen, G. Li, K. P. Schultz, H. Q. Tran, I. A. Guzei, D. H. Evans, *J. Am. Chem. Soc.* **2008**, *130*, 11620–11622.

[7] C. Kahlfuss, E. Saint-Aman, C. Bucher in *Organic Redox System: Redox-Controlled Intramolecular Motions Triggered by pi-Dimerization and Pimerization Process* (Ed: T. Nishinaga), Wiley, Hoboken, **2015**, Chap. 3, pp. 39-88.

[8] D.-L. Sun, S. V. Rosokha, S. V. Lindeman, J. K. Kochi, *J. Am. Chem. Soc.* **2003**, *125*, 15950–15963.

[9] D. Sun, S. V. Rosokha, J. K. Kochi, *J. Am. Chem. Soc.* **2004**, *126*, 1388–1401.

[10] G. Pognon, C. Boudon, K. J. Schenk, M. Bonin, B. Bach, J. Weiss, *J. Am. Chem. Soc.* **2006**, *128*, 3488–3489.

[11] A. Takai, C. P. Gros, J.-M. Barbe, R. Guilard, S. Fukuzumi, *Chem. Eur. J.* **2009**, *15*, 3110–3122.

[12] D. J. Hill, M. J. Mio, R. B. Prince, T. S. Hughes, J. S. Moore, *Chem. Rev.* **2001**, *101*, 3893–4012.

[13] D.-W. Zhang, X. Zhao, Z.-T. Li, *Acc. Chem. Res.* **2014**, *47*, 1961–1970.

[14] Z. Yu, S. Hecht, *Chem. Commun.* **2016**, *52*, 6639–6653.

[15] Y. Ferrand, I. Huc, *Acc. Chem. Res.* **2018**, *51*, 970–977.

[16] C. Kahlfuss, A. Milet, J. Wytko, J. Weiss, E. Saint-Aman, C. Bucher, *Org. Lett.* **2015**, *17*, 4058–4061.

[17] C. Kahlfuss, E. Métay, M.-C. Duclos, M. Lemaire, A. Milet, E. Saint-Aman, C. Bucher, *Chem. Eur. J.* **2015**, *21*, 2090–2106.

[18] T. Suzuki, W. Nojo, Y. Sakano, R. Katoono, Y. Ishigaki, H. Ohno, K. Fujiwara, *Chem. Lett.* **2016**, *45*, 720–722.

[19] W. Geuder, S. Hünig, A. Suchy, *Tetrahedron* **1986**, *42*, 1665–1677.

[20] A. Trabolsi, N. Khashab, A. C. Fahrenbach, D. C. Friedman, M. T. Colvin, K. K. Cotí, D. Benítez, E. Tkatchouk, J.-C. Olsen, M. E. Belowich, et al., *Nat. Chem.* **2010**, *2*, 42–49.

[21] Y. Wang, M. Frasconi, J. F. Stoddart, *ACS Cent Sci* **2017**, *3*, 927–935.

[22] J. Ferraris, D. O. Cowan, V. Walatka, J. H. Perlstein, *J. Am. Chem. Soc.* **1973**, *95*, 948–949.

[23] K. Bechgaard, K. Carneiro, F. B. Rasmussen, M. Olsen, G. Rindorf, C. S. Jacobsen, H. J. Pedersen, J. C. Scott, *J. Am. Chem. Soc.* **1981**, *103*, 2440–2442.

[24] T. Suzuki, Y. Tokimizu, Y. Sakano, R. Katoono, K. Fujiwara, S. Naoe, N. Fujii, H. Ohno, *Chem. Lett.* **2013**, *42*, 1001–1003.

[25] T. Suzuki, Y. Sakano, Y. Tokimizu, Y. Miura, R. Katoono, K. Fujiwara, N. Yoshioka, N. Fujii, H. Ohno, *Chem. Asian J.* **2014**, *9*, 1841–1846.

[26] S. Arae, T. Mori, T. Kawatsu, D. Ueda, Y. Shigeta, N. Hamamoto, H. Fujimoto, M. Sumimoto, T. Imahori, K. Igawa, et al., *Chem. Lett.* **2017**, *46*, 1214–1216.

[27] M. Daniels, F. de Jong, K. Kennes, C. Martín, J. Hofkens, M. Van der Auweraer, W. Dehaen, *Eur. J. Org. Chem.* **2018**, *2018*, 4683–4688.

[28] T. Janosik, A. Rannug, U. Rannug, N. Wahlström, J. Slätt, J. Bergman, *Chem. Rev.* **2018**, *118*, 9058–9128.

[29] E. J. Dale, N. A. Vermeulen, M. Juríček, J. C. Barnes, R. M. Young, M. R. Wasielewski, J. F. Stoddart, *Acc. Chem. Res.* **2016**, *49*, 262–273.

[30] L. Striepe, T. Baumgartner, *Chem. Eur. J.* **2017**, *23*, 16924–16940.

[31] M. Hasegawa, H. Enozawa, Y. Kawabata, M. Iyoda, *J. Am. Chem. Soc.* **2007**, *129*, 3072–3073.

[32] H. Tamaoki, R. Katoono, K. Fujiwara, T. Suzuki, *Angew. Chem. Int. Ed Engl.* **2016**, *55*, 2582–2586.

[33] M. Stolar, C. Reus, T. Baumgartner, *Adv. Energy Mater.* **2016**, *6*, 1600944.

[34] L. Striepe, M. Vespa, T. Baumgartner, *Org. Chem. Front.* **2017**, *4*, 717–723.

[35] T. Inabe, *Bull. Chem. Soc. Jpn.* **2005**, *78*, 1373–1383.

[36] Y.-T. Wu, J. S. Siegel, *Chem. Rev.* **2006**, *106*, 4843–4867.

[37] H. Imahori, T. Umeyama, K. Kurotobi, Y. Takano, *Chem. Commun.* **2012**, *48*, 4032–4045.

[38] W. Zhang, T. Fukushima, T. Aida, *Supramol. Chem.: Mol. Nanomater.* **2012**, *8*, 3791–3807.

[39] T. Kubo, *Chem. Rec.* **2015**, *15*, 218–232.

[40] F. Hirayama, *J. Chem. Phys.* **1965**, *42*, 3163–3171.

[41] L. Chen, H. Wang, D.-W. Zhang, Y. Zhou, Z.-T. Li, *Angew. Chem. Int. Ed Engl.* **2015**, *127*, 4100–4103.

[42] S. V. Rosokha, C. L. Stern, J. T. Ritzert, *CrystEngComm* **2013**, *15*, 10638–10647.

[43] A. V. Dyuba, T. V. Vygodina, A. A. Konstantinov, *Biochemistry* **2013**, *78*, 1358–1365.

Chapter 3

Development of aromatic amine with molecular film forming ability applicable to molecular diode/junction

3-1. Conventional diodes and molecular diodes

A diode is an element which has rectifying function that allows one-way flow of electricity. The diode has several important functions for modern electrical devices such as regulating current, making the voltage constant, and detecting the waves. Therefore, it is incorporated as an essential component in almost all current devices such as light-emitting devices (LED), radios, logic gates, and photodetectors. Firstly, vacuum diodes were developed, and then PN junction diodes, in which p-type and n-type semiconductors are connected, were developed and commonly used (Figure 1).[1] In the case of semiconductor junctions, the electronic properties including rectification properties are regulated by controlling the chemical species doped and their concentration in the semiconductor. On the other hand, in the organic molecules, the properties can be controlled by designing molecules based on advanced synthesis techniques (Figure 2).[2-8]

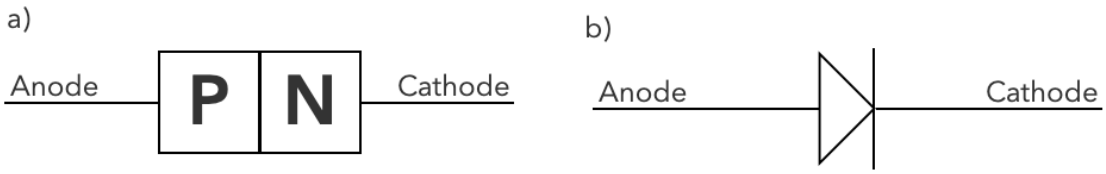

Figure 1 | a) Schematic diagram and b) graphic symbol of the diode.

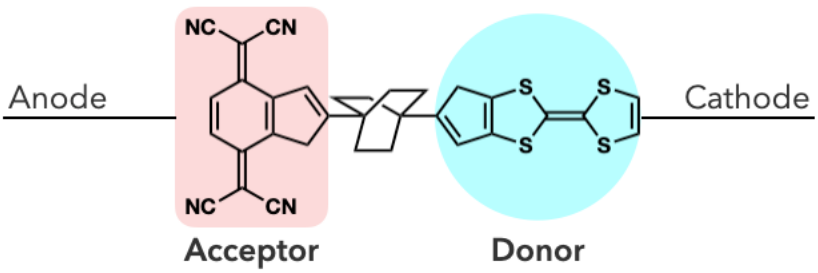

Figure 2 | Schematic diagram of the first suggested molecular diode.

3-2. A history of molecular diodes

Currently, molecular devices such as diodes, transistors, switches, and sensors based on functional organic molecules have been studied.[9-11] Molecular diodes, which were first proposed as molecular electronics, have been the main object of research among them. The first work on molecular diodes was the theoretical prediction by Ratner and Aviram in 1974 as shown in Chapter 1.[12,13] Then, the molecular diodes were first fabricated by the Langmuir-Blodgett (LB) technique,[4] in which a thin-molecular LB film was sandwiched between the top and bottom metal electrodes (Figure 3). Since then, the electronic rectification properties of the diodes have been intensively studied. Although various studies have been carried out using single-molecule systems or monolayers with multiple molecules,[5,14-16] the formation of electrodes has been hampered by the atomic contact between the top and bottom electrodes and the easy breakage of monolayers, which has caused problems in attaining the reproducibility and performance of the devices, so that the rectification ratio has not been very high. In order to improve the low quality of such rectification properties, a self-assembled-monolayer (SAM)-based diode has been developed.[17-19]

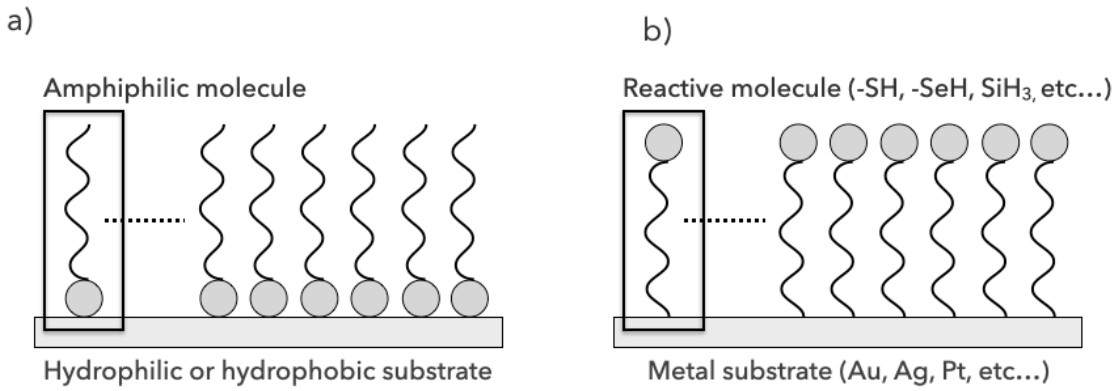

Figure 3 | Schematic diagram of a) Langmuir-Blodgett (LB) film and b) self-assembled-monolayer (SAM) film.

3-3. Molecular diodes of next generation

Prof. Christian A. Nijhuis in the National University of Singapore used a eutectic liquid alloy of gallium and indium (EGaIn) as a top electrode of the molecular diodes, and successfully made a soft electrical contact with a ferrocene-terminated alkanethiolate SAM, forming a stable tunnel junction with high yields (70~90%).[20] The rectification ratio, R = 100, was observed to be higher than the previously reported ratio (R < 30) (Figure 4).

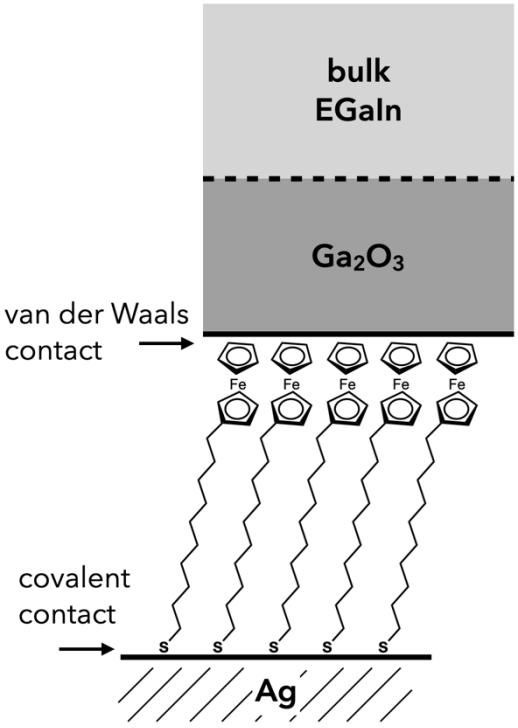

Figure 4 | Schematic showing tunneling junctions consisting of template-stripped Ag bottom-electrodes, supporting SAMs, and contacted by Ga_2O_3/EGaIn. The SAMs are: (A) SC11 Fc are drawn roughly to scale.

It has also been shown that this rectification property is further enhanced by increasing the number of conducting orbitals (HOMO and HOMO+1).[18,19] Chen et al. investigated the molecular diodes of ferrocene dimers using EGaIn to the top electrode. The R value was shown to increase gradually with the addition of voltage, with a maximum number beyond 100000 (Figure 5).

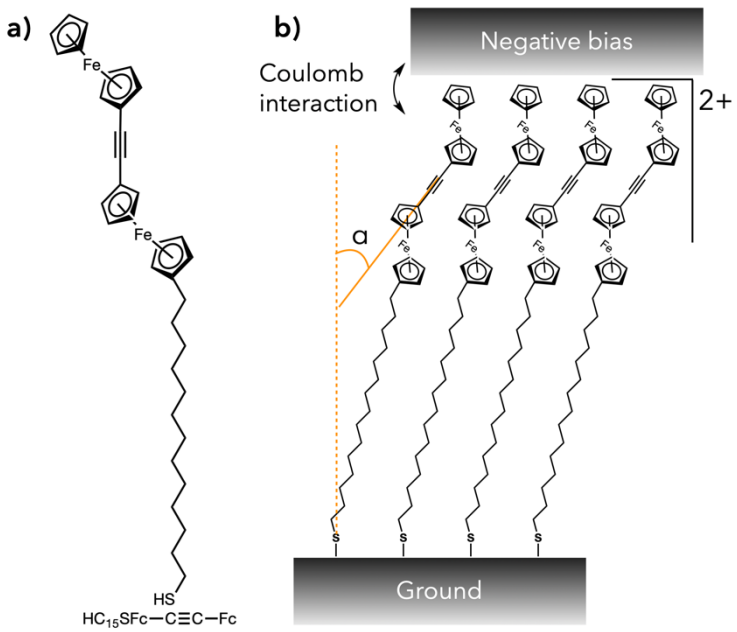

Figure 5 | The junctions and mechanism of rectification. **a**, Molecular structure of HSC_{15} Fc–C≡C–Fc. **b**, Schematic illustration of the junctions, where α is the tilt angle of the Fc–C≡C–Fc unit. Double arrows indicate the Coulomb or van der Waals interaction between the Fc–C≡C–Fc unit and the negatively or positively biased top electrode, respectively.

In addition, in the study of the diodes with a ferrocene as a donor moiety and polychlorotriphenylmethyl as an acceptor moiety,[21] an increase in the R value was observed due to the raise in HOMO energy-level caused by the charge transfer interaction between the donor and the acceptor unit (Figure 6).

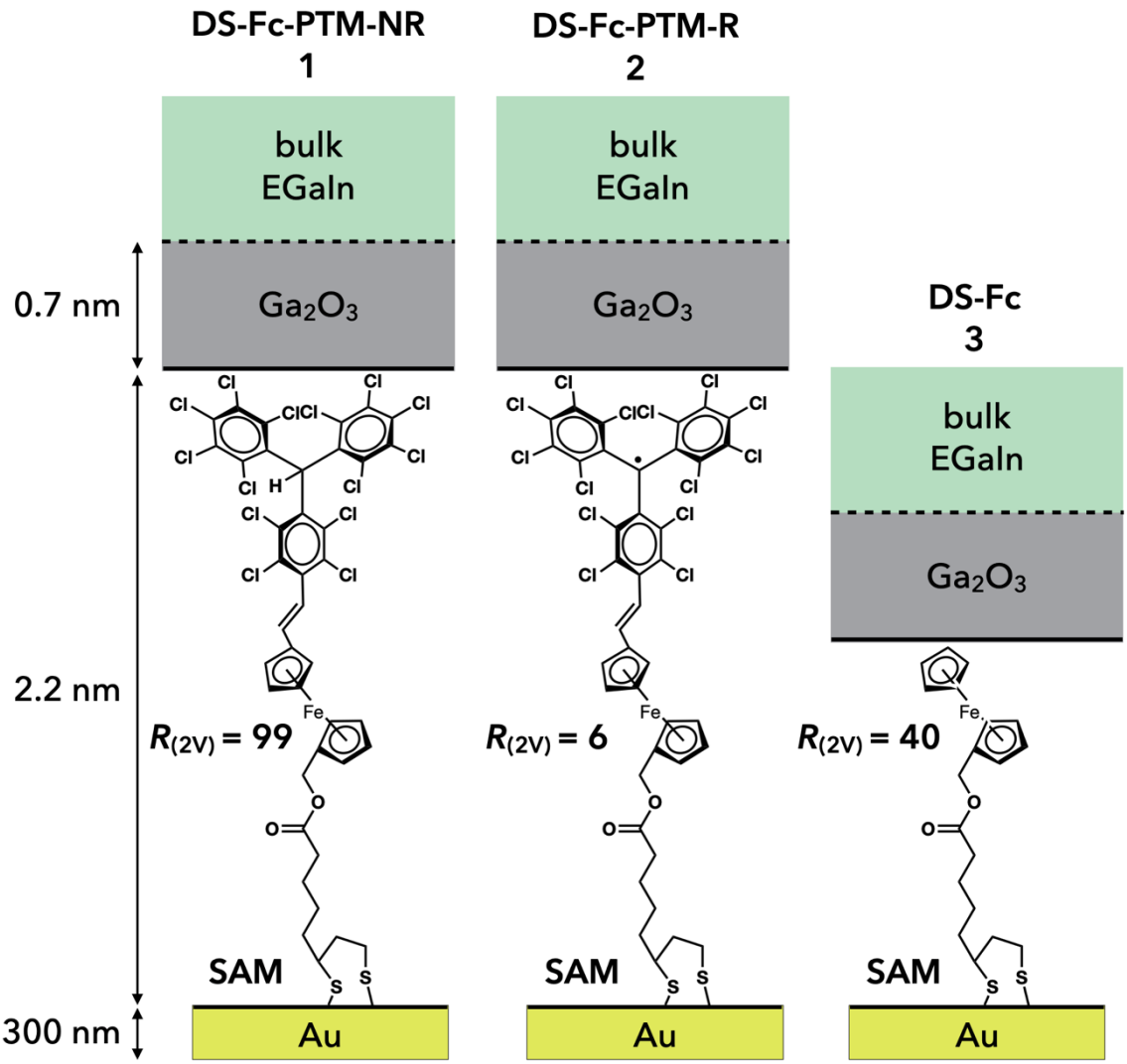

Figure 6 | Idealized schematic representations of the junctions based on Au bottom electrodes, SAMs **1**, **2**, and **3**, and Ga_2O_3/EGaIn top electrodes.

3-4. New design of molecular diode in this study

Although some innovative results have been reported by using ferrocene as a donor, there are few examples of studies using donor skeleton other than ferrocene, and there are no studies of D-σ-A type diodes, as proposed by Ratner and Aviram, in which the donor and acceptor skeletons are connected by an insulating σ-bridge. Therefore, in this doctoral dissertation, the author has decided to synthesize the diodes with novel donor skeleton and donor-acceptor system. The author proceeds the study in collaborating with Prof. Nijhuis, a leading expert in molecular diode research.

As the donor molecule, benzindolocarbazole (BIC)[22,23] was selected, which was also used in Chapter 2. In one of the successful previous studies, improved rectification performance has been observed in chromophores that allow two-electron oxidation such as ferrocene dimers. In this context, there are two reasons to choose BIC as a donor skeleton. (1) BIC is a π-extended phenylenediamine derivative that is capable of two-electron oxidation. (2) Due to that π-extension, on-site Coulombic repulsion is reduced, and the potential gap between the first (E_{ox}^1) and second (E_{ox}^2) oxidation potentials is smaller than that of corresponding phenylenediamine. As an acceptor skeleton, the author decided to use nitrofluorenone derivatives, which are typical two-electron reducible molecules.[24,25] This choice also considers the easy structural varifation in modulating the electron-withdrawing ability by changing the number and position of the substituted nitro groups or replacing the ketone moiety to dicyanomethylene. In addition, lipoic acid, which was a disulfide substituent used in a previous study, was introduced at the metal biding site to the bottom electrode.[21]

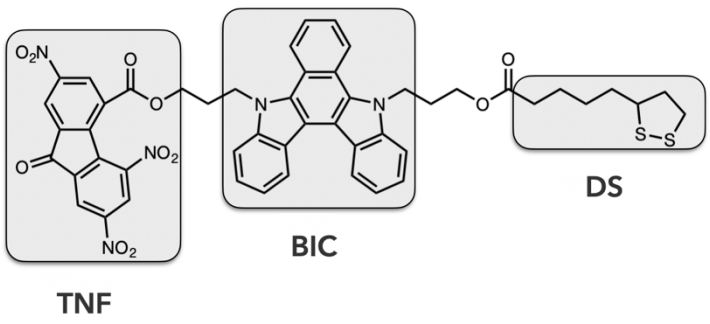

Figure 7 | Molecular design of newly designed diode.

3-5. Preparation of novel molecular diode

One of the features of the BIC skeleton is that a substituent can be introduced on the N atom of the carbazole at the previous stage of formation of the BIC skeleton, as was also utilized in Chapter 1. In this work, the author also planned to take advantage of this feature to prepare the diode molecules (Scheme 1). Benzocarbazole **5** was prepared by treating **4** with NaH and 3-iodo-1-propanol. Benzocarbazole with metal-biding moiety **6** was prepared by the condensation reaction of α-lipoic acid in dichloromethane in the presence of EDCI and DMAP. The target DA-dyad **1** was derived from **6** upon exposure to nitrene insertion conditions (160 °C in 1,2-dichlorobenzene), followed by substitution of propanol on the other N atom and condensation reaction with electron-accepting trinitrofluorenone attached with carboxylic acid. In addition, TNF-BIC **2** which does not have metal-binding site, was prepared using the same synthetic method. Thus, to a solution of mono-butylated-BIC **9** in dry DMF was added NaH and 3-iodo-1-propanol to obtain **10**, which was converted to **2** upon condensation reaction with TNF-carboxylic acid (Scheme 2).

Scheme 1

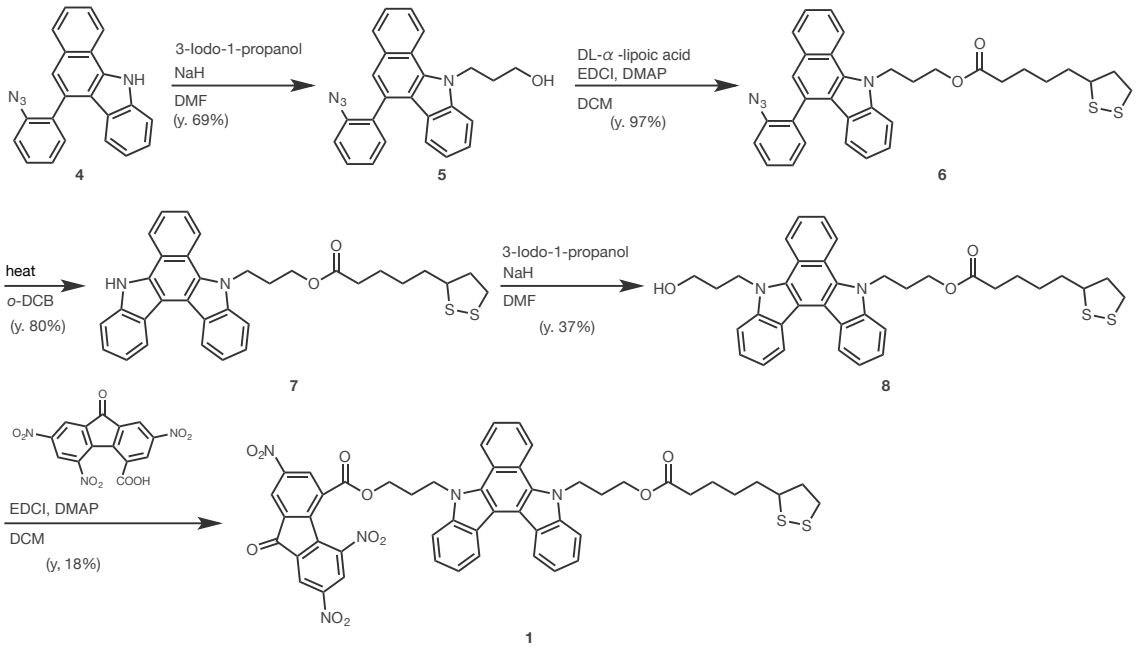

Scheme 2

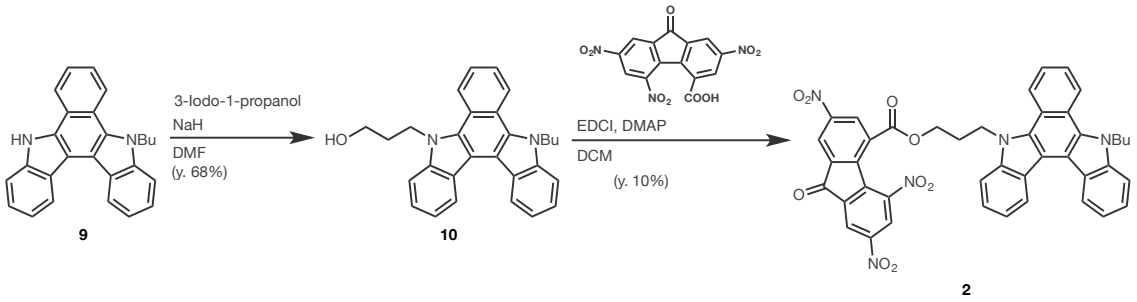
HN
NBu
9
3-Iodo-1-propanol
NaH
DMF
(y. 68%)
HO
N
NBu
10
O
O2N
NO2
NO2
COOH
EDCI, DMAP
DCM
(y. 10%)
O2N
O
O
O
N
NBu
NO2
NO2
2

3-6. Electrochemical properties of the molecular diode

CV and DPV measurements of dibutylated-BIC and MeOCO-TNF showed two-stage one-electron oxidation and reduction waves, respectively. These results indicated that each chromophore undergoes two-electron oxidation/reduction. On the other hand, the voltammograms of molecular diode TNF-BIC-DS and its reference compound TNF-BIC exhibit two-stage one-electron oxidation as well as two-stage one-electron reduction, as shown in Figures 8 and 9. The positive and negative shifts in the oxidation and reduction waves derived from BIC and TNF, respectively, suggest that the charge-transfer (CT) interaction between the donor and acceptor units lowers HOMO-level where as the LUMO-level is raised, thus, stabilizing the neutral state and prevents the unintentional oxidation and reduction reactions (Table 1).

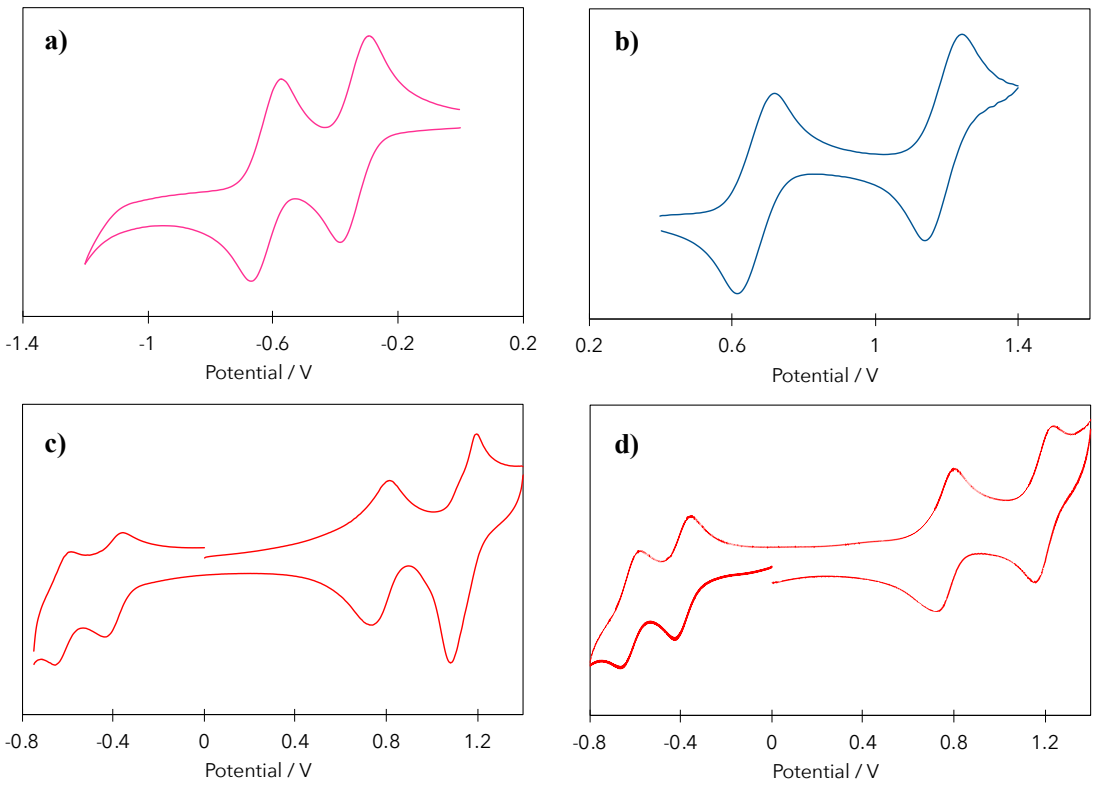

Figure 8 | Cyclic voltammograms of **a)** dibutylated-BIC, **b)** TNF-COOMe, **c)** TNF-BIC-DS (**1**), and **d)** TNF-BIC (**2**) measured in CH_2Cl_2 (*E*/V vs SCE, 0.1 M Bu_4NPF_6 as a supporting electrolyte, Pt electrode, scan rate 100 mV/s). Vertical axes indicate the electric current.

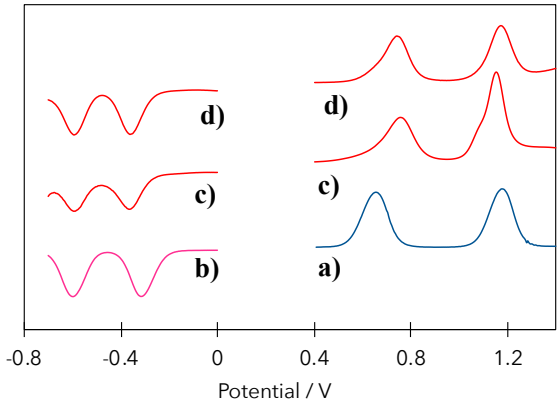

Figure 9 | Differential pulse voltammograms of **a)** dibutylated-BIC, **b)** TNF-COOMe, **c)** TNF-BIC-DS (**1**), and **d)** TNF-BIC (**2**) measured in CH_2Cl_2 (*E*/V vs SCE, Pt electrode, 0.1 M Bu_4NPF_6).

Table 1 | Oxidation potentials of TNF-BIC-DS (**1**), TNF-BIC (**2**), dibutylated-BIC, and TNF-COOMe, measured by DPV method in CH_2Cl_2.

compd.	E^{red}_2	E^{red}_1	E^{ox}_1	E^{ox}_2
TNF-BIC-DS (**1**)	-0.60	**-0.37**	**+0.76**	+1.16
TNF-BIC (**2**)	-0.59	**-0.36**	**+0.74**	+1.17
Bu-BIC-Bu	—	—	+0.65	+1.17
MeOCO-TNF	-0.60	-0.32	—	—

3-7. UV-Vis-NIR spectra of the molecular diode

In the UV-Vis-NIR spectra of BIC, TNF-COOMe, and BIC-TNF-DS **1**, new absorption band derived from the CT interaction was observed in the molecular diode **1** (Figure 10). In preliminary investigations at our collaborators, a decrease in HOMO and an increase in LUMO on the substrate were observed as suggested by voltammetry measurements, and it is also determined that the rectification ratio of this molecule is about 80. Furthermore, the formation of SAMs on metallic substrates has been revealed, and of particular interest, the temperature-dependent reversal of the rectification effect has been observed. This unique phenomenon will be investigated in due course. It should be noted that the properties of author's molecular diode are evaluated by sandwiched-structure of the molecular layer by the electrodes, thus the device can be also considered as a molecular junction.

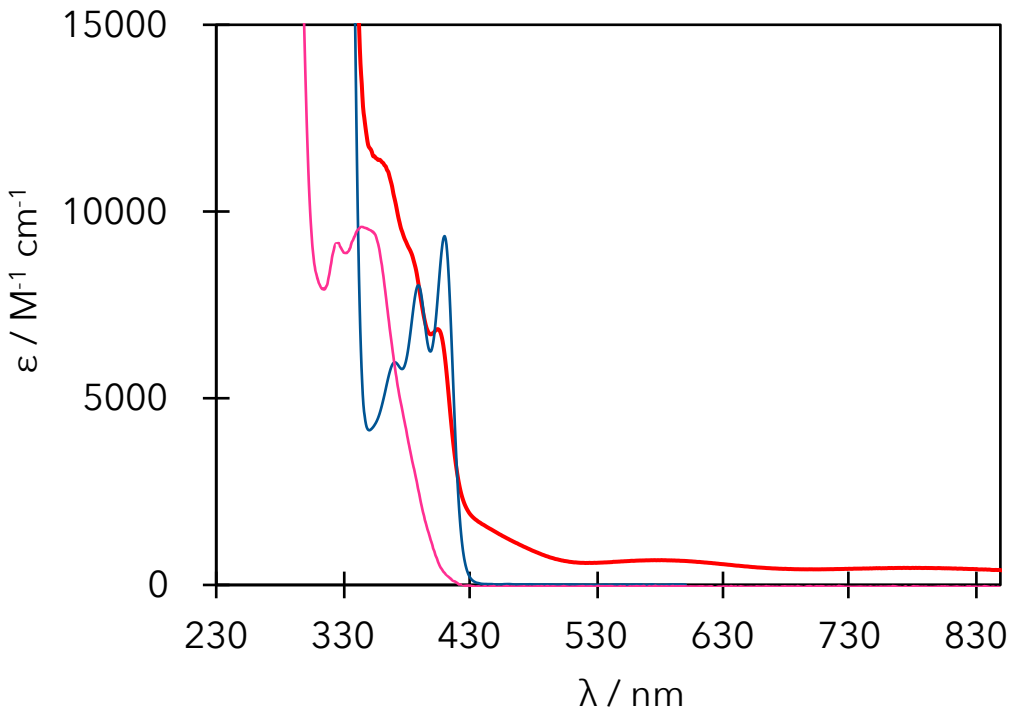

Figure 10 | UV-Vis-NIR spectra of dibutylated-BIC (blue), TNF-COOMe (pink), and **1** (red) measured in CH_2Cl_2.

3-8. Molecular junctions: principal, progress, and problem

A molecular junction refers to a metal electrode cross-linked at both ends of a molecule, which can be divided into two categories: a single-molecule junction and a molecular-film junction.[26-29] The first example of the single-molecule junction is the molecular diode, which was proposed in 1974.[12] If a single molecule can have rectification or transistor functions, the ultimate size of electronic devices can be realized, and device performance can be dramatically improved. Although various research groups have been actively working on single molecule junctions, this area of research has not deviated from the level of basic research due to the poor stability of single molecule junctions or poor reproducibility of observing single molecules sandwiched between the electrodes.

On the other hand, molecular-film junction has developed using LB films or SAMs. As described in the introduction of molecular diodes, the formation of electrode has been problematic, but the improved electrode formation method was developed by Prof. Nijhuis and colleagues at NUS (Figure 11).

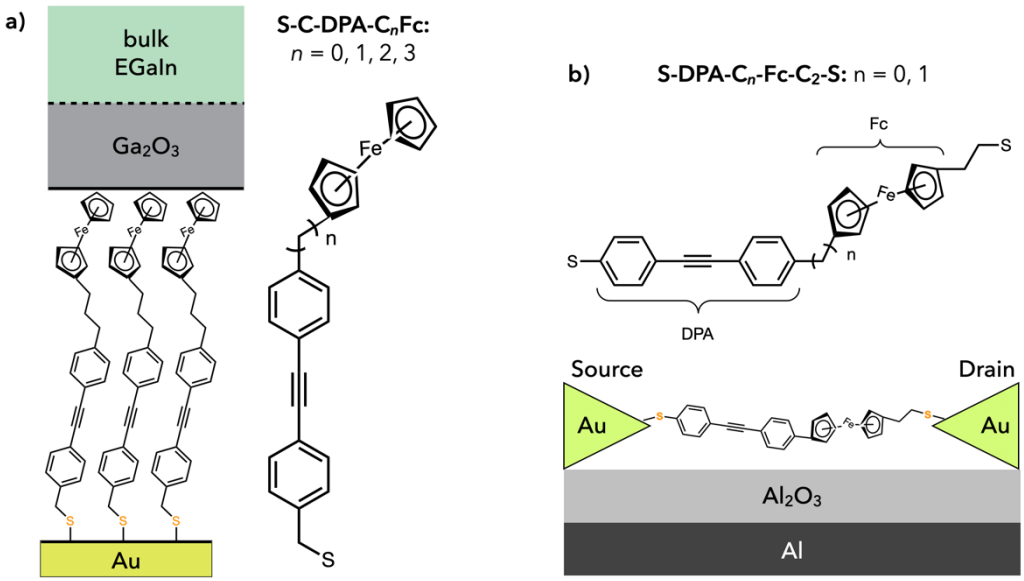

Figure 11 | Illustrations of the junctions and description of the combined Marcus–Landauer model. **a**, Illustration of the SAM-based junction with the chemical structure of the S-C-DPA-C_n -Fc (n = 0, 1, 2, 3). **b**, Schematic illustration of the single-molecule transistor with S-DPA-C-Fc-C_2-S or S-DPA-FcC_2-S, where a second thiol anchoring group was used to form a contact to the electrode (separated by a -CH_2CH_2- tether from the Fc unit).

3-9. Molecular junctions with conductivity ON/OFF switching

Molecular junctions are expected to possess various functions such as molecular diodes and molecular transistors, depending on the molecule used. If functional molecules whose conductivity can be changed by external stimuli are adopted as components of the junction, a highly functional molecular junction that can switch the conductivity in a ON/OFF manner by the external stimuli could be created. One of the advantages of organic molecules is the availability of various stimuli such as UV-Vis light irradiation, magnetic field or pH changes and so on.[30] For example, in photoswitch-type molecular junctions,[31] it has been observed that light irradiation causes cis/trans isomerization of the molecule, resulting in a difference in conductivity at the detecting potential (Figure 12).

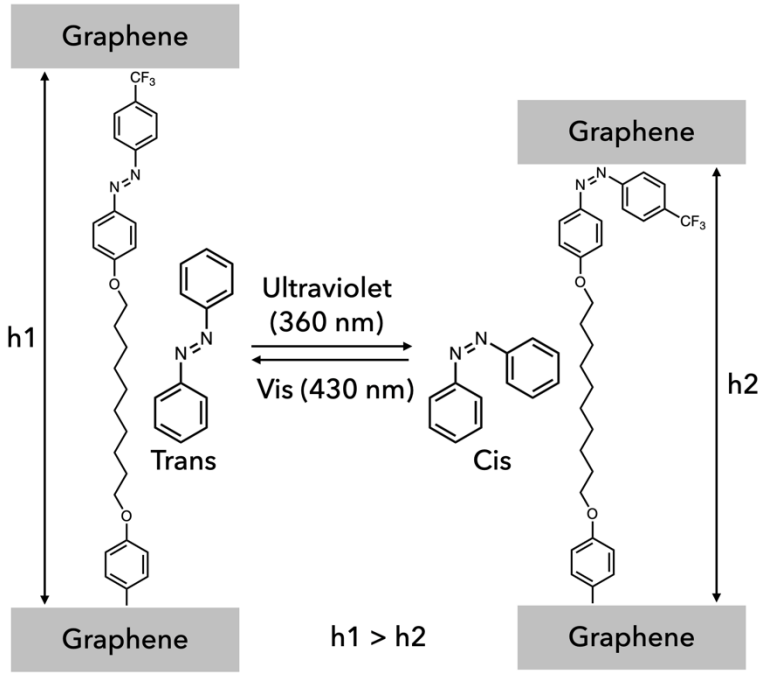

Figure 12 | Photo-switching of graphene-aryl azobenzene monolayer–graphene devices. (**a**) Molecular tunneling barriers (with h1 and h2 being the vertical distance between the two graphene electrodes) corresponding to conformational changes in aryl azobenzene molecules with light irradiation.

3-10. Electrically-switchable molecular junctions

However, when external stimuli such as light and heat are used, other devices such as light sources and heat sources are required to provide external stimuli. To overcome this problem, the author aimed to develop and electrically-switchable molecular junction that can directly oxidize/reduce the molecules via electrodes, using the potential input as an external stimulus. Although the potential input has the characteristic advantage without requiring other external devices for input, the development has been hampered on molecular junction whose conductivity is changed by using electrical input as an external stimulus until now.[32-34]

3-11. Challenges of electrically-switchable molecular junction

It is an essential condition for a conductivity switching molecular junction to possess two stable states with different electrical conductivity at the same detection potential. However, such condition is hardly realized in the conventional redox molecules. Figure 13 shows the voltammogram of a typical redox molecule. When the redox wave is over the top, the molecule is oxidized/reduced and changed from neutral state (state A) to oxidized state (state B), or from reduced state (state A) to neutral state (state B). The state A shown in the green and the state B shown in the pink do not coexist at any potential. In other words, there is no region in which two states (A and B) can coexist simultaneously. Accordingly, it is impossible to construct a molecular junction with a conductivity change using conventional redox molecules.

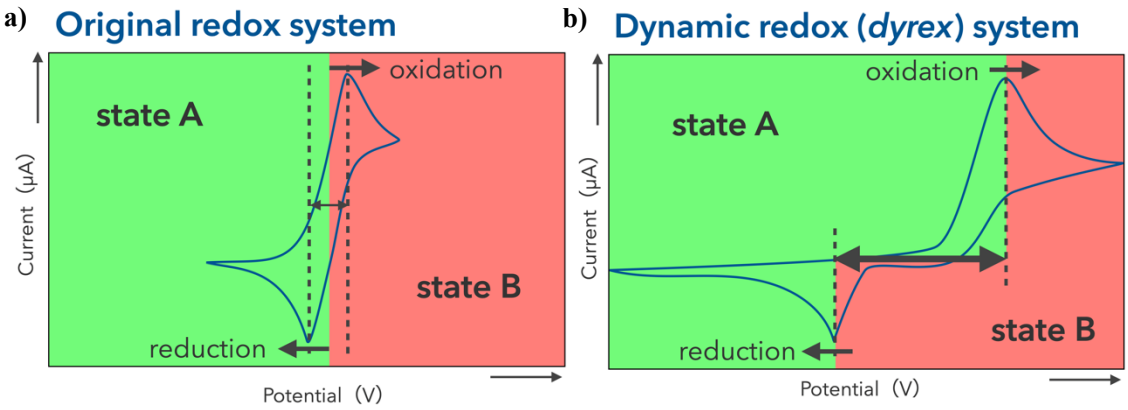

Figure 13 | Plausible cyclic voltammograms of **a**) original redox system, and **b**) dynamic redox (*dyrex*) system.

To solve this issue, the author focused on a recently developed skeleton called dynamic redox (dyrex) system molecules.[35,36] Dyrex molecules are characterized by a large separation between the oxidation and reduction potentials due to a large structural change upon redox reaction. As a result of this phenomenon, there actually exist the region where states A and B can coexist stably, so that the region of two stable states at the same potential can be used for detection purpose. Therefore, these molecules can be utilized as molecular junctions with conductivity-switching function.

3-12. Dynamic redox (*dyrex*) system

As dyrex molecules, two-series of compounds, namely hexaphenylethane (HPE) type[37] and bis(diarylethenyl) (BDAE) type,[38] were investigated. HPE type exists as a bond-formed configuration as the neutral state, but when oxidized, the bond is cleaved form two units of triarylmethylium, which are twisted around the central biphenyl moiety thus undergoing a structural change. This skeleton can be utilized as a highly responsive device because of the rapid formation and cleavage of the bond upon redox reaction. On the other hand, BDAE-type compounds adopt twisted configuration at the neutral state, and the large structural change in accompanied by reducing the twisting angle occurs by forming a bond between the diarylethenyl moieties. The latter class has a large structural change between neutral and oxidized state, and a larger shift in redox potential than the HPE type skeleton has been observed. Thanks to these characteristics, BDEA type skeleton can be expected to exhibit a larger potential range of bistability. The author considered that utilizing the properties of dyrex molecules could be suitable to develop electrically-switchable molecular junctions. Tuning of the redox potentials can be easily done by controlling the electron donating properties of the substituted aryl group, which makes the dyrex skeleton more attractive from the view point of fine-tunability.

Scheme 3

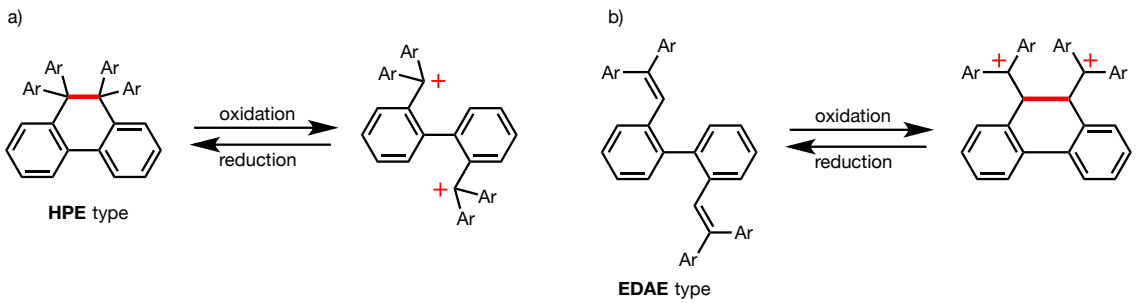

3-13. Preliminary examination of previously synthesized molecule

In related to the work on molecular junction, the author also continued to collaborate Prof. Nijhuis, his collaborator in molecular diodes, who firstly conducted preliminary investigations of EDAE-type compound **3A** synthesized by author's lab member, Dr. Ohta.[39]

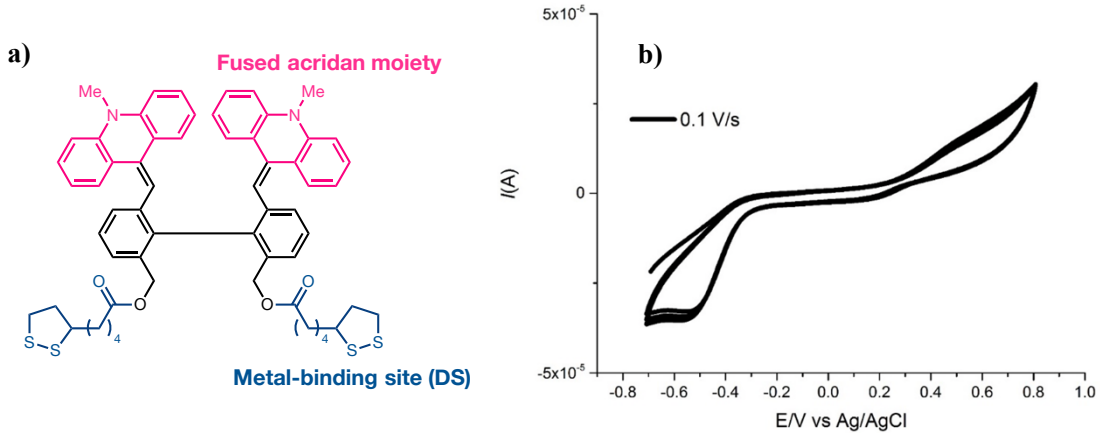

Figure 14 | **a**) Molecular structure of EDAE-type compound **3A**, and **b)** cyclic voltammogram of **3A**-monolayer on Au^{TS} surface.

According to the measurement of the redox behavior on the gold electrode, the separation of the redox waves was observed similar to the solution state. This result shows that the large structural change of the molecule upon redox reaction is maintained on the electrode (Figure 14). The voltage-dependent conductivity of the resulting molecular film on the substrate was also measured at the same detection potential. The measurements showed that the conductive ON/OFF function definitely appeared. When the time-dependence of the ON/OFF ratio of conductivity was investigated, the ratio increased as time passed, and the maximum value of R = 40 was attained, which is much higher than the conventional one. This result is outstanding because it is an exceptional value. However, the author was informed by collaborators that the R value just after switching from OFF to ON is very low (<5), which is the major problem in the response time (Figure 15). Based on the above-mentioned considerations, the author thought that a novel molecular design was needed to solve the problem with overcoming the slow response time.

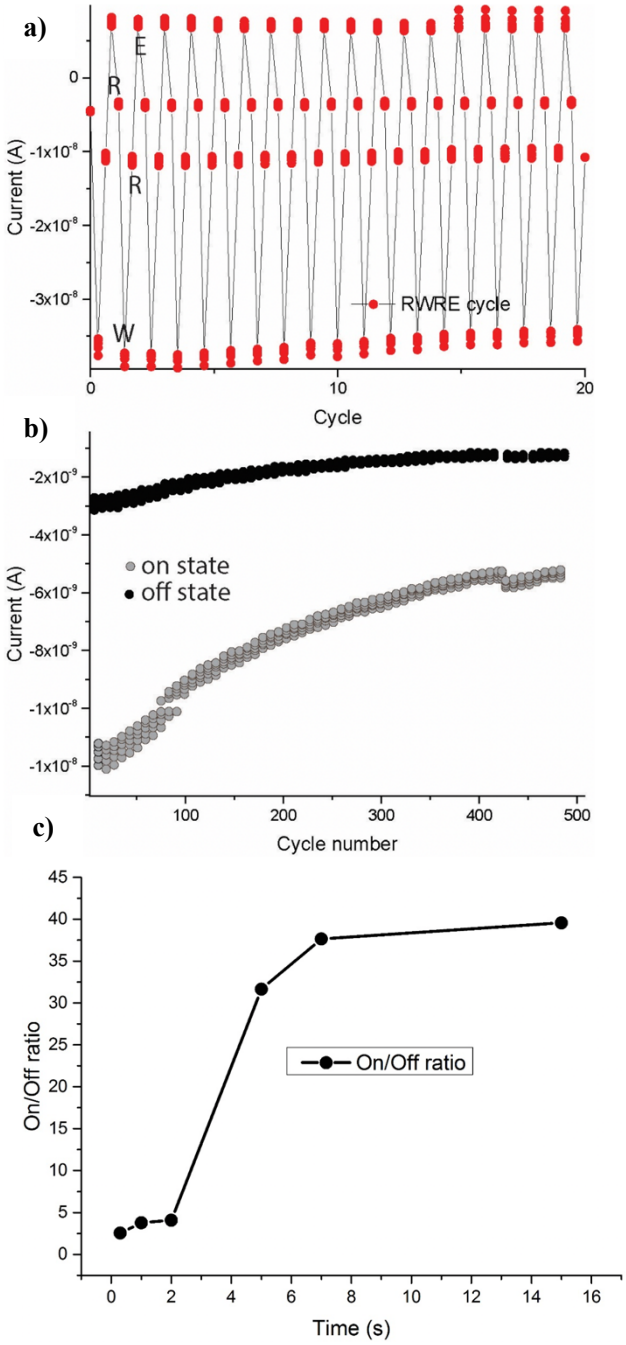

Figure 15 | **a**), **b**) Write-multiple read-erase-multiple read (WRER) cycles of **3A**-monolayer. The writing, reading, erasing, and reading voltages were -1.0, -0.7, 1.0, -0.7 V, respectively. **c)** On/Off ratio as a function of time delay between Write-read cycle. This suggested that dyrex based molecular junctions useful for designing monolayer based memory devices, the values are lower than that of the industrial requirement for on/off ratio of 100. It will reach higher on/off ratio with time.

3-14. Considerations for accelerating the reaction rate

The author believes that the slow response rate may be related to the reaction rate of structural change, so the author performed detailed electrochemical measurement including multiple cycles of redox reactions of **3A** during cyclic voltammetry measurements (Figure 16). According to the voltammogram, a new oxidation wave was observed at -0.12 V in the second oxidation cycle, which was not observed in the first cycle. Here, the reaction scheme of the EDAE-type skeleton is now considered. The skeleton, which exists as a torsional form in the neutral state, is converted into a stable dication state upon C–C bond formation between the two diarylethyl radical moieties resulting from 2e-oxidation. In the subsequent reduction step, the resulting neutral diradicals are converted to the original bis(diarylethenyl) compound through a process of bond cleavage. Since the new oxidation wave in the second cycle observed by the voltammogram is attributed to the neutral diradical species, the author thought that the process from open-shell diradical species to closed-shell double-bonded species should be slow in **3A**, and thus the new design is necessary to accelerated this step (Scheme 3). It is highly likely that the bulkiness of the tricyclic cationic skeleton hampers co-planarization of the 2p-orbital of the radical with the breaking C–C σ-bond.

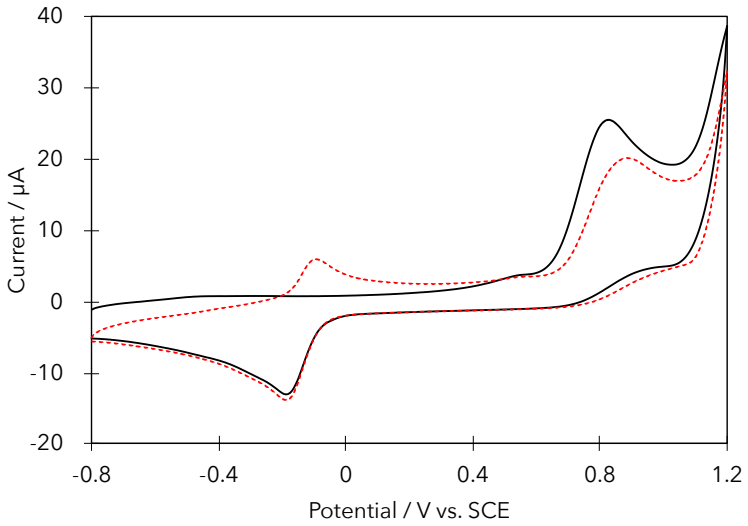

Figure 16 | Cyclic voltammograms of **3A** measured in CH_2Cl_2 (*E*/V vs SCE, 0.1 M Bu_4NPF_6 as a supporting electrolyte, Pt electrode, scan rate 100 mV/s). Black solid line indicates the 1st cycle, and red dot line indicates 2nd cycle, respectively.

Scheme 3 | Redox scheme of BDAE-type compound **3A**.

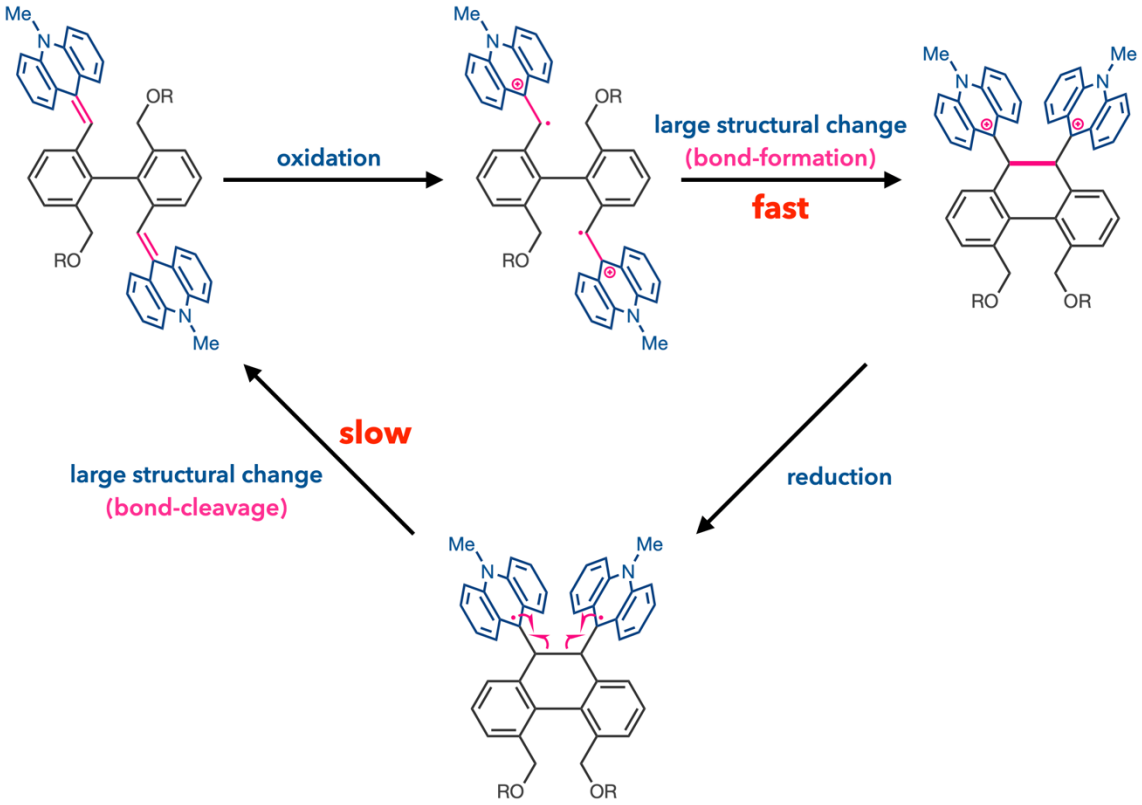

3-15. Molecular design for superior molecular junction

Based on the above considerations, the author decided to prepared three kinds of compounds based on two molecular design guidelines for developing better molecular junctions: 1) to introduce a non-fused aromatic substituent in order to eliminate the bulkiness and to accelerate the bond cleavage process, 2) to prepare several derivatives with different electron-donating properties in order to adjust the potential in accordance with the needs (Figure 17). As the substituent, aromatic amines were used for the purpose of maintaining the stability at the dication state.

Figure 17

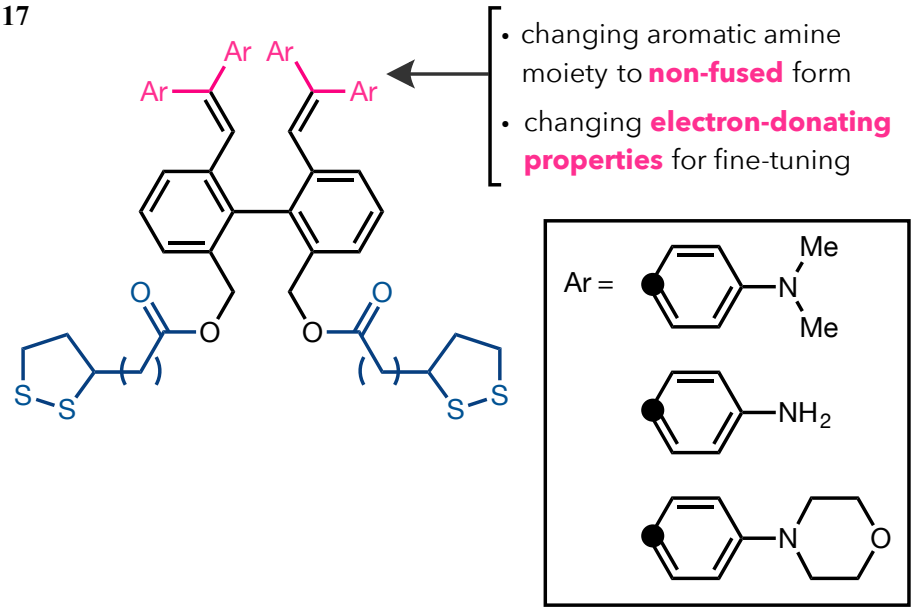

3-16. Preparation of new BDAE compounds undergoing rapid response

To a solution of 1,3-dibromobenzene which is a commercially available was added LDA followed by iodine to obtain 1,3-dibromo-2-iodobenzene. Then, copper-catalyzed Ullmann coupling was conducted to generate biphenyl **12**. **12** was converted to dialdehyde **13** by diformylation by dilithiation, which was converted into **15** through reduction by $NaBH_4$ and TBS protection of the resulting alcohol. Dialdehyde **16** was prepared by formylation via another dilithiation of the remaining dibromo groups using *sec*-BuLi. **16** is a common intermediate in the preparation of several derivatives.[39] Easy introduction of different substituents at the end of scheme is an important point in this method (Scheme 4). The target BFAE derivatives **3X** (**X** = **D**, **M**, **P**) were prepared by subjecting dialdehyde **16** to Horner-Wadsworth-Emmons (HWE) reactions using the corresponding HWE reagent, followed by deprotection of the TBS group and condensation of lipoic acid at the benzyl alcoholic moiety, respectively.

Scheme 4

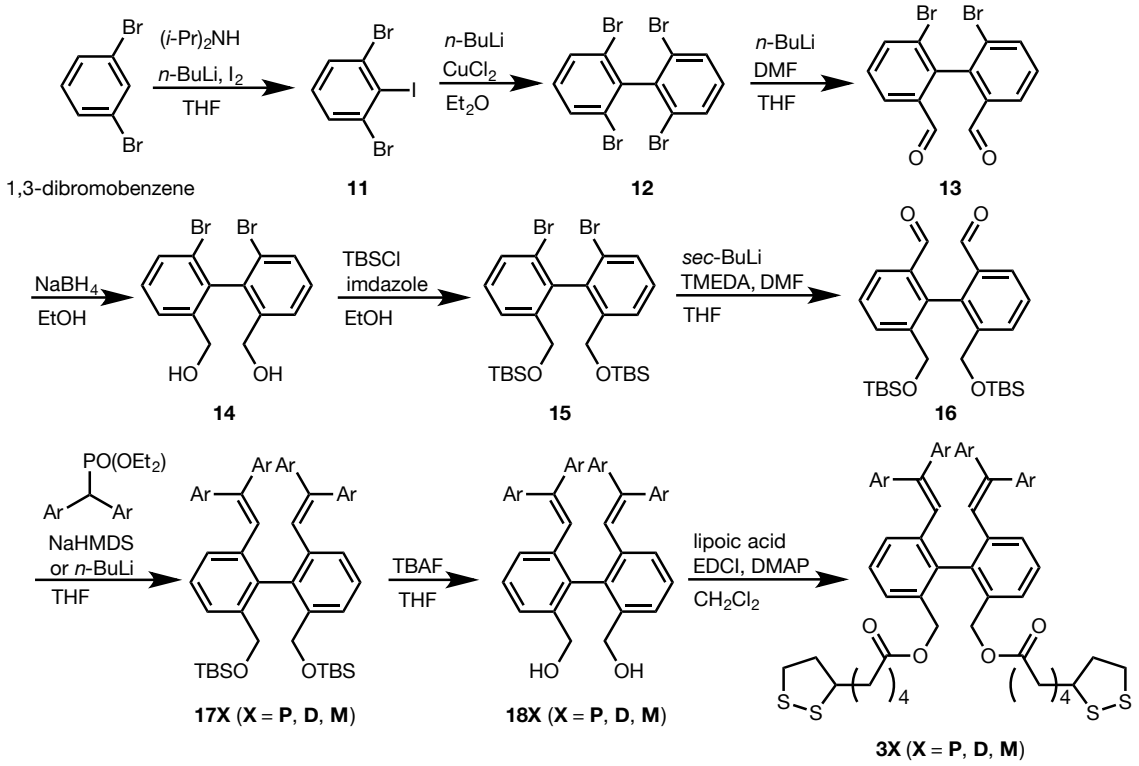

3-17. Electrochemical properties of newly prepared BDEA compounds

The voltammograms of the newly synthesized compound **3X** (**X** = **P**, **D**, **M)** showed characteristic dyrex behavior (Figure 18 and Table 3). There is no oxidation waves after the second cycle, which had been observed in the compound **3A** containing the tricyclic acridine units. Thus, the neutral diradical species **3X˙˙** (**X** = **P**, **D**, **M)** produced by the reduction of **3X** are rapidly converted to a closed-shell double-bonded structure with facile C–C bond fission. In addition, as the author had expected, the modulation of the electron-donating nature of the substituent was remarkably evident in the shift of the redox potentials. For the substituent with the highest electron-donating group, the oxidation potential is +0.76 V and the reduction potential is -0.43 V, so the working potential is between -0.43 V and +0.76 V, then for the high electron-donating group, the working potential is between -0.31 V and +0.80 V, then for the low electron-donating group, the working potential is between -0.18 V and +1.04 V. It was clearly showing that the modulation of the working potential can be achieved based on the same synthetic strategy just by changing the substituent at the end of the synthetic scheme. In the future, measurements will be performed on these derivatives, which can help developing a novel molecular junction.

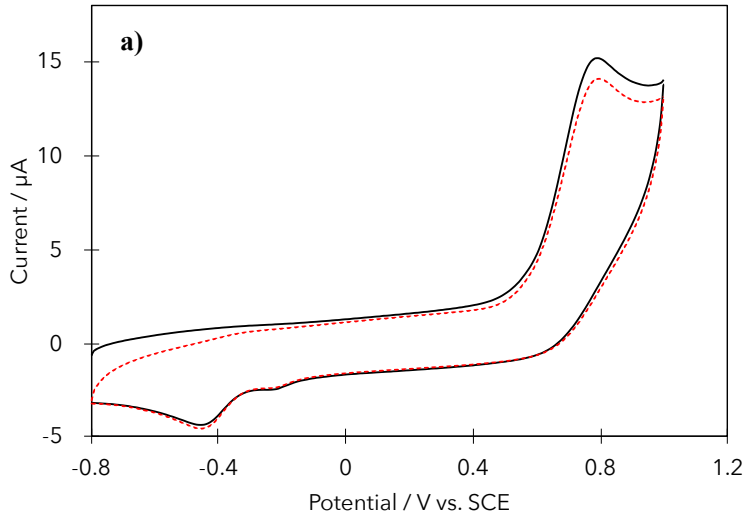

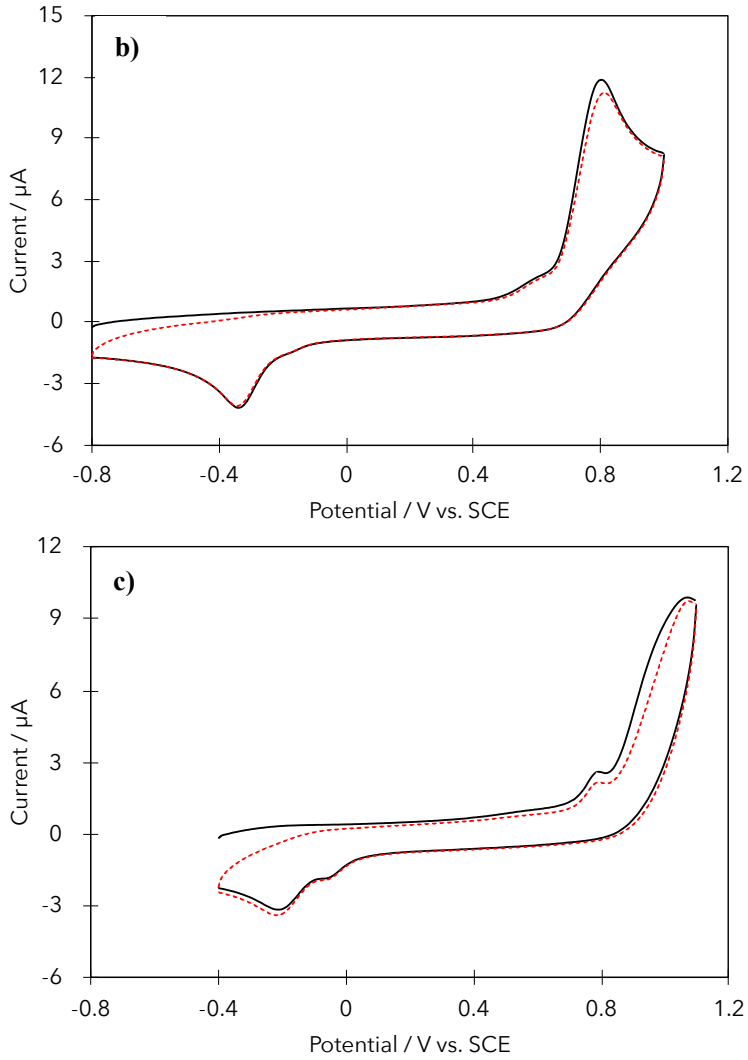

Figure 18 | Cyclic voltammograms of a) **3P** ,b) **3D**, and c) **3M** measured in CH_2Cl_2 (*E*/V vs SCE, 0.1 M Bu_4NPF_6 as a supporting electrolyte, Pt electrode, scan rate 100 mV/s). Black solid line indicates the 1st cycle, and red dot line indicates 2nd cycle, respectively.

Table 3 | Oxidation potentials of **3A**, **3M**, **3D**, and **3P** measured by DPV method in CH_2Cl_2.

compd.	E^{ox} (V)	E^{red} (V)	E^{ox}(diradical) (V)
3A (acridane)	+0.80	-0.16	-0.12
3M (morphorino)	+1.04	-0.18	—
3D (dimethylamino)	+0.80	-0.31	—
3P (pyrodinino)	+0.76	-0.43	—

Experimental Section

General

^{1}H NMR spectra were recorded on Bruker AVANCE III HD (400 MHz). IR spectra were taken on a JEOL JIR-WINSPEC100 FT/IR spectrophotometer. Mass Spectra were recorded on JEOL JMS-T100GCV spectrometer in FD/FI, EI mode (GC-MS & NMR Laboratory, Graduate School of Agriculture, Hokkaido University). Column chromatography was performed on silica gel I-6-40 (YMC) of particle size 40-63 μm. Melting points were measured on Yamato MP-21 or Yanagimoto micro melting point apparatus and reported uncorrected. UV/Vis/NIR spectra were recorded on a Hitachi U-3500 spectrophotometer or PerkinElmer Lambda 900S at the Open Facility of Hokkaido University. CD spectra were measured on a JASCO J-820 spectropolarimeter. Fluorescence spectra were measured on a Hitachi F-7000 fluorescence spectrophotometer. All commercially available compounds were used without further purification. Solvents were purified prior to use.

<Preparation of molecular diode 1>

1) Preparation of **5**

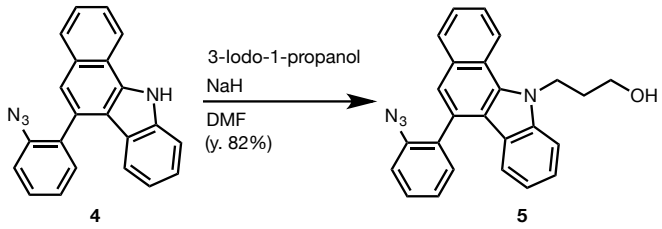

4 5

To a stirred solution of **4** (501 mg, 1.50 mmol) in dry DMF (15 mL) under argon was added NaH (78 mg, 1.95 mmol, 60% in mineral oil) at room temperature. After stirring for 10 min, a solution of 3-iodo-1-propanol (558 mg, 3.00 mmol) in dry DMF (1 mL) was added dropwise over 5 min to the mixture. After stirring for 1.5 h at room temperature, the mixture was diluted with H_2O and extracted with Et_2O three times. The combined organic layer was washed with H_2O and brine, dried over anhydrous $MgSO_4$, and concentrated in vacuo. The residue was chromatographed on silica-gel (hexane:CH_2Cl_2 =

2:1 to 1:1) to give **5** (480 mg, 82%) as a pale-yellow solid.

Mp 59 °C; IR (KBr) ν/cm^{-1} :3397, 3051, 2927, 2117, 1574, 1559, 1489, 1468, 1452, 1433, 1370, 1334, 1301, 1284, 1246, 1165, 1128, 1096, 1050, 1029, 742, 710; ^{1}H NMR (400 MHz, DMSO-*d*6) δ/ppm : 8.66 (d, 1H, *J* = 8.7 Hz), 8.03 (dd, 1H, *J* = 8.1, 1.4 Hz), 7.65 (d, 1H, *J* = 8.7 Hz), 7.63 (dd, 1H, *J* = 8.7, 1.4 Hz), 7.59 (dd, 1H, *J* = 8.7, 1.4 Hz), 7.55 (d, 1H, *J* = 7.4, 1.2 Hz), 7.49 (s, 1H), 7.48 (dd, 1H, *J* = 8.2, 1.2 Hz), 7.42 (dd, 1H, *J* = 7.4, 1.2 Hz), 7.38 (dd, 1H, *J* = 8.1, 1.2 Hz), 7.33 (dd, 1H, *J* = 7.4, 1.2 Hz), 6.98-7.05 (m, 2H), 5.02 (t, 2H, *J* = 5.6 Hz), 3.81 (t, 2H, *J* = 5.6 Hz), 2.38 (qn, 2H, *J* = 5.6 Hz); ^{13}C NMR (100 MHz, DMSO-*d*6) δ/ppm:140.80, 138.77, 134.51, 133.08, 133.02, 131.95, 131.65, 129.63, 129.36, 125.65, 125.00, 124.97, 124.62, 122.34, 122.01, 121.75, 121.68, 121.19, 119.63, 118.56, 118.09, 109.02, 59.82, 45.58, 32.69; HRMS (FD, m/z) [(M+H^{+})]calcd. for $C_{25}H_{20}N_4O_1$: 392.1637; found: 392.1621.

2) Preparation of **6**

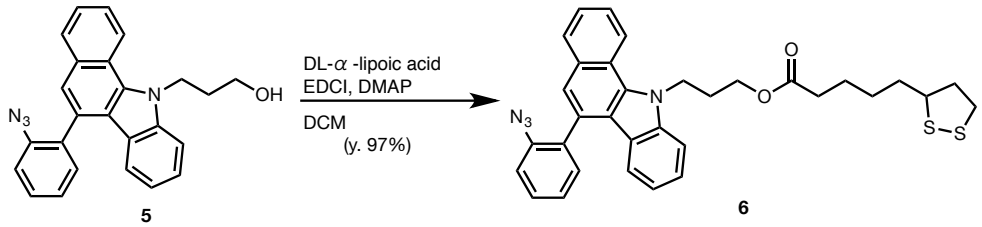

5 **6**

A solution of **5** (484 mg, 1.23 mmol), DL-α-lipoic acid (510 mg, 2.47 mmol), 1-(3-dimethylaminopropyl)-3-ethylcarbodiimide hydrochloride (EDCI, 497 mg, 2.59 mmol) and 4-dimethylaminopyridine (DMAP, 316 mg, 2.59 mmol) in dry CH_2Cl_2 (12 mL) under argon was stirred for 1 h at room temperature. After stirring, the resulting mixture was filtered through the pad of silica-gel and eluted with mixed solvent (CH_2Cl_2:EtOAc = 4:1) and evaporated the solvent to give **6** (694 mg, 97%) as a pale-yellow solid.

Mp 88°C; IR (KBr) ν/cm^{-1} :3440, 3052, 2926, 2861, 2113, 2090, 1728, 1467, 1453, 1443, 1432, 1376, 1372, 1336, 1301, 1164, 1132, 1094, 1038, 934, 868, 740; ^{1}H NMR (400 MHz, DMSO-*d*6) δ/ppm : 8.56 (d, 1H, *J* = 8.6 Hz), 8.05 (dd, 1H, *J* = 8.3, 1.2 Hz), 7.63 (dd, 1H, *J* = 7.6, 1.5 Hz), 7.54-7.61 (m, 3H), 7.50 (s, 1H), 7.48 (dd, 1H, *J* = 7.6, 1.5 Hz), 7.42 (dd, 1H, *J* = 7.6, 1.5 Hz), 7.39 (dd, 1H, *J* = 8.3, 1.2 Hz), 7.34 (dd, 1H, *J* = 7.5, 1.1 Hz), 6.99-7.05 (m, 2H), 4.97 (t, 2H, *J* = 6.5 Hz), 4.27 (t, 2H, *J* = 6.5 Hz), 3.58 (qn, 1H, *J*

= 6.5 Hz), 3.08-3.21 (m, 2H), 2.39-2.51 (m, 5H), 1.91 (sext, 1H, *J* = 6.8 Hz), 1.67-1.76 (m, 4H), 1.45-1.59 (m, 2H); ^{13}C NMR (100 MHz, DMSO-*d*6) δ/ppm: 173.28, 140.56, 138.76, 134.39, 133.06, 132.96, 132.00, 131.62, 129.77, 129.41, 125.68, 125.05, 125.00, 124.70, 122.77, 121.90, 121.70, 121.48, 121.32, 119.81, 118.57, 118.18, 108.73, 61.73, 56.33, 42.97, 40.23, 32.50, 34.64, 34.04, 29.18, 28.82, 24.70; HRMS (FD, m/z) [(M+H$^+$)]calcd. for $C_{33}H_{32}N_4O_2S_2$: 580.1967; found: 580.1946.

3) Preparation of **7**

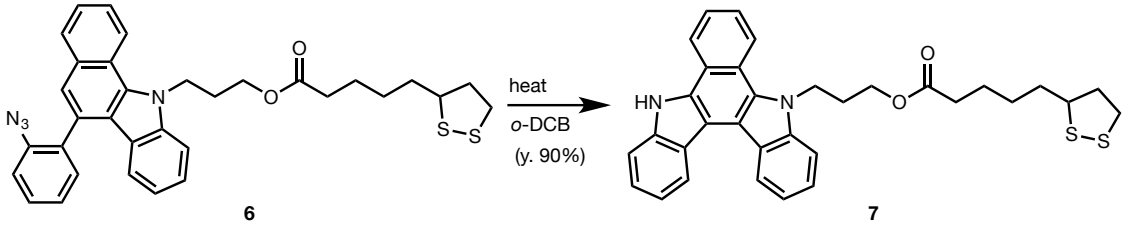

6 **7**

A solution of **6** (467 mg, 804 μmol) in 1,2-dichlorobenzene (10 mL) under argon was stirred for 18 h at 160 °C. After cooling to room temperature, the resulting mixture was chromatographed on silica-gel (hexane only to hexane:EtOAc = 3:1) to give **7** (400 mg, 90%) as a pale-yellow solid.

Mp 119 °C; IR (KBr) ν/cm^{-1} :3335, 3047, 2926, 1703, 1698, 1682, 1485, 1468, 1446, 1435, 1407, 1384, 1364, 1337, 1258, 1244, 1184, 1153, 1137, 1137, 1092, 737; ^{1}H NMR (400 MHz, DMSO-*d*6) δ/ppm : 12.28 (s, 1H), 8.89 (d, 1H, *J* = 8.2 Hz), 8.83 (dd, 2H, *J* = 8.2, 3.2 Hz), 8.76 (dd, 1H, *J* = 7.0, 2.4 Hz), 7.90 (d, 1H, *J* = 8.2 Hz), 7.73-7.79 (m, 3H), 7.54 (dd, 1H, *J* = 7.3, 7.3 Hz), 7.48 (dd, 1H, *J* = 7.6, 7.6 Hz), 7.43 (dd, 1H, *J* = 7.3, 7.3 Hz), 7.38 (dd, 1H, *J* = 7.6, 7.6 Hz), 5.08 (t, 2H, *J* = 7.0 Hz), 4.10 (t, 2H, *J* = 5.08 Hz), 3.53 (td, 1H, *J* = 2.7, 6.2 Hz), 3.04-3.18 (m, 2H), 2.28-2.38 (m, 3H), 2.23 (t, 2H, *J* = 6.6 Hz), 1.91 (sext, 1H, *J* = 6.8 Hz), 1.42-1.63 (m, 4H), 1.28-1.35 (m, 2H); ^{13}C NMR (100 MHz, DMSO-*d*6) δ/ppm: 173.28, 140.56, 138.76, 134.39, 133.06, 132.96, 132.00, 131.62, 129.77, 129.41, 125.68, 125.05, 125.00, 124.70, 122.77, 121.90, 121.70, 121.58, 121.32, 119.81, 118.57, 118.18, 108.73, 61.73, 56.33, 42.97, 40.23, 38.50, 34.64, 34.04, 29.18, 28.81, 24.70; HRMS (FD, m/z) [(M+H$^+$)]calcd. for $C_{33}H_{32}N_2O_2S_2$: 552.1905; found: 552.1895.

4) Preparation of **8**

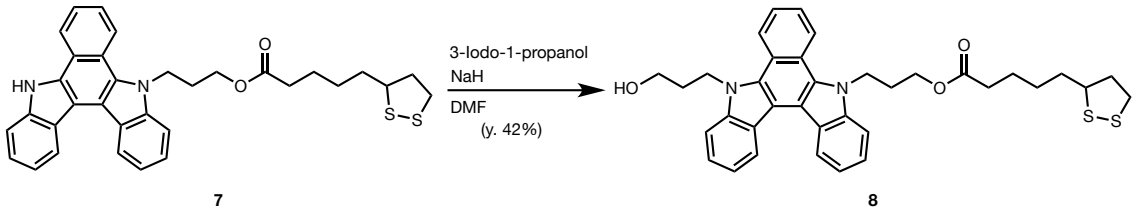

7 **8**

To a stirred solution of **7** (287 mg, 520 μmol) in dry DMF (10 mL) under argon was added NaH (31 mg, 780 mmol, 60% in mineral oil) at room temperature. After stirring for 10 min, a solution of 3-iodo-1-propanol (193 mg, 1.04 mmol) in dry DMF (1 mL) was added dropwise over 5 min to the mixture. After stirring for 1.5 h at room temperature, the mixture was diluted with saturated aqueous solution of NH_4Cl and extracted with EtOAc three times. The combined organic layer was washed with H_2O and brine, dried over anhydrous Na_2SO_4, and concentrated in vacuo. The residue was chromatographed on silica-gel (hexane:EtOAc = 3:2) to give **8** (134 mg, 42%) as a pale-yellow solid.

Mp 57 °C; IR (KBr) ν/cm^{-1} :3426, 3252, 3042, 2924, 2844, 2354, 2337, 1728, 1722, 1715, 1467, 1463, 1402, 1342, 1335, 1167, 1154, 1138, 1055, 917, 735; ^{1}H NMR (400 MHz, DMSO-*d*6) δ/ppm : 8.86-8.94 (m, 4H), 7.91 (dd, 2H, *J* = 2.6, 8.4 Hz), 7.77 (dd, 2H, *J* = 3.0, 6.6 Hz), 7.55 (dd, 2H, *J* = 3.0, 7.4 Hz), 7.42 (d, 2H, *J* = 7.4 Hz), 5.06 (t, 2H, *J* = 7.0 Hz), 5.00 (t, 2H, *J* = 7.0 Hz), 4.86 (t, 1H, *J* = 5.7 Hz), 4.07 (t, 2H, *J* = 5.7 Hz), 3.62 (dt, 2H, *J* = 5.0, 5.7 Hz), 3.52 (tdd, 2H, *J* = 2.5, 2.5, 6.8 Hz), 3.04-3.17 (m, 2H), 2.26-2.38 (m, 3H), 2.15-2.24 (m, 4H), 1.80 (sext, 1H, *J* = 6.8 Hz), 1.53-1.63 (m, 1H), 1.42-1.51 (m, 3H), 1.27-1.36 (m, 2H); ^{13}C NMR (100 MHz, DMSO-*d*6) δ/ppm: 173.12, 141.36, 141.30, 131.16, 130.95, 125.47, 125.41, 124.87, 124.86, 123.97, 123.62, 122.80, 122.71, 122.30, 122.27, 122.26, 122.11, 119.90, 119.80, 114.66, 114.28, 110.69, 110.68, 61.95, 58.81, 56.47, 43.79, 43.59, 40.31, 38.54, 34.47, 33.68, 33.33, 28.98, 28.57, 24.58 ; HRMS (FD, m/z) [$(M+H^+)$]calcd. for $C_{36}H_{38}N_2O_3S_2$: 610.2324; found:610.2338.

5) Preparation of **1**

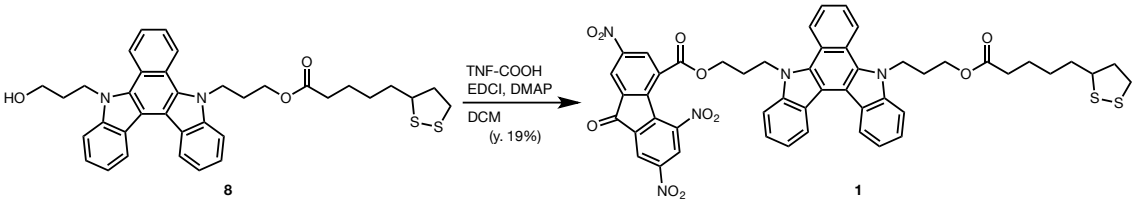

A solution of **8** (70 mg, 114 μmol), 2,5,7-trinitrofluorenone-4-carboxylic acid (164 mg, 456 μmol), 1-(3-dimethylaminopropyl)-3-ethylcarbodiimide hydrochloride (EDCI, 92 mg, 479 μmol) and 4-dimethylaminopyridine (DMAP, 59 mg, 479 μmol) in dry 1,2-dichloroethane (5 mL) under argon was stirred for 19 h at 60 °C. After cooling to room temperature, the mixture was diluted with CH_2Cl_2 and H_2O and filtered through the pad of Celite 545. The filtrate was extracted with CH_2Cl_2 three times. The combined organic layer was washed with H_2O and brine, and dried over anhydrous $MgSO_4$, and concentrated in vacuo. The residue was chromatographed on silica-gel (hexane:CH_2Cl_2 = 3:1 to 1:1) to give **1** (21 mg, 19%) as a dark-green solid.

Mp 85 °C; IR (KBr) ν/cm^{-1} :3447, 3088, 3053, 2923, 2861, 1731, 1613, 1592, 1533, 1466, 1424, 1399, 1341, 1311, 1279, 1229, 1173, 1085, 1041, 919, 830, 735, 706; ^{1}H NMR (400 MHz, DMSO-*d*6) δ/ppm :8.64 (d, 1H, *J* = 8.5 Hz), 8.46 (d, 1H, *J* = 8.5 Hz), 8.39 (d, 1H, *J* = 8.1 Hz), 8.19 (s, 1H), 8.16 (d, 1H, *J* = 8.1 Hz), 7.92 (d, 1H, *J* = 8.4 Hz), 7.80 (d, 1H, *J* = 8.4 Hz), 7.65 (s, 1H), 7.61 (dd, 1H, *J* = 7.8, 7.8 Hz), 7.60 (dd, 1H, *J* = 7.5, 7.5 Hz), 7.46 (dd, 1H, *J* = 7.8, 7.8 Hz), 7.40 (dd, 1H, *J* = 7.5, 7.5 Hz), 7.29 (dd, 1H, *J* = 7.5 Hz), 7.02 (dd, 1H, *J* = 7.5 Hz), 5.04 (br s, 2H), 4.93 (t, 2H, *J* = 7.2 Hz), 4.29 (br s, 2H), 4.24 (t, 2H, *J* = 5.72 Hz), 3.59 (tdd, 1H, *J* = 2.3, 2.3, 7.6 Hz), 3.06-3.20 (m, 2H), 2.44 (br s, 2H), 2.30-2.39 (m, 5H), 1.85 (sext, 1H, *J* = 6.8 Hz), 1.62-1.69 (m, 1H), 1.51-1.60 (m, 3H), 1.35-1.43 (m, 2H) ; ^{13}C NMR (100 MHz, DMSO-*d*6) δ/ppm:173.23, 141.21, 140.68, 130.55, 130.54, 125.29, 125.19, 124.90, 124.42, 123.49, 123.29, 122.62, 122.24, 121.59, 121.59, 121.43, 121.09, 119.91, 119.19, 114.01, 113.82, 110.74, 110.48, 66.09, 62.04, 56.51, 44.06, 43.65, 40.34, 38.56, 34.50, 33.77, 29.10, 28.63, 27.67, 24.68; HRMS (FD, m/z) [(M+H^+)]calcd. for $C_{50}H_{41}N_5O_{11}S_2$: 951.2244; found:951.2228.

<Preparation of reference molecular diode 2>

6) Preparation of **10**

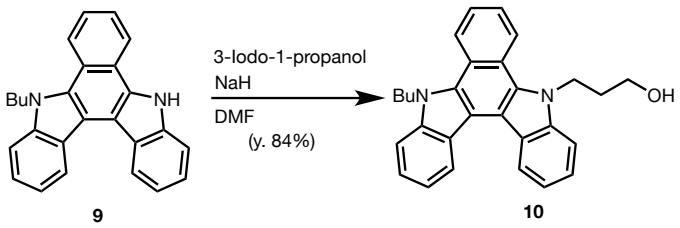

9 **10**

To a stirred solution of **9** (150 mg, 414 μmol) in dry DMF (5 mL) under argon was added NaH (25 mg, 621 μmol, 60% in mineral oil) at room temperature. After stirring for 10 min, a solution of 3-iodo-1-propanol (154 mg, 828 μmol) in dry DMF (1 mL) was added dropwise over 5 min to the mixture. After stirring for 5 h at room temperature, the mixture was diluted with H_2O, and extracted with EtOAc three times. The combined organic layer was washed with H_2O and brine, dried over anhydrous Na_2SO_4, and concentrated in vacuo. The residue was chromatographed on silica-gel (hexane:EtOAc = 2:1) to give **10** (147 mg, 84%) as a pale-yellow solid.

Mp 123 °C; IR (KBr) ν/cm^{-1} :3250, 3048, 2953, 2923, 2810, 1607, 1484, 1467, 1423, 1396, 1361, 1339, 1256, 1233, 1198, 1171, 1158, 1141, 1107, 1092, 1037, 1011, 918, 727, 668; ^{1}H NMR (400 MHz, DMSO-*d*6) δ/ppm :8.92 (dd, 1H, *J* = 3.4, 7.0 Hz), 8.89 (d, 2H, *J* = 8.2 Hz), 8.80 (dd, 1H, *J* = 2.0, 8.7 Hz), 7.91 (d, 2H, *J* = 8.7 Hz), 7.88 (d, 2H, *J* = 8.2 Hz), 7.77 (tt, 2H, *J* = 2.0, 3.5, 7.0 Hz), 7.55 (td, 2H, *J* = 3.5, 7.6 Hz), 7.42 (td, 2H, *J* = 3.5, 7.6 Hz), 5.00 (t, 2H, *J* = 7.5 Hz), 4.92 (t, 2H, *J* = 7.5 Hz), 4.86 (t, 1H, *J* = 5.0 Hz), 3.62 (td, 2H, *J* = 5.0, 6.0 Hz), 2.19 (td, 2H, *J* = 6.0, 7.5 Hz), 1.94 (qn, 2H, *J* = 7.5 Hz), 1.43 (sext, 2H, *J* = 7.5 Hz), 0.94 (t, 2H, *J* = 7.5 Hz) ; ^{13}C NMR (100 MHz, DMSO-*d*6) δ/ppm:141.38, 141.30, 131.09, 131.02, 125.42, 125.41, 124.83, 124.82, 123.93, 123.60, 122.77, 122.74, 122.31, 122.23, 122.19, 122.13, 119.77, 119.75, 114.48, 114.30, 110.76, 110.67, 58.51, 46.19, 43.78, 33.34, 32.10, 19.97, 14.21; HRMS (FD, m/z) [(M+H$^+$)]calcd. for $C_{29}H_{28}N_2O_1$: 420.2202; found: 420.2181.

7) Preparation of **2**

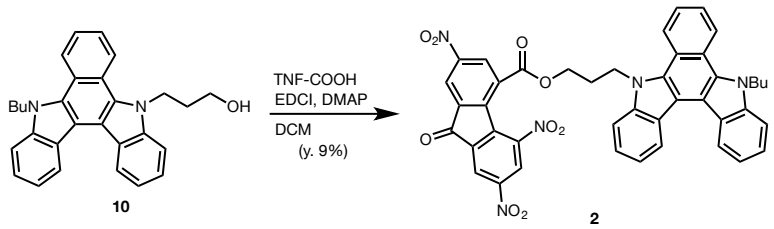

A solution of **10** (31 mg, 74 μmol), 2,5,7-trinitrofluorenone-4-carboxylic acid (26 mg, 74 μmol), 1-(3-dimethylaminopropyl)-3-ethylcarbodiimide hydrochloride (EDCI, 18 mg, 94 μmol) and 4-dimethylaminopyridine (DMAP, 11 mg, 94 μmol) in dry CH_2Cl_2 (1 mL) under argon was stirred for 3 days at room temperature. The resulting mixture was chromatographed on silica-gel (hexane:EtOAc = 3:1 to 1:1) to give **2** (5 mg, 9%) as a dark-green solid.

Mp 135 °C; IR (KBr) ν/cm^{-1} :3426, 3092, 2957, 2926, 2854, 2360, 1732, 1618, 1614, 1593, 1536, 1467, 1401, 1341, 1312, 1280, 1229, 1175, 1158, 1086, 1038, 917, 735; ^{1}H NMR (400 MHz, DMSO-*d*6) δ/ppm :8.68 (d, 1H, *J* = 8.2 Hz), 8.45 (d, 1H, *J* = 8.1 Hz), 8.40 (d, 1H, *J* = 8.2 Hz), 8.22 (d, 1H, *J* = 8.1 Hz), 7.97 (s, 1H), 7.91 (d, 1H, *J* = 8.4 Hz), 7.84 (d, 1H, *J* = 8.4 Hz), 7.78 (s, 1H), 7.72 (s, 1H), 7.64 (dd, 1H, *J* = 7.4, 7.4 Hz), 7.62 (dd, 1H, *J* = 7.4, 7.4 Hz), 7.50 (dd, 1H, *J* = 7.4, 7.4 Hz), 7.43 (dd, 1H, *J* = 7.6, 7.6 Hz), 7.31 (dd, 1H, *J* = 7.6, 7.6 Hz), 7.05 (dd, 1H, *J* = 7.4, 7.4 Hz), 5.07 (br s, 2H), 4.82 (t, 2H, *J* = 7.3 Hz), 4.34 (br s, 2H), 2.00-2.069 (m, 2H), 1.58 (sext, 2H, *J* = 7.3 Hz), 1.36-1.52 (m, 2H), 1.06 (t, 3H, *J* = 7.3 Hz); HRMS (FD, m/z) [(M+H^+)]calcd. for $C_{43}H_{31}N_5O_9$: 761.2122; found: 761.2113.

<Preparation of dyrex molecule 3M (Ar = morphorinophenyl)>

8) Preparation of **17M**

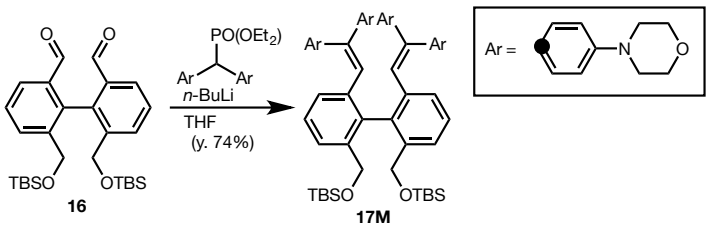

To a solution of diethyl bis(4-morphorinophenyl)methylphosphonate (716 mg, 1.51 mmol) in dry THF (8 mL) under argon was added a solution of *n*-BuLi (1.55 M in *n*-hexane, 0.97 mL, 1.51 mmol) at -78 °C. After stirring for 2 h at -78 °C, to the resulting solution was added a solution of dialdehyde **16** (150 mg, 0.30 mmol in THF 2 mL) at -78 °C. The mixture was allowed to warm and then stirred for 14.5 h at room temperature. After addition of saturated aqueous NH_4Cl_4, the resulting mixture was extracted with EtOAc for three times. The combined organic layer was washed with brine and dried over anhydrous Na_2SO_4, then concentrated in vacuo. The residue was reprecipitated with MeOH/*n*-Hexane to give **17M** (253 mg, 74% yield based on **16**) as a white solid.

Mp 164-165 °C; IR (KBr) ν /cm^{-1}: 3447, 3064, 3034, 2956, 2927, 2892, 2854, 2821, 1607, 1559, 1515, 1471, 1450, 1427, 1379, 1333, 1303, 1256, 1231, 1194, 1151, 1123, 1069, 1051, 1005, 958, 930, 850, 775, 669, 656, 612; ^{1}H NMR (400 MHz, $CDCl_3$) δ /ppm: 7.35 (d, 2H, J = 7.6 Hz), 7.08 (d, 4H, J = 8.8 Hz), 6.95 (dd, 2H, J = 7.6, 7.6 Hz), 6.95 (d, 4H, J = 8.8 Hz), 6.81 (d, 2H, J = 7.6 Hz), 6.75 (d, 4H, J = 8.8 Hz), 6.33 (d, 4H, J = 8.8 Hz), 6.28 (s, 2H), 4.35 (d, 2H, J = 13.7 Hz), 4.29 (d, 2H, J = 13.7 Hz), 3.84 (t, 8H, J = 4.7 Hz), 3.80 (t, 8H, J = 4.7 Hz), 3.14 (t, 8H, J = 4.7 Hz), 3.02 (t, 8H, J = 4.7 Hz), 0.91 (s, 18H), 0.02 (s, 6H), 0.00 (s, 6H); ^{13}C NMR (100 MHz, $CDCl_3$) δ /ppm: 150.3, 149.7, 142.54, 142.53, 137.97, 137.22, 136.52, 135.65, 131.85, 131.78, 129.22, 129.13, 126.74, 124.72, 124.63, 114.8, 114.79, 114.57, 66.9, 66.9, 63.15, 49.02, 48.88, 26.01, 26.01, 18.46, -5.35, -5.4; HRMS (FD, m/z) [(M+H$^+$)] calcd. for $C_{70}H_{90}N_4O_6Si_2$: 1138.63989; found: 1138.63834.

9) Preparation of **3M**

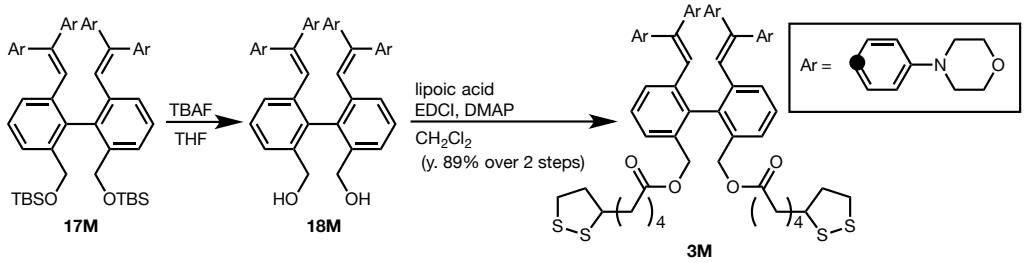

To a solution of **17M** (200 mg, 0.18 mmol) in dry THF (5 mL) under argon was added tetrabutylammonium fluoride (1.0 M in THF, 0.53 mL, 0.53 mmol) at room temperature. After stirring for 1.5 h at room temperature, the mixture was quenched with saturated aqueous NH_4Cl and extracted with EtOAc for three times. The combined organic layer was washed with brine and dried over anhydrous Na_2SO_4, then concentrated in vacuo to give **18M**, which was used without further purification.

To a solution of the crude diol **18M** in CH_2Cl_2 (5 mL) under argon was added 1-(3-dimethylaminopropyl)-3-ethylcarbodiimide hydrochloride (103 mg, 0.54 mmol), 4-dimethylaminopydirine (21 mg, 0.18 mmol), and DL-α-lipoic acid (110 mg, 0.54 mmol) at room temperature. After stirring for 14 h, the solvent was removed and the residue was chromatographed on Al_2O_3 (*n*-Hexane/EtOAc = 2/1 to 1/1 to 1/2) to give **3M** (201 mg, 89% yield over 2 steps) as pale yellow amorphous.

IR (KBr) ν /cm^{-1}: 3451, 2955, 2852, 2574, 1732, 1605, 1514, 1495, 1461, 1449, 1416, 1380, 1334, 1303, 1257, 1229, 1193, 1121, 1068, 1051, 928, 861, 824, 769, 609; ^{1}H NMR (400 MHz, $CDCl_3$) δ /ppm: 7.18 (d, 2H, *J* = 7.5 Hz), 7.10 (d, 4H, *J* = 8.7 Hz), 6.96 (dd, 2H, *J* = 7.8, 7.5 Hz), 6.95 (d, 4H, *J* = 8.7 Hz), 6.88 (d, 2H, *J* = 7.8 Hz), 6.78 (d, 4H, *J* = 8.7 Hz), 6.36 (s, 2H), 632 (d, 4H, *J* = 8.7 Hz), 4.84 (d, 2H, *J* = 12.5 Hz), 4.77 (d, 2H, *J* = 12.5 Hz), 3.84 (t, 8H, *J* = 4.7 Hz), 3.80 (t, 8H, *J* = 4.7 Hz), 3.54 (dddd, 2H, *J* = 12.2, 6.5, 6.5, 1.2 Hz), 3.15 (t, 8H, *J* = 4.7 Hz), 3.13-3.05 (m, 4H), 3.01 (t, 8H, *J* = 4.7 Hz), 3.27 (tdd, 2H, *J* = 12.2, 6.5, 1.2 Hz), 3.18-3.04 (m, 12H), 2.45-2.34 (m, 2H), 2.33 (t, 4H, *J* = 7.4 Hz), 1.87 (dq, 2H, *J* = 12.2, 6.5 Hz), 1.70-1.63 (m, 8H), 1.48-1.40 (m, 4H); ^{13}C NMR (100 MHz, $CDCl_3$) δ /ppm: 172.99, 150.49, 149.88, 143.21, 138.52, 138.35, 135.31, 133.19, 133.17, 131.82, 131.37, 130.65, 129.22, 127.21, 126.89, 124.32, 114.84, 114.6, 66.9, 66.89, 64.68, 56.33, 56.31, 48.96, 48.83, 40.22, 38.51, 34.66, 34.65, 34.04, 28.83, 28.81, 24.66; HRMS (FD, m/z) [(M+H$^+$)]

calcd. for $C_{74}H_{86}N_4O_8S_4$: 1286.53285; found: 1286.53442.

<Preparation of dyrex molecule 3D (Ar = dimethylaminophenyl)>

10) Preparation of **17D**

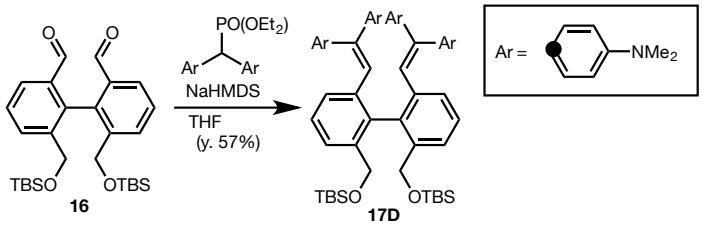

To a solution of diethyl bis(4-dimethylaminophenyl)methylphosphonate (949 mg, 2.43 mmol) in dry THF (25 mL) under argon was added a solution of sodium hexamethyl-disilazide (1.0 M in *n*-hexane, 2.43 mL, 2.43 mmol) at 0 °C. After stirring for 90 min at 0 °C, to the resulting solution was added a solution of dialdehyde **16** (303 mg, 0.61 mmol in THF 5 mL) at 0 °C. The mixture was allowed to warm and then stirred for 15.5 h at room temperature. After addition of saturated aqueous NH_4Cl_4, the resultant mixture was extracted with EtOAc for three times. The combined organic layer was washed with brine and dried over anhydrous $MgSO_4$ and concentrated in vacuo. The residue was chromatographed on Al_2O_3 (*n*-hexane/EtOAc = 10/1) and washed with ether and *n*-hexane to give **17D** (335 mg, 57% yield based on **16**) as a pale yellow solid.

Mp 229 °C; IR (KBr) ν /cm^{-1}: 3035, 2953, 2927, 2883, 2854, 2800, 1610, 1520, 1471, 1461, 1444, 1408, 1355, 1253, 1226, 1192, 1167, 1106, 1065, 1005, 947, 838, 817, 776, 664, 565; ^{1}H NMR (400 MHz, $CDCl_3$) δ /ppm: 7.32 (d, 2H, J = 7.7 Hz), 7.08 (d, 4H, J = 8.8 Hz), 6.96 (d, 4H, J = 8.8 Hz), 6.95 (dd, 2H, J = 7.7, 7.5 Hz), 6.86 (d, 2H, J = 7.5 Hz), 6.58 (d, 4H, J = 8.8 Hz), 6.24 (d, 4H, J = 8.8 Hz), 6.19 (s, 2H), 4.38 (d, 2H, J = 14.0 Hz), 4.31 (d, 2H, J = 14.0 Hz), 2.92 (s, 12H), 2.82 (s, 12H), 0.91 (s, 18H), 0.03 (s, 6H), 0.01 (s, 6H); ^{13}C NMR (100 MHz, $CDCl_3$) δ /ppm: 149.73, 149.27, 143.27, 137.98, 137.62, 136.38, 133.02, 131.89, 131.44, 129.36, 128.98, 128.94, 126.53, 123.94, 122.92, 112.09, 111.73, 111.61, 65.84, 63.18, 40.47, 40.38, 26.04, 18.46, -5.33, -5.38; HRMS (FD, m/z) [(M+H$^+$)] calcd. for $C_{62}H_{82}N_4O_2Si_2$: 970.59763; found: 970.59723.

11) Preparation of **3D**

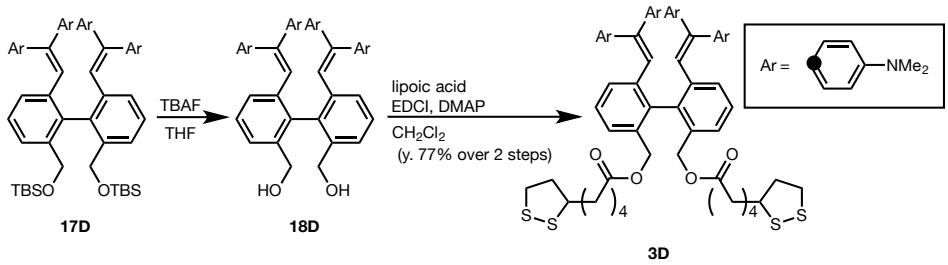

To a solution of **17D** (289 mg, 0.30 mmol) in dry THF (7.5 mL) under argon was added tetrabutylammonium fluoride (1.0 M in THF, 0.91 mL, 0.91 mmol) at room temperature. After stirring for 1 h at room temperature, the mixture was quenched with saturated aqueous NH_4Cl and extracted with EtOAc for three times. The combined organic layer was washed with brine and dried over anhydrous $MgSO_4$, then concentrated in vacuo to give **18D**, which was used without further purification.

To a solution of the crude diol **18D** in CH_2Cl_2 (6 mL) under argon was added 1-(3-dimethylaminopropyl)-3-ethylcarbodiimide hydrochloride (174 mg, 0.91 mmol), 4-dimethylaminopydirine (36 mg, 0.30 mmol), and DL-α-lipoic acid (187 mg, 0.91 mmol) at room temperature. After stirring for 17 h, the solvent was removed and the residue was chromatographed on Al_2O_3 (*n*-Hexane/EtOAc = 3/1 to 2/1) to give **3D** (254 mg, 77% yield over 2 steps) as a pale yellow amorphous.

IR (KBr) ν /cm^{-1}: 3340, 2925, 2799, 1732, 1608, 1551, 1520, 1479, 1443, 1353, 1226, 1192, 1166, 1062, 946, 819, 765; ^{1}H NMR (400 MHz, $CDCl_3$) δ /ppm: 7.15 (dd, 2H, *J* = 6.4, 5.8 Hz), 7.10 (d, 4H, *J* = 8.8 Hz), 6.96 (d, 4H, *J* = 8.8 Hz), 6.96 (d, 2H, *J* = 6.4 Hz), 6.94 (d, 2H, *J* = 5.8 Hz), 6.61 (d, 4H, *J* = 8.8 Hz), 6.27 (s, 2H), 6.22 (d, 4H, *J* = 8.8 Hz), 4.84 (d, 2H, *J* = 12.5 Hz), 4.78 (d, 2H, *J* = 12.5 Hz), 3.53 (dddd, 2H, *J* = 12.9, 6.5, 6.5, 1.2 Hz), 3.18-3.04 (m, 4H), 2.93 (s, 12H), 2.82 (s, 12H), 2.41 (tdd, 2H, *J* = 12.9, 6.5, 1.2 Hz), 2.33 (t, 4H, *J* = 7.3 Hz), 1.87 (tdd, 2H, *J* = 12.9, 6.5, 1.2 Hz), 1.70-1.60 (m, 8H), 1.50-1.36 (m, 4H); ^{13}C NMR (100 MHz, $CDCl_3$) δ /ppm: 173.07, 149.85, 149.38, 143.9, 139.03, 138.44, 133.06, 133.05, 132.63, 131.83, 130.59, 129.33, 128.49, 126.98, 126.53, 122.63, 112.11, 111.73, 64.87, 56.31, 56.28, 40.44, 40.34, 40.17, 38.47, 34.61, 34.06, 34.04, 28.79, 28.76, 24.65; HRMS (FD, m/z) [($M+H^+$)] calcd. for $C_{66}H_{78}N_4O_4S_4$: 1118.49059; found: 1118.49158.

<Preparation of dyrex molecule 3P (Ar = pyrrolidinnophenyl)>

12) Preparation of **17P**

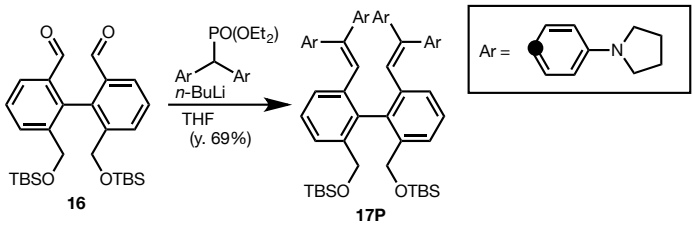

To a solution of diethyl bis(4-pyrrolidinophenyl)methylphosphonate (668 mg, 1.51 mmol) in dry THF (8 mL) under argon was added a solution of *n*-BuLi (1.55 M in *n*-hexane, 0.97 mL, 1.51 mmol) at -78 °C. After stirring for 4 h at -78 °C, to the resulting solution was added a solution of dialdehyde **16** (150 mg, 0.30 mmol in THF 2 mL) at -78 °C. The mixture was allowed to warm and then stirred for 19 h at room temperature. After addition of saturated aqueous NH_4Cl_4, the resultant mixture was extracted with EtOAc for three times. The combined organic layer was washed with brine and dried over anhydrous Na_2SO_4 and concentrated in vacuo. The residue was suspended to EtOAc and the precipitation was filtered through *Kiriyama* funnel. The residue was washed with EtOAc to give **17P** (222 mg, 69% based on **16**) as a yellow solid.

Mp 285 °C (decomp.); IR (KBr) ν /cm^{-1}: 3433, 3064, 3038, 3009, 2955, 2926, 2891, 2853, 1610, 1520, 1487, 1462, 1425, 1373, 1251, 1227, 1186, 1159, 1105, 1071, 1004, 966, 937, 853, 837, 811, 776; ^{1}H NMR (400 MHz, $CDCl_3$) δ /ppm: 7.31 (d, 2H, J = 6.7 Hz), 7.08 (d, 4H, J = 8.7 Hz), 6.97 (d, 4H, J = 8.7 Hz), 6.95 (dd, 2H, J = 6.7, 6.7 Hz), 6.90 (d, 2H, J = 6.7 Hz), 6.43 (d, 4H, J = 8.7 Hz), 6.16 (s, 2H), 6.08 (d, 4H, J = 8.7 Hz), 4.40 (d, 2H, J = 14.0 Hz), 4.32 (d, 2H, J = 14.0 Hz), 3.27 (t, 8H, J = 6.4 Hz), 3.16 (t, 8H, J = 6.4 Hz), 1.98 (t, 8H, J = 6.4 Hz), 1.93 (t, 8H, J = 6.4 Hz), 0.92 (s, 18H), 0.03 (s, 6H), 0.01 (s, 6H); ^{13}C NMR (100 MHz, $CDCl_3$) δ /ppm: 147.06, 146.66, 143.69, 138.03, 137.73, 136.31, 132.26, 132.05, 132.05, 129.54, 129.54, 128.87, 128, 126.47, 123.65, 122.13, 111.26, 110.88, 63.21, 47.53, 47.41, 26.05, 25.51, 25.41, 18.46, -5.32, -5.36; HRMS (FD, m/z) [(M+H$^+$)] calcd. for $C_{70}H_{90}N_4O_2Si_2$: 1074.66023; found: 1074.66014.

13) Preparation of **3P**

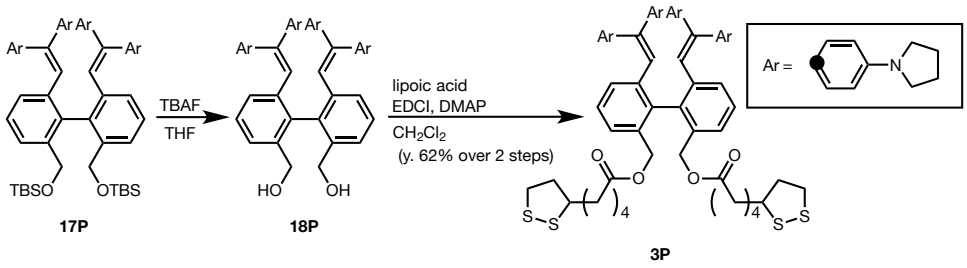

To a solution of **17P** (222 mg, 0.21 mmol) in dry THF (5 mL) under argon was added tetrabutylammonium fluoride (1.0 M in THF, 0.63 mL, 0.63 mmol) at room temperature. After stirring for 2 h at room temperature, the mixture was quenched with saturated aqueous NH_4Cl and extracted with EtOAc for three times. The combined organic layer was washed with brine and dried over anhydrous Na_2SO_4, then concentrated in vacuo to give **18P**, which was used without further purification.

To a solution of the crude diol **18P** in CH_2Cl_2 (5 mL) under argon was added 1-(3-dimethylaminopropyl)-3-ethylcarbodiimide hydrochloride (121 mg, 0.63 mmol), 4-dimethylaminopydirine (25 mg, 0.21 mmol), and DL-α-lipoic acid (130 mg, 0.63 mmol) at room temperature. After stirring for 24 h, the solvent was removed and the residue was chromatographed on Al_2O_3 (*n*-Hexane/EtOAc = 5/1) to give **3P** (155 mg, 62% yield over 2 steps) as yellow amorphous.

IR (KBr) ν /cm^{-1}: 3451, 3131, 3124, 2965, 2928, 2839, 2360, 2343, 1734, 1608, 1551, 1548, 1536, 1519, 1503, 1485, 1461, 1432, 1415, 1372, 1245, 1186, 965, 816, 762; ^{1}H NMR (400 MHz, $CDCl_3$) δ /ppm: 7.13 (d, 2H, *J* = 6.7 Hz), 7.09 (d, 4H, *J* = 8.6 Hz), 7.00-6.91 (m, 8H), 6.44 (d, 4H, *J* = 8.6 Hz), 6.23 (s, 2H), 6.07 (d, 4H, *J* = 8.6 Hz), 4.80 (s, 4H), 3.52 (td, 2H, *J* = 7.4, 6.6 Hz), 3.27 (d, 4H, *J* = 4.6 Hz), 3.18-3.04 (m, 12H), 2.45-2.34 (m, 2H), 2.32 (t, 4H, *J* = 7.4 Hz), 1.98 (t, 8H, *J* = 6.0 Hz), 1.93 (t, 8H, *J* = 6.0 Hz), 1.88-1.83 (m, 2H), 1.68-1.59 (m, 8H), 1.48-1.38 (m, 4H); ^{13}C NMR (100 MHz, $CDCl_3$) δ /ppm: 173.1, 147.21, 146.77, 144.29, 139.2, 138.49, 133.09, 133.08, 131.99, 131.9, 130.51, 129.49, 127.57, 126.92, 126.37, 121.91, 111.33, 110.95, 64.93, 56.31, 56.26, 47.56, 47.4, 40.16, 40.14, 38.48, 34.61, 34.06, 28.78, 28.74, 25.52, 25.42, 24.66; HRMS (FD, m/z) [$(M+H^+)$] calcd. for $C_{74}H_{86}N_4O_4S_4$: 1222.55319; found: 1222.55162.

References

[1] S. M. Sze, K. K. Ng, *Physics of Semiconductor Devices*, John Wiley & Sons, **2006**.

[2] R. M. Metzger, *Chem. Rev.* **2015**, *115*, 5056–5115.

[3] D. Xiang, X. Wang, C. Jia, T. Lee, X. Guo, *Chem. Rev.* **2016**, *116*, 4318–4440.

[4] W.-Y. Lo, N. Zhang, Z. Cai, L. Li, L. Yu, *Acc. Chem. Res.* **2016**, *49*, 1852–1863.

[5] M. Iwane, S. Fujii, M. Kiguchi, *Sensors* **2017**, *17*, 956–971.

[6] A. Vilan, D. Aswal, D. Cahen, *Chem. Rev.* **2017**, *117*, 4248–4286.

[7] H. Jeong, D. Kim, D. Xiang, T. Lee, *ACS Nano* **2017**, *11*, 6511–6548.

[8] P. T. Mathew, F. Fang, *Proc. Est. Acad. Sci. Eng.* **2018**, *4*, 760–771.

[9] C. P. Collier, E. W. Wong, M. Belohradsky, F. M. Raymo, J. F. Stoddart, P. J. Kuekes, R. S. Williams, J. R. Heath, *Science* **1999**, *285*, 391–394.

[10] H. Jeong, D. Kim, D. Xiang, T. Lee, *ACS Nano* **2017**, *11*, 6511–6548.

[11] B. Chen, K. Xu, *Nano: Brief Reports and Reviews* **2019**, *14*, 1930007.

[12] A. Aviram, M. A. Ratner, *Chem. Phys. Lett.* **1974**, *29*, 277–283.

[13] A. S. Martin, J. R. Sambles, G. J. Ashwell, *Phys. Rev. Lett.* **1993**, *70*, 218–221.

[14] I. Díez-Pérez, J. Hihath, Y. Lee, L. Yu, L. Adamska, M. A. Kozhushner, I. I. Oleynik, N. Tao, *Nat. Chem.* **2009**, *1*, 635–641.

[15] M. Elbing, R. Ochs, M. Koentopp, M. Fischer, C. von Hänisch, F. Weigend, F. Evers, H. B. Weber, M. Mayor, *Proc. Natl. Acad. Sci. U. S. A.* **2005**, *102*, 8815–8820.

[16] N. J. Tao, *Nat. Nanotechnol.* **2006**, *1*, 173–181.

[17] L. Yuan, N. Nerngchamnong, L. Cao, H. Hamoudi, E. del Barco, M. Roemer, R. K. Sriramula, D. Thompson, C. A. Nijhuis, *Nat. Commun.* **2015**, *6*, 6324.

[18] L. Yuan, R. Breuer, L. Jiang, M. Schmittel, C. A. Nijhuis, *Nano Lett.* **2015**, *15*, 5506–5512.

[19] X. Chen, M. Roemer, L. Yuan, W. Du, D. Thompson, E. Del Barco, C. A. Nijhuis, *Nat. Nanotechnol.* **2017**, *12*, 797–803.

[20] C. A. Nijhuis, W. F. Reus, G. M. Whitesides, *J. Am. Chem. Soc.* **2009**, *131*, 17814–17827.

[21] M. Souto, L. Yuan, D. C. Morales, L. Jiang, I. Ratera, C. A. Nijhuis, J. Veciana, *J. Am. Chem. Soc.* **2017**, *139*, 4262–4265.

[22] T. Suzuki, Y. Tokimizu, Y. Sakano, R. Katoono, K. Fujiwara, S. Naoe, N. Fujii, H. Ohno, *Chem. Lett.* **2013**, *42*, 1001–1003.

[23] T. Suzuki, Y. Sakano, Y. Tokimizu, Y. Miura, R. Katoono, K. Fujiwara, N. Yoshioka, N. Fujii, H. Ohno, *Chem. Asian J.* **2014**, *9*, 1841–1846.

[24] D. F. Perepichka, I. F. Perepichka, A. F. Popov, M. R. Bryce, A. S. Batsanov, A. Chesney, J. A. K. Howard, N. I. Sokolov, *J. Organomet. Chem.* **2001**, *637*, 445–462.

[25] C. Browning, J. M. Hudson, E. W. Reinheimer, F.-L. Kuo, R. N. McDougald Jr, H. Rabaâ, H. Pan, J. Bacsa, X. Wang, K. R. Dunbar, et al., *J. Am. Chem. Soc.* **2014**, *136*, 16185–16200.

[26] B. Xu, N. J. Tao, *Science* **2003**, *301*, 1221–1223.

[27] L. Cui, R. Miao, C. Jiang, E. Meyhofer, P. Reddy, *J. Chem. Phys.* **2017**, *146*, 092201.

[28] M. Thoss, F. Evers, *J. Chem. Phys.* **2018**, *148*, 030901.

[29] L. Yuan, L. Wang, A. R. Garrigues, L. Jiang, H. V. Annadata, M. Anguera Antonana, E. Barco, C. A. Nijhuis, *Nat. Nanotechnol.* **2018**, *13*, 322–329.

[30] H. Jeong, D. Kim, D. Xiang, T. Lee, *ACS Nano* **2017**, *11*, 6511–6548.

[31] S. Seo, M. Min, S. M. Lee, H. Lee, *Nat. Commun.* **2013**, *4*, 1920.

[32] J. E. Green, J. W. Choi, A. Boukai, Y. Bunimovich, E. Johnston-Halperin, E. DeIonno, Y. Luo, B. A. Sheriff, K. Xu, Y. S. Shin, et al., *Nature* **2007**, *445*, 414–417.

[33] J. Lee, H. Chang, S. Kim, G. S. Bang, H. Lee, *Angew. Chem. Int. Ed Engl.* **2009**, *48*, 8501–8504.

[34] S. Seo, J. Lee, S.-Y. Choi, H. Lee, *J. Mater. Chem.* **2012**, *22*, 1868–1875.

[35] T. Suzuki, E. Ohta, H. Kawai, K. Fujiwara, T. Fukushima, *Synlett* **2007**, *2007*, 0851–0869.

[36] C. Kahlfuss, E. Saint-Aman, C. Bucher in *Organic Redox System: Redox-Mediated Reversible σ-Bond Formation/*Cleavage (Ed: T. Nishinaga), Wiley, Hoboken, **2015**, Chap. 2, pp. 13-38.

[37] T. Suzuki, J.-I. Nishida, T. Tsuji, *Chem. Commun.* **1998**, *0*, 2193–2194.

[38] H. Higuchi, E. Ohta, H. Kawai, K. Fujiwara, T. Tsuji, T. Suzuki, *J. Org. Chem.* **2003**, *68*, 6605–6610.

[39] E. Ohta, H. Uehara, Y. Han, K. Wada, H. Noguchi, R. Katoono, Y. Ishigaki, H. Ikeda, K. Uosaki, T. Suzuki, *Chempluschem* **2017**, *82*, 1043–1047.

Acknowledgements

All the studies described in this dissertation were carried out under the supervision of Professor Dr. Takanori Suzuki, Department of Chemistry, Faculty of Science, Hokkaido University. The author would like to express deeply his sincere gratitude to Professor Suzuki for his consistent guidance, suggestion, valuable discussions, and so much encouragement throughout the course of this work.

The author would like to be thankful to Dr. Ryo Katoono, and Dr. Yusuke Ishigaki, Department of Chemistry, Faculty of Science, Hokkaido University, and Professor Dr. Kenshu Fujiwara, Department of Life Science, Faculty of Engineering Science, Akita University, for their helpful guidance, suggestion and encouragement.

The author expresses sincere thanks to Professor Dr. Hiroaki Ohno and Mr. Yuiki Kawada, Graduate School and Faculty of Pharmaceutical Sciences, Kyoto University, and Professor Dr. Tomoyuki Akutagawa, and Dr. Takashi Takeda, Institute of Multidisciplinary Research for Advanced Materials, Tohoku University, for giving him the opportunity to make experiments for the contents of Chapter 2.

The author would like to express his deep gratitude to Associate Professor Dr. Christian A. Nijhuis and Dr. Karuppannan Senthil Kumar, Department of Chemistry, National University of Singapore, for their valuable and helpful suggestions and measurements of the behavior on the metal substrates in Chapter 3.

The author is deeply grateful to Professor Dr. Michael M. Haley and his laboratory members, Department of Chemistry and Biochemistry, University of Oregon, for his heartfelt guidance, suggestion, valuable discussions, and so much encouragement during my stay in his laboratory.

The author would like to express his gratitude to Dr. Eri Fukushi, and Mr. Yusuke Takata at GC-MS & NMR Laboratory, Faculty of Agriculture, Hokkaido University, Mr. Yasunori Kumaki, High Resolution NMR Laboratory, Graduate School of Science, Hokkaido University, for the measurements of mass and NMR spectra and elemental analyses. The author is deeply thankful to Mr. Tomohiro Hirose, Ms. Nozimi Takeda, Ms. Ai Tokumitsu, Ms. Satomi Sawasato, Instrumental Analysis Division, Equipment Management Center, Creative Research Institution, Hokkaido University, for the measurements of elemental analyses.

The author gives a special thanks to Dr. Hitomi Tamaoki, Dr. Yasuto Uchimura, Dr. Yuto Sakano, Dr. Takuto Sato, Dr. Takayuki Tsunoda, Dr. Takafumi Saito, Mr. Yoshitaka Nomura, Mr. Satoshi Okamoto, Mr. Yuki Saito, Mr. Yuse Kuriyama, and Mr. Yudai Obara for their helpful encouragement. The author also thanks to all other members in Laboratory of Organic Chemistry 1 (Suzuki's group). They often afforded beneficial advice to the author and encouraged him.

The author would like to be thankful to Scholarship of Japan Chemical Industry Association for its financial support.

Finally, the author expresses the largest gratitude to his parents, Tatsuru and Rieko Nojo, and his sister, Aoi Nojo for their financial support, encouragement, and understanding of hits outlook on life.

Wataru Nojo